12-2012

Role of human arylamine N-acetyltransferase in carcinogen metabolism and human breast cancer progression.

Carmine Simone Leggett
University of Louisville

Follow this and additional works at: https://ir.library.louisville.edu/etd

ROLE OF HUMAN ARYLAMINE *N*-ACETYLTRANSFERASE IN CARCINOGEN
METABOLISM AND HUMAN BREAST CANCER PROGRESSION

By

Carmine Simone Leggett
B.S., Spelman College, 2006
M.S., Delaware State University, 2008
M.S., University of Louisville School of Medicine, 2010

A Dissertation
Submitted to the Faculty of the
School of Medicine of the University of Louisville
in Partial Fulfillment of the Requirements
for the Degree of

Doctor of Philosophy

Department of Pharmacology and Toxicology
University of Louisville School of Medicine
Louisville, Kentucky

December 2012

ROLE OF HUMAN ARYLAMINE *N*-ACETYLTRANSFERASE IN CARCINOGEN
METABOLISM AND HUMAN BREAST CANCER PROGRESSION

By

Carmine Simone Leggett
B.S., Spelman College, 2006
M.S., Delaware State University, 2008
M.S., University of Louisville School of Medicine, 2010

A Dissertation Approved on

August 16, 2012

by the following Dissertation Committee:

_____

David W. Hein, Ph.D.

_____

Ramesh C. Gupta, Ph.D.

_____

Kenneth E. Palmer, Ph.D.

_____

J. Christopher States, Ph.D.

_____

John O. Trent, Ph.D.

DEDICATION

This dissertation is dedicated to my parents, The Reverend and Mrs. Johnny and Connie Leggett, and grandparents, the late Mr. and Mrs. Doshie and Ola Marks, who instilled in me the value of education and fearlessly pursing my dreams. I especially would like to thank my parents for providing me with the strength to continue during difficult times through their unconditional love, prayers, and support.

ACKNOWLEDGEMENTS

ABSTRACT

ROLE OF HUMAN ARYLAMINE *N*-ACETYLTRANSFERASE IN CARCINOGEN METABOLISM AND HUMAN BREAST CANCER PROGRESSION

Carmine S. Leggett

August 16, 2012

Human arylamine *N*-acetyltransferase (NAT) is a phase II cytosolic enzyme that occurs as two isozymes, NAT1 and NAT2. This family of polymorphic enzymes catalyzes the detoxification and/or activation of many aromatic and heterocyclic amine drugs and carcinogens. These metabolism reactions can lead to detoxification of xenobiotics by *N*-acetylation, or bioactivation by *O*-acetylation which is preceded by cytochrome P450 (CYP) hydroxylation. This study evaluates the role of human arylamine *N*-acetyltransferase in carcinogen metabolism as it pertains to substrate selectivity, kinetic activity towards arylamine and alkylaniline substrates, and toxicological risk. Here we introduce the use of immortalized human fibroblasts (GM4429) to investigate the effects of combinations of human NAT1, human NAT2 haplotypes (*NAT2*4*, *NAT2*5B*, or *NAT2*7B*), and varying CYP1A2 enzymatic activity on carcinogen metabolism. We determined the apparent Michaelis-Menten constants of human NAT1 and human NAT2 for several well-characterized and

putative environmental carcinogens. We utilized these data to investigate NAT substrate selectivity for these compounds of interest.

NAT1 has been implicated in several cancers including urinary bladder, colorectal, lung, and breast cancer. Studies suggest that NAT1 plays an important role in cell growth and survival, as well as in cell proliferation and cell invasion, which are hallmarks of metastatic cancer. Here we describe the use of computational screening to identify effective, novel small molecule inhibitors of the molecular target NAT1. Our lead compound, Compound 10, suppressed carcinogen metabolism and 4-aminobiphenyl (ABP) -induced DNA adducts. The results in this study show that upon NAT1 inhibition there is a significant decrease in ABP activation, cell invasion, and cell proliferation in human breast adenocarcinoma cells. We also show that NAT1 inhibition in human breast cancer cells resulted in mitotic arrest, which supports findings suggesting that NAT1 plays an important role in human breast cancer progression. Our results indicate that human NAT1 is a molecular target for cancer therapy.

TABLE OF CONTENTS

CHAPTERS

I.   BACKGROUND AND SIGNIFICANCE

II.   FUNCTIONAL EFFECTS OF HUMAN NAT1, HUMAN NAT2 HAPLOTYPES (*NAT2*4, NAT2*5B,* AND *NAT2*7B*), AND HIGH AND LOW CYP1A2 ENZYMATIC ACTIVITY ON CARCINOGEN METABOLISM

III.   IDENTIFICATION AND CHARACTERIZATION OF NOVEL HUMAN ARYLAMINE *N*-ACETYLTRANSFERASE SMALL MOLECULE INHIBITORS

LIST OF TABLES

LIST OF FIGURES

CHAPTER I

BACKGROUND AND SIGNIFICANCE

Arylamine *N*-Acetyltransferase Function and Characterization

Human arylamine *N*-acetyltransferase (NAT) is a phase II xenobiotic metabolizing enzyme that catalyzes the *N*- and *O*- acetylation of many arylamine drugs and environmental carcinogens (Figure 1.1). NAT catalyzes the *N*-acetylation of substrates by transferring an acetyl group from acetyl coenzyme A to the exocyclic nitrogen of aromatic or heterocyclic amines. This step is described as the detoxification pathway because these innocuous *N*-acetylated substrates are excreted from the body. If compounds are first *N*-hydroxylated by cytochrome P450 (CYP) enzymes, the *N*-hydroxlated substrates can then be further activated by NAT-catalyzed *O*-acetylation. This bioactivation reaction leads to the formation of *N*-acetoxy substrates. These very unstable *N*-acetoxy metabolites spontaneously form highly reactive electrophilic arylnitrenium ions that can react with DNA producing DNA adducts that can lead to mutagenesis and initiate cancer.
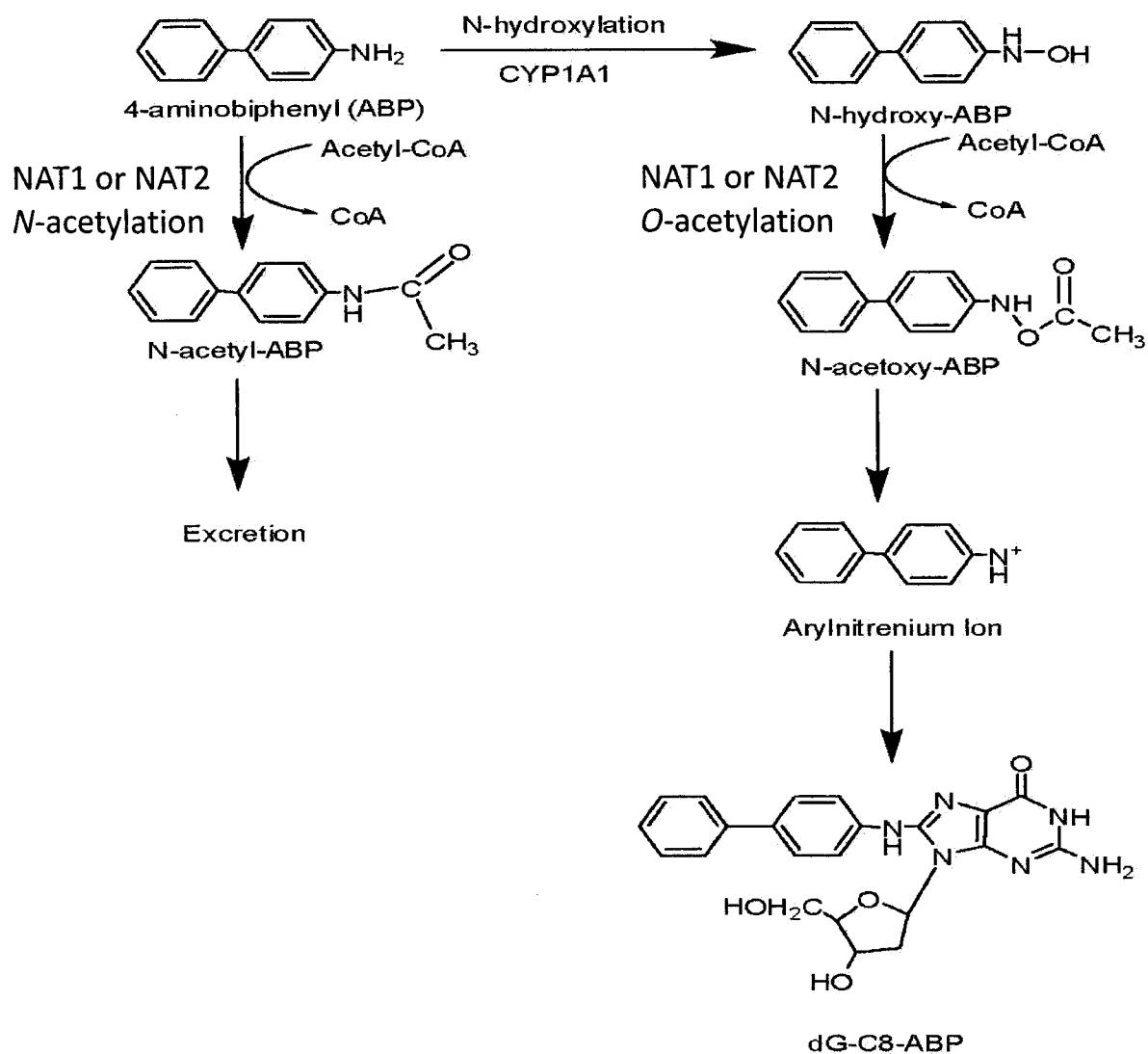
Figure 1.1 Metabolism reactions catalyzed by arylamine *N*-acetyltransferase. Adapted from Bendaly et al., 2007.

Arylamine *N*-acetyltransferase occurs in two human isozymes, NAT1 and NAT2, that share 87% nucleotide homology. Despite their high homology, they differ in substrate specificity and tissue distribution (Hein, 2002). Human NAT1 has a widespread distribution in adult tissues including the liver, while human NAT2 is expressed mainly in the liver and intestine (Russell et al., 2009). Both isozymes possess a functional Cys-His-Asp catalytic triad that allows the transfer of an acetyl group for acetyl coenzyme A in a ping-pong bi-bi reaction mechanism (Hein, 2009). Site-directed mutagenesis of individual amino acids demonstrated that substrate selectivity is strongly influenced by three key active site loop residues F125, Y127, and R129 (Goodfellow et al., 2010). For example, NAT1 selectively acetylates p-aminobenzoic acid (PABA) and p-aminosalicyclic acid (PAS), whereas NAT2 preferentially acetylates sulphamethazine (SMZ) and procainamide.

p-Aminobenzoylglutamate (PABG), a folic acid catabolite, is the only known endogenous substrate for NAT. PABG is *N*-acetylated by NAT1 suggesting an endogenous role for NAT in folate metabolism and embryonic development (Minchin, 1995). NAT1 polymorphisms have been associated with incidences of spina bifida and limb deficiency defects further suggesting that there is a critical endogenous role for *N*-acetyltransferases (Minchin, 1995). The endogenous role of NAT is not fully understood. Studies are needed investigated to determine the role that NAT plays in development and carcinogen metabolism.
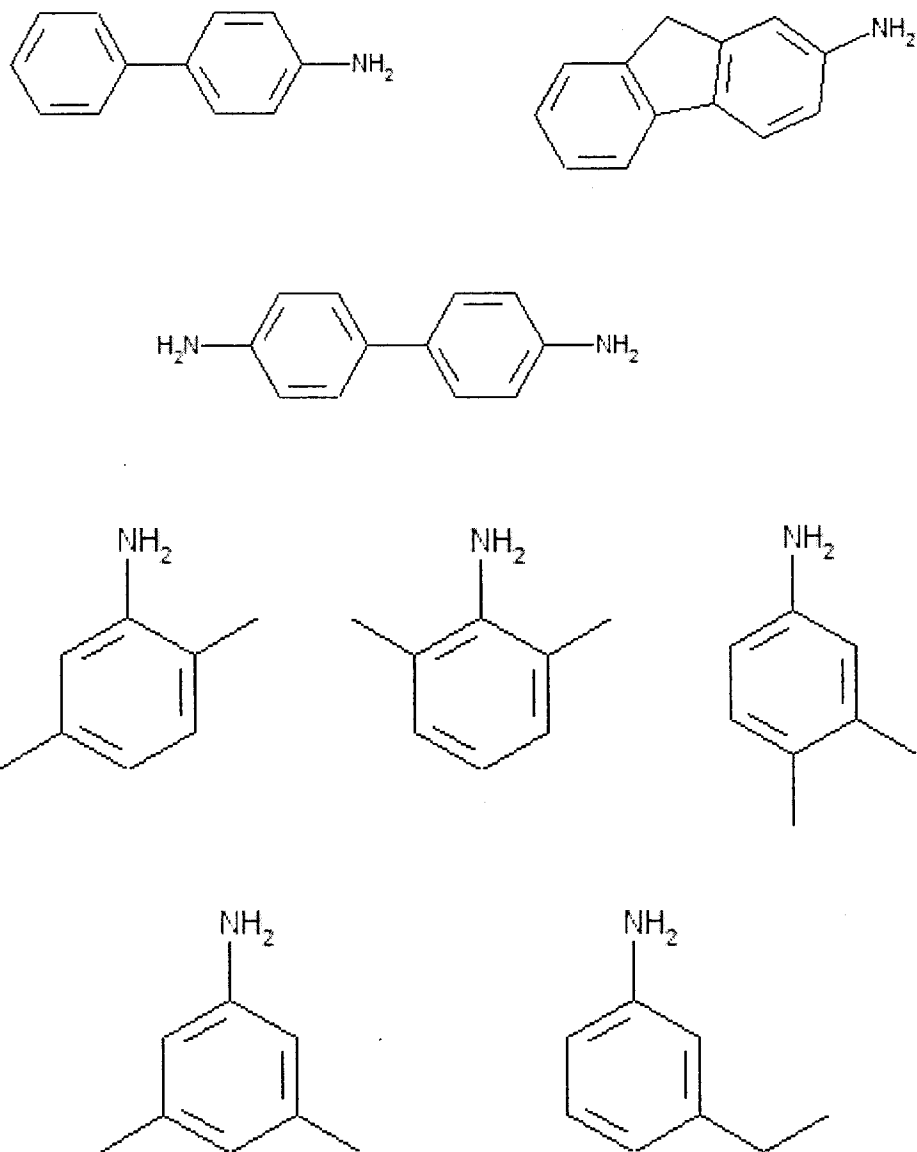
Figure 1.2 Chemical structures of selected *N*-acetyltransferase substrates. Arylamine environmental carcinogens 4-aminobiphenyl, 2-aminofluorene, benzidine and alkyanilines 2,5-dimethylaniline, 2,6-dimethylaniline, 3,4-dimethylaniline, 3,5-dimethylaniline, and 3-ethylaniline. (from left to right).

4

As seen in Figure 1.2, *N*-acetyltransferase metabolizes a number of aromatic and heterocyclic amine carcinogens. Some examples include environmental carcinogens found in cigarette smoke and meats cooked at high temperatures, such as 4-aminobiphenyl (ABP), 2-aminofluorene (AF), and 2-amino-1-methyl-6-phenylimidazo [4,5-b]pridine (PhIP) (Walker et al., 2009).

Exposure to ABP, which is present in tobacco smoke (2.4 - 4.6 ng per cigarette), has been associated with bladder cancer risk (Liu et al., 2007). AF, whose *N*-acetylated derivative was developed as an insecticide, is associated with mutagenesis (Sugamori et al., 2003). Although some arylamine substrates such as ABP and AF are metabolized by both NAT1 and NAT2, each NAT isozyme exhibits substrate specificity (Liu et al., 2007). Capacities of human NAT1 to catalyze the metabolic activation of *N*-hydroxy-2-acetylaminofluorene and *N*-hydroxy-4-acetylaminobiphenyl via *N,O*-acetylation were lower than the metabolic rates of *N*-hydroxy-2-aminofluorene and *N*-hydroxy-4-aminobiphenyl via *O*-acetylation (Hein et al., 1993). ABP and AF both produce dG-C8-adducts, but the mutation pattern for each compound is different. dG-C8-AF produces both frameshift and base-substitution (G to T) mutations, and dG-C8-ABP produces only base-substitution (G to A) mutations (Beland et al., 1983).

Other compounds metabolized by NAT enzymes include alkylaniline (monocyclic arylamines) genotoxicants 2,5-dimethylaniline (2,5-DMA), 2,6-dimethylaniline (2,6-DMA), 3,4-dimethylaniline (3,4-DMA), 3,5-dimethylaniline (3,5-DMA), and 3-ethylaniline (3-EA). Arylamine genotoxicants 2,6-DMA and 3,5-DMA are present in cigarette smoke and pollution from industrial sources.

The alkylanilines 2,6-DMA , 3,5-DMA, and 3-EA are associated with bladder cancer among the general population including non-smokers (Liu et al., 2007). Exposure to these alkylanilines (monocyclic arylamines) is of particular interest to toxicological risk studies because of the wide distribution of these compounds in the environment resulting in ubiquitous exposure (Skipper et al., 2010). Since these compounds are present in cigarette smoke, indoor spaces contaminated with cigarette smoke exhibit higher levels of alkylanilines than in uncontaminated spaces. Industrial sources also provide significant levels of exposure to these compounds (Skipper et al., 2010).

It is important to note that in previous studies conducted in Italy, 2,6-DMA levels were higher among non-smokers than smokers illustrating the environmental significance of monocyclic arylamine exposure is extensive and is not confined to groups such as active smokers or those subjected to occupational exposure (Skipper et al., 2010). This suggests that environmental exposure is as important as active smoking exposure. The arylamine compounds explored in this study were chosen because they are general environmental pollutants that potentially have a detrimental impact on the total population due to the possibility of toxicological risk.

Both NAT1 and NAT2 are capable of N-acetylating arylamines and alkylanilines to innocuous compounds that are less reactive and excreted. Since these isozymes are differentially expressed in tissues, substrate selectivity may have a profound effect on the detoxification or bioactivation of alkylanilines. NAT2 polymorphisms have been shown to play an important role in the

6

bioactivation and detoxification of arylamine and hydrazine drugs and carcinogens. While previous studies have sought to better understand the carcinogenicity and genotoxicity of these compounds, none have determined the effects of NAT2 genetic polymorphisms on the metabolism of alkylanilines.

Human Arylamine *N*-Acetyltransferase Genetic Variants

and Functional Genomic Studies

Human arylamine *N*-acetyltransferase polymorphisms were first identified when patients prescribed the anti-tuberculosis drug isoniazid experienced varying toxic side-effects. It was later discovered that *N*-acetyltransferase polymorphisms were responsible not only for the variations in metabolism of this hydrazine drug, but also of environmental carcinogens consequently altering risk posed by the activation of carcinogens. Polymorphisms in the NAT genes have been shown to affect the acetylator phenotype (Hein, 2006).

Molecular epidemiological studies have reported associations between NAT polymorphisms and individual risk of several diseases including cancer. Functional genomic studies have been done in *E. coli* (Hein et al., 1994), yeast (Fretland et al., 2001), COS-1 cells (Zang et al., 2007) and Chinese hamster ovary cells (Metry et al., 2007) to better understand the relationship between haplotype and disease risk. These studies have provided valuable information adding to our understanding of the effects that genetic variations have on disease susceptibility and toxicological risk, but these relationships are not fully understood.

The reference allele *NAT2*4,* which is associated with rapid acetylation, and over 32 *NAT2* allelic variants have been identified in human populations (Walker et al., 2009). These alleles contain nucleotide substitution sites throughout the NAT2 coding regions that cause functional consequences of

altered (rapid or slow) acetylator phenotype. Two alleles of interest associated with slow acetylator phenotype are *NAT2*5B* and *NAT2*7B*. *NAT2*5B* possesses three single nucleotide polymorphisms (SNPs) in the NAT2 open reading frame T341C (I114T), C481T (synonymous), and A803G (K268R), whereas *NAT2*7B* is associated with two SNPs in the *NAT2* open reading frame C282T (synonymous) and G857A (G286E) (Bendaly et al., 2009). Studies have shown that the T341C SNP associated with the *NAT2*5B* allele causes a reduction in protein due to enhanced protein aggregation and/or targeting for degradation (Walraven et al., 2008). It is postulated that this polymorphism reduces hydrophobic interactions at the interface between the domain II beta barrel and the domain I helix, altering protein folding resulting in protein degradation. The G857A SNP associated with the *NAT2*7B* allele results in altered active site access and altered substrate affinity which causes substrate-dependent activity changes. It is believed that this polymorphism alters the conformation of the C-terminal tail adjacent to the active site opening due to steric clashes with nearby residues.

Although epidemiological studies suggest that genetic polymorphisms are associated with increased susceptibility to various cancers related to environmental carcinogen exposure, further experimental studies are needed to strengthen these findings. Previous studies in our laboratory investigated the effects of NAT2 genetic variants on 2-amino-1-methyl-6-phenylimidazo[4,5b]pyridine (PhIP) induced DNA adduct formation and mutagenesis in nucleotide excision repair (NER)-deficient Chinese hamster ovary

(CHO) cells that recombinantly express human CYP1A2 and human *NAT2*4* or *NAT2*5B* alleles (Metry et al., 2007). This study provides evidence in support of the ability to study mutagenesis and DNA damage in a cell line stably transfected with human *NAT2* alleles and human CYP1A2.

Arylamine *N*-Acetyltransferase 1 and Cancer

NAT1 is found in almost all tissues of the body (Hein, 2009). NAT1 mRNA levels have been associated with several cancers including breast, urinary bladder, esophageal, and gastric cancers (Tiang et al., 2010). Analysis of gene expression profiles of 39 breast cancers showed that NAT1 clustered with expression of the estrogen receptor (ER) (Walker et al., 2009). Studies also revealed the higher expression of NAT1 in luminal carcinomas compared to basal-like carcinomas (Zheng et al., 1999). These reports support the use of NAT1 as a biomarker and potential molecular target for cancers, especially breast cancer.

Studies suggest that NAT1 plays an important role in cell growth and survival, as well as in cell proliferation and cell invasion, which are hallmarks of metastatic cancer (Tiang et al., 2010). When NAT1 was over-expressed in an immortalized breast epithelial cell line, cells showed increased proliferative capacity and the ability to grow in low serum media (Adam et al., 2003). In a RNAi-mediated knock-down study, Tiang et al. (2011) showed that NAT1 knock down in colon adenocarcinoma cells resulted in a marked increase in cell-cell contact growth inhibition, a loss of cell viability at confluence, and an up-regulation of the cell adhesion molecule E-cadherin (Tiang et al., 2011). The human NAT1 gene is overexpressed highly in ER+ breast cancer cells and in invasive ductal and lobular breast carcinomas (Adam et al., 2003) suggesting that NAT1 is important to cancer progression and cancer cell biology, particularly breast cancer. There have been many molecular epidemiological studies

associating NAT1 polymorphisms and increased cancer risk. (Minchin et al., 2007). The close association between NAT1 polymorphisms and risk for cancer suggests a potential clinical benefit of NAT1 inhibition. For example, in comparison with all other NAT1 genotypes the rapid acetylator genotype (*NAT1*10*) was elevated in human bladder (Bell et al., 1995) and breast (Zheng et al., 1999) cancers. These data suggest that NAT1 plays an important role in cancer progression which supports the use of NAT1 as a molecular target for novel cancer therapeutics.

Specific Aims and Hypotheses

This dissertation project encompasses two specific aims. Listed are the specific aims and the hypothesis behind each aim. The following chapters describe the experiments performed to test these hypotheses, the analyses of the results, and conclusions.

Specific Aim I Hypothesis

We hypothesize that xenobiotic-metabolizing enzyme phenotypes (i.e., rapid or slow) and substrate selectivity will impact carcinogen metabolism.

Specific Aim I

To investigate the effects of combinations of human NAT1, human NAT2 haplotypes (*NAT2*4*, *NAT2*5B*, or *NAT2*7B*), and varying CYP1A2 enzymatic activity on carcinogen metabolism in immortalized human fibroblasts.

Specific Aim II Hypothesis

We hypothesize that the inhibition of NAT1 enzymatic activity will reduce carcinogen activation and experimental cancer progression.

Specific Aim II

To identify novel small molecule inhibitors of human NAT1, and to evaluate the effects of inhibition of NAT1 on carcinogen metabolism and experimental cancer initiation and progression.

CHAPTER II

FUNCTIONAL EFFECTS OF HUMAN NAT1, HUMAN NAT2 HAPLOTYPES
(*NAT2*4*, *NAT2*5B*, AND *NAT2*7B*), AND HIGH AND LOW CYP1A2
ENZYMATIC ACTIVITY ON CARCINOGEN METABOLISM

INTRODUCTION

Susceptibility to chronic diseases, such as cancer, involves interactions between genetic variations in the genes of xenobiotic metabolizing enzymes (XMEs) and the environment. The effects of genetic variance on toxicological risk are not fully understood and require further investigation. Environmental arylamine and heterocyclic amine carcinogens are metabolized by XMEs such as arylamine *N*-acetyltransferases (NATs). Two isozymes, NAT1 and NAT2, catalyze the detoxification of aromatic and heterocyclic amines by *N*-acetylation (Hein et al., 2000). NAT1 and NAT2 also catalyze the bioactivation of aromatic and heterocyclic amines. This bioactivation occurs by *O*-acetylation which is preceded by cytochrome P450 hydroxylation (Hein, 2000). The resulting arylamine acetoxy products are capable of spontaneously forming electrophilic arylnitrenium ions that covalently bond to DNA and proteins. These environmental carcinogen-induced DNA adducts can lead to mutagenesis and initiate cancer.

NAT1 and NAT2 are highly polymorphic genes. The polymorphisms result in differences in the rate at which drugs and carcinogens are metabolized.

Polymorphisms in the NAT genes were first discovered after differences in toxicity were seen in patients treated with the anti-tuberculosis drug isoniazid (Hein, 2000). The differences in side effects such as numbness and tingling in the fingers, as well as other progressive damage to the nervous system, were attributed to single nucleotide polymorphisms (SNPs) in the NAT gene. To date over 32 human NAT2 polymorphisms have been identified as rapid, intermediate, and slow acetylator phenotypes. These SNPs determine acetylator phenotype by modifying enzyme function and stability. The functional roles of this family of enzymes have been studied to better understand the association of these polymorphic alleles with cancer risk.

Carcinogens 4-aminobiphenyl (ABP) and 2-aminofluorene (AF) are metabolized by both NAT isozymes, illustrating that both NAT1 and NAT2 play an important role in arylamine carcinogen metabolism (Grant et al., 1990) Exposure to ABP, which is present in tobacco smoke, has been associated with bladder cancer risk (Liu et al., 2008). AF, whose N-acetylated derivative was developed as an insecticide, is associated with mutagenesis (Sugamori et al., 2007). Although some arylamine substrates such as ABP and AF are metabolized by both NAT1 and NAT2, each of the isozymes exhibits substrate specificity (Liu et al., 2007).

In addition to substrate specificity, allelic variations in the NAT2 locus also play an important role in acetylation capacity, metabolic activation, and cancer risk (Hein, 2000). Many studies suggest a relationship between NAT2 slow acetylator phenotype and cancers such as urinary bladder, colorectal,

breast, and lung cancers (Zang et al., 2007). The results of these studies were inconsistent due to several factors including misclassification of smoking or occupational status, a misinterpretation of genotype and phenotype, and limited statistical power (Walker et al., 2009). Acetylator phenotype may increase vulnerability to arylamine induced toxicological outcomes. Functional genomic studies that incorporate effects of acetylator phenotype did not consider other limitations. These study confounders include substrate specificity, genetic variations, and the study of interactions of various XMEs.

In this study, we undertook experiments to assess the intrinsic capacities and substrate specificities of human NAT1 and NAT2 to catalyze the *N*-acetylation of several environmental arylamine and alkylaniline carcinogens. We utilized nucleotide excision repair (NER) - deficient immortalized human fibroblasts to examine the effects of combinations of human NAT1, 3 common human NAT2 haplotypes (*NAT2*4, NAT2*5B*, or *NAT2*7B*), and high and low CYP1A2 enzymatic activity on carcinogen metabolism. These human fibroblasts endogenously express human NAT1, and therefore provide a model to better understand the role that human NAT1 and NAT2 play in carcinogen metabolism. This human cell model also enables us to study NAT1 and NAT1 intrinsic capacities and substrate specificities.

This study investigates the functional effects of altered CYP1A2 activity and *NAT2* haplotypes on carcinogen metabolism, DNA adduct levels, and mutagenesis in NER-deficient Simian Virus 40 (SV40)-transformed human skin fibroblast line GM4429. GM4429 cells were derived from a Caucasian

16

Xeroderma Pigmentosum (XP) complementation group A (XPA) patient exhibiting a delayed onset of neurological disease. These cells are widely used as a model of NER deficiency due to mutation of XPA (States et al., 1996). Simian Virus 40, an oncogenic DNA virus, induces malignant transformation and causes a loss of cell cycle checkpoint control (States et al., 1996). The large T-antigen of the SV40 virus accomplishes abrogation of the cell cycle checkpoint by sequestering p53 which stops both G1 and G2 checkpoints (States et al., 2002).

This study determines the specificity constants of recombinant human NAT1 and NAT2 for seven arylamine carcinogens benzidine, ABP, AF, 2,5-DMA, 3,4-DMA, 3,5-DMA, and 3-EA. Here we provide new insight into the metabolic detoxification of persistent environmental carcinogens by arylamine *N*-acetyltransferase *N*-acetylation.

MATERIALS AND METHODS

Cells and Culture Conditions

A clone of SV40-transformed human skin fibroblasts (GM4429) was the kind gift of Dr. J. Christopher States. GM4429 cells express endogenous NAT1, and are nucleotide excision repair deficient (NIGMS Human Mutant Cell Repository, Coriell Institute, Camden, NJ). Cells were cultured in alpha modification of minimal essential media (Cambrex, Walkersville, MD) supplemented with 10% fetal bovine serum (Hyclone, Logan, UT), 100 U/mL penicillin (Lonza), 100 U/mL streptomycin (Lonza), and 2 mM L-glutamine (Lonza) at 37°C in 5% CO_2. Culture media was supplemented with appropriate selective agents (hygromycin and geneticin) to maintain stable transfectants.

Stable Transfection

Stable transfections were carried out in GM4429 fibroblasts using the Flp-In system (Invitrogen) as described previously in CHO cells by Metry et al., (2007). These cells were transfected with the pFRT/_lacZeo_ plasmid resulting in a single integrated FRT site. Cells were split 24 h after transfection and treated with medium supplemented with Zeocin (200 µg/mL) 48 h after transfection, for selection according to the manufacturer's protocol. Zeocin – resistant clones were picked with cloning cylinders. The cell lines with a single intergrated FRT site determined by real-time polymerase chain reaction (PCR) and Southern blot screening were selected for additional transfection. The pIRES plasmid containing cDNAs of human _CYP1A2_ and NADPH-cytochrome P450 reductase

gene (Invitrogen), was transfected into the newly constructed GM4429-FRT cell line using Effectene Transfection Reagent kit (Qiagen). Geneticin-resistant clones were isolated using cloning cylinders. Human *NAT2* alleles (*NAT2*4*, *NAT2*5B*, or *NAT2*7B*) were transfected using the pcDNA5/FRT plasmid and co-transfected with pOG44 (Invitrogen), a Flp recombinase expression plasmid, into GM4429-FRT-CYP1A2 cells. Stably transfected cells were selected by geneticin and hygromycin resistance.

NAT mRNA expression (Taqman Quantitative RT-PCR Assays)

TaqMan assays were used to assess levels of *NAT1 and NAT2* mRNA expressed in each cell line. TaqMan Universal Master Mix (Applied Biosystems, Foster City, California, USA), primers and probes, 96 well optical plates and caps were used. Synthesis of first strand cDNA were carried out using Superscript III ReverseTranscriptase (Invitrogen) following the manufacturer's protocol using 1 µg of DNase-treated total RNA. PCR with 1x final concentration of TaqMan Universal Master Mix, 300 nM of each primer and 100 nM of probe in 20 µl were performed using Applied Biosystems StepOnePlus Real-Time PCR Systems (Applied Biosystems). For quantitative RT-PCR of *NAT1* (Husain et al, 2007a) and *NAT2* (Husain et al., 2007b), forward primer and reverse primer were used with TaqMan probe.

NAT1 Genotyping

DNA was extracted from human fibroblast samples using the "Qiagen DNA Purification kit" (Qiagen, Valencia. CA). NAT1 genotype was determined as previously described (Doll and Hein, 2002). Briefly, *NAT1* amplification was carried out in an Applied Biosystems StepOnePlus Real-Time PCR Systems with two initial hold steps (50 °C for 2 min., followed by 95 °C for 10 min.) and 40 thermocycles of a two-step PCR: 92°C for 15 s, 60° C for 1min. The fluorescence intensity of each sample was measured to monitor amplification of the NAT1 gene. Primers, probes, and DNA were added to final concentrations of 300 nM, 100 nM, and 0.5 -2.5 ng/μl, respectively.

Measurement of Cytochrome P450 (CYP1A2) Activity

Whole cells from geneticin-resistant clones were assayed for CYP1A2 activity. Whole cell samples were assayed for 7-ethoxyresorufin *O*-deethylase activity by fluorimetric determination as described by Bendaly et al., (2007). This reaction was conducted in a 96-well plate, containing 1 million cells in 10 μL of PBS with 5 mM glucose and 5 μM 7-ethoxyresorufin. The reaction was incubated at 37°C for 10 minutes. Resorufin formation was measured by fluorescence at emission wavelength of 585 nm and excitation wavelength of 530 nm. Cell lines exhibiting similar 7-ethoxyresorufin *O*-deethylase activity comparable to the parent cell line (GM4429) were utilized for additional characterization and study.

Measurement of N-Acetyltransferase Activity (in vitro)

N-acetylation of the NAT1 specific substrate para-aminobenzoic acid (PABA), the NAT2 specific substrate sulfamethazine (SMZ), and selected arylamines 4- aminobiphenyl (ABP), 2-aminofluorene (AF), benzidine, 2,5-dimethylaniline (2,5-DMA), 2,6-dimethylaniline (2,6-DMA), 3,4-dimethylaniline (3,4-DMA), 3,5-dimethylaniline (3,5-DMA), and 3-ethylaniniline (3-EA) were measured using in vitro assays, and acetylated products were separated utilizing reverse phase high performance liquid chromatography (HPLC). Reactions were prepared with acetyl- coenzyme A (1 mM), substrates (300 μM), and 50 μL cell lysate and incubated at 37°C for 10 min. Reactions were stopped by adding 1/10 volume of 1 M acetic acid and centrifugation at 15,000g for 10 min. Reaction products in the resulting supernatant were separated by reverse-phase HPLC. HPLC separation for sulphamethazine NAT2 assays was achieved on a C18 LiChrospher® 125x4mm column using a gradient 91:9 sodium perchlorate (pH 2.5) / acetonitrile to 71:29 sodium perchlorate (pH 2.5) / acetonitrile over 5 min at 260 nm. HPLC separation for p-aminobenzoic acid NAT1 reactions was achieved using a gradient 96:4 sodium perchlorate (pH 2.5)/ 88:11acetonitrile at 280nm (Hein et. al., 2006). HPLC separation for 2,6-DMA, 3,5-DMA, and 3-EA was achieved using 50:50 acetonitrile and 0.01M potassium phosphate buffer (pH 5) at 1 ml/min at 210 nm (Martin et al., 1996).

N-acetylation Activity (in situ)

In situ N-acetylation activity was measured in whole cell assays using human fibroblasts, grown to confluency in culture medium supplemented with substrates PABA, SMZ, ABP, AF, benzidine, 2,5-DMA, 2,6-DMA, 3,4-DMA, 3,5-DMA, or 3-EA. The cells were incubated at 37°C and media was collected after 4h, 1/10 volume of 1 M acetic acid was added, and the reaction was centrifuged at 13,000g for 10 min. The supernatant was analyzed on the reverse phase HPLC column and the N-acetyl substrate was separated and quantitated as described above.

Glutathione S-Transferase (GST) Activity

GST activity was measured in human fibroblast lysate using the substrate 1-chloro-2,4-dinitrobenzene (CDNB). A solution of 100 mM potassium phosphate buffer pH 6.5 (980 µl), 200 mM glutathione (10 µl, Sigma Aldrich), and 100 mM CDNB (10 µl, Sigma Aldrich) was added to a 1 ml quartz cuvette and mixed. Sample lysate was added to the quartz cuvette containing the substrate solution. The absorbance was read at 340 nm on a spectrophotomer every 30 seconds over a period of 5 minutes after a lag time of 1 minute. The increase in absorbance is directly proportional to total GST activity. The GST specific activity was calculated using the following equation:

$[\Delta A_{340}/\text{minute (background)} - \Delta A_{340}/\text{minute (sample)}] / [A^m \text{ (CDNB extinction coefficient)} \times \text{mg protein added}] = X \text{ nmol/min/mg protein}$

Determination of Michaelis Menten Constants towards human NAT1 and NAT2

Kinetic parameters for ABP, AF, benzidine, 2,5-DMA, 2,6-DMA, 3,4-DMA, 3,5-DMA, and 3-EA were determined using lysates of yeast that stably express human NAT1 or human NAT2. *N*-acetylation reactions were conducted as described above, but using 0 – 1000 µM substrate. Data were fit to the Michaelis-Menten equation and apparent kinetic parameters were determined using GraphPad Prism 5 (GraphPad Software, San Diego, CA).

Measurement of O-acetyltransferase Enzymatic Activity

N-hydroxy-4-aminobiphenyl (N-OH-ABP) *O*-acetyltransferase activity was evaluated using reverse phase HPLC as described by Hein et al. (2006). Briefly, reaction mixtures containing 100 µg total protein, 1 mg/mL deoxyguanosine (dG), 100 µM *N*-OH-ABP, and 1 mM acetyl coenzyme A were incubated at 37°C for 10 min. Reactions were stopped with the addition of 100 µL of water saturated ethyl acetate and centrifuged for 10 minutes at 13, 000 g. The organic phase was removed, evaporated to dryness, and re-suspended in 100 µM of 10% acetonitrile. HPLC separation was achieved using 80:20 sodium perchlorate (pH 2.5): acetonitrile over 3 minutes to 50:50 sodium perchlorate (pH 2.5)/acetonitrile. dG-C8-ABP adducts were detected by absorbance at 300 nm.

DNA Isolation and DNA Adduct Quantitation

DNA adduct levels were measured as previously described in our laboratory (Metry et al., 2007). DNA was isolated from cells grown in 10 cm plates treated with ABP, AF, 2,6-DMA, 3,5-DMA, or 3-EA. ABP was used as a positive control in the present study. Cells were harvested after 48 h and incubated in 50 μl of 10% SDS and 20 μg/ml proteinase K for 45 min at 37 °C. DNA was extracted by phenol:chloroform:isoamyl alcohol (25:24:1) and precipitated using cold isopropanol and centrifuged for 1 min. Supernatant was removed and the pellet washed with ethanol, dried, and resuspended in buffer containing 5 mM Tris HCl, 1 mM $CaCl_2$, 1 mM $MgCl_2$, and 1 mM $ZnCl_2$. DNA was quantified at A_{260}.

DNA samples were treated with 10 units DNAase I (US Biological, Swampscott, MA) for 1 h at 37°C and 1 unit nuclease P1 (US Biological) for 6 h, followed by overnight treatment with 5 units of alkaline phosphatase (Sigma). Two volumes of acetonitrile were added to stop the reaction. Samples were filtered using a 5,000 nominal molecular weight limit centrifugal filter device (Millipore, Bedford, MA) and were concentrated to 50 μL. DNA samples were reconstituted in 5% acetonitrile to a final volume of 100 μL. Samples were submitted for LC-MS-MS analysis to the University of Louisville Biomolecular Mass Spectrometry Core Facility. Samples used for quantitative analysis were spiked with 1 ng deuterated internal standard (dG-C8-ABP-d5) before any sample treatment. The samples were reconstituted with 25 μL 5% ACN in 2.5 mM NH_4HCO_3 just before analysis and 5 μL of the sample was analyzed by

nanoAcquity Ultra High Performance Liquid Chromatography (UPLC) (Waters, Milford, MA) coupled with a LTQ-Orbitrap XL mass spectrometer (Thermo Scientific, San Jose, CA). Samples were loaded onto a C18 micro-precolumn cartridge (LC Packings, Thermo Scientific, San Jose, CA) and separated with an in-house packed C18 capillary column (125 mm × 75 μ m × 5 μm). A 15 min binary solvent gradient (Solvent A: 0.1% formic acid and Solvent B: ACN/0.1% formic acid) at 400 nL/min was used. The gradient started from 10% Solvent B, increased linearly to 80% Solvent B in 10 min, and then remained at 80% B for 5 min. The eluates were ionized with a nanospray source and dG-C8-ABP and dG-C8-ABP-d5 were detected with linear ion trap using the transitions of m/z 435.2 to m/z 319.2 (dG-C8-ABP) and m/z 440.2 to m/z 324.2 (dG-C8-ABP-d5). Amounts of dG-C8-ABP were calculated from peak areas of dG-C8-ABP and dG-C8-ABP-d5 with a calibration curve from dG-C8-ABP and dG-C8-ABP-d5 standards.

Assays for Mutagenesis at the Hypoxanthine Phosphoribosyl Transferase (HPRT) Locus

To evaluate mutagenesis at the *HPRT* locus we employed methods previously used in our lab (Metry et al., 2007). Cells were grown for 12 doublings, with selective agents in complete HAT medium (30 μM hypoxanthine, 0.1 μM aminopterin, and 30 μM thymidine). After which cells were grown in the prescence of ABP (0 – 500 μM). Survival was determined by colony forming assay and expressed as percent of vehicle control. The remaining cells were re-plated and sub-cultured. After 7 days of growth, cultures were plated for cloning

efficiency in complete media and for mutations in complete medium containing 40 µM 6-thioguanine (6-TG) (Sigma). Ten dishes were seeded with 1 x 10^5 cells /100 mm and incubated for 7 days; cloning efficiency dishes were seeded with 100 cells/ well/ 6-well plate and incubated for 6 days.

RESULTS

Stable Transfections: CYP1A2 EROD Activity, NAT1 mRNA Expression, and Endogenous NAT1 genotype.

We constructed NER-deficient SV40-transformed human fibroblast cells that stably express human NAT2 alleles (*NAT2*4*, *NAT2*5B*, or *NAT 2*7B*) and human CYP1A2, using the Flp-In system (Invitrogen, Carlsbad, CA) as described in the methods. No significant differences (p>0.05) in CYP1A2 7-ethoxyresorufin oxidation catalytic activity were observed between GM4429/CYP1A2 cells and the clones of cells further transfected with *NAT2* alleles (Figure 2.1). No significant (p>0.05) differences in relative NAT1 mRNA levels were observed among all cell lines (Figure 2.2). The NAT1 genotype of GM4429 cells was *NAT1*4/*4*.

PABA and SMZ N-Acetylation and NAT2 mRNA Expression Following Stable Transfections

p-Aminobenzoic acid (PABA) is a NAT1-selective substrate. No significant difference (p>0.05) in PABA *N*-acetylation activity was observed among the NAT2-transfected GM4429 cells lines (Figure 2.2). Sulfamethazine (SMZ) is a NAT2-selective substrate. All *NAT2* -transfected cells had significantly higher (P<0.01) SMZ *N*-acetylation activity than the cell lines not transfected with NAT2 expression constructs (Figure 2.3). SMZ *N*-acetylation activity in the cell lines transfected with the *NAT2*4* allele was found to be thirty-five-fold higher than in cell lines not transfected with NAT2 expression constructs. Lysates collected

from cells transfected with *NAT2*5B* and *NAT2*7B* showed significantly lower SMZ *N*-acetylation activity when compared to lysates of cells transfected with the reference allele *NAT2*4* ($p<0.001$). Activity in GM4429 cells not transfected with *NAT2* were below the level of detection for SMZ *N*-acetyltransferase (<0.15 nmoles/min/mg). No significant ($p>0.05$) difference in relative NAT2 mRNA levels were observed among all NAT2-transfected cell lines (Figure 2.3.).

Apparent Michaelis-Menten Kinetics

As seen in Table 1, recombinant human NAT1 had the highest reaction velocity for the *N*-acetylation of benzidine, AF, and 3,4-DMA. Apparent intrinsic activities (V_{max}/K_m) of recombinant human NAT1 for the selected substrates were in the order of benzidine>3,4-DMA>AF>ABP>3-EA>3,5-DMA>2,5-DMA. Recombinant human NAT1 had much lower affinity (higher K_m) for the tested compounds compared to human NAT2, and catalyzed the *N*-acetylation of these compounds at a much higher rate.

As seen in Table 2.1, recombinant human NAT2 had the highest velocity for the *N*-acetylation of 3,4-DMA, 3,5-DMA, and ABP. Apparent intrinsic activities (V_{max}/K_m) of recombinant human NAT2 were 3,5-DMA>3-EA>AF>ABP> AF> benzidine >3,4-DMA > 2,5-DMA. Despite having a high affinity (lower K_m) for the tested compounds recombinant human NAT2 catalyzed the *N*-acetylation of these compounds at a much slower rate that recombinant human NAT1. Recombinant human NAT2 specificity constants for these compounds were in

the order of 3,5-DMA>2,5-DMA>3-EA>ABP>AF>3,4-DMA,>benzidine. Neither NAT1 nor NAT2 catalyzed the N-acetylation of 2,6-DMA at detectable levels.

N-Acetyltransferase Activity In Human Fibroblast Lines Following Transfections

Lysates collected from NAT2-transfected and non-transfected cells showed no significant difference ($p > 0.05$) in N-acetylation of benzidine, 3,4-DMA, and AF (Figure 2.4). Lysates collected from cells transfected with NAT2*4, NAT2*5B and NAT2*7B showed significantly higher ($p < 0.01$) N-acetylation of 3,5-DMA, 2,5-DMA, 3-EA, and ABP when compared to cells not transfected with NAT2 (Figure 2.5). Lysates collected from cells transfected with NAT2*5B and NAT2*7B showed significantly ($p < 0.01$) lower N-acetylation 3,5-DMA when compared to lysates from cells transfected with the reference allele NAT2*4.

High and Low CYP1A2 EROD Activity in Human Fibroblast Cell Lines Following NAT2 Transfections

In order to evaluate the effects of varying (high or low) CYP1A2 activity on N-acetylation of environmental carcinogens, we confirmed the construction of NER-deficient SV40-transformed human fibroblast cell lines that stably express human NAT2 alleles (NAT2*4, NAT2*5B, or NAT2*7B) and varying human CYP1A2 activity. Cell lines that are designated "low CYP1A2" had significantly lower ($p < 0.05$) EROD activity than the cell lines designated "high CYP1A2" (Figure 2.6). EROD activity in cell lines expressing alleles NAT2*4, NAT2*5B, and NAT2*7B having high CYP1A2 activity were 3, 5, and 8-fold higher than cell

lines with the corresponding NAT2 allele and low CYP1A2 activity, respectively. Cell lines transfected only with CYP1A2 had 12-fold higher EROD activity than the null cell line.

Glutathione S-transferase (GST) Activity

GST is a human phase II cytosolic xenobiotic metabolizing enzyme that performs detoxification of carcinogens and other environmental pollutants. Lysates collected from our transfected cell lines showed no significant difference ($p > 0.05$) in glutathione S-transferase activity (Figure 2.7).

In situ PABA and SMZ N-acetylation Activity in Human Fibroblast Lines with High and Low EROD Activity Following NAT2 Transfections

As shown in Figure 2.8A, no significant difference ($p>0.05$) in PABA N-acetylation in situ activity was observed among the GM4429 cells lines. All NAT2 -transfected cells had significantly higher ($P<0.01$) SMZ N-acetylation in situ activity than the non-transfected cell lines (Figure 2.8B). SMZ N-acetylation in situ activity in the cell lines transfected with the NAT2*4 allele was found to be significantly higher ($p<0.05$) than in cells transfected with NAT2*5B and NAT2*7B. Activity in GM4429 cells not transfected with NAT2 was non-detectable.

N-acetyltransferase Activity in Human Fibroblast Lines with High and Low CYP1A2 Activity

When measuring benzidine (a NAT1 selective substrate) N-acetylation at 20 µM substrate, no significant differences ($p > 0.05$) were observed when comparing cells lines with high or low CYP1A2 activity and the same NAT2 allele (i.e., HighCYP1A2/ NAT2*4 vs. LowCYP1A2/NAT2*4). No significant differences ($p > 0.05$) in benzidine N-acetylation activity were observed between GM4429/CYP1A2 cells and cell lines further transfected with NAT2 (Figure 2.9A). At 200 µM substrate, when comparing the same allele and high or low CYP1A2 enzymatic activity, N-acetylation in HighCYP1A2/NAT2*4 cells was significantly higher ($p < 0.05$) than that of LowCYP1A2/NAT2*4 cell lines (Figure 2.9b). HighCYP1A2/NAT2*7B cells had significantly lower ($p < 0.05$) benzidine N-acetylation activity than LowCYP1A2/NAT2*7B cells. CYP1A2 cells had significantly lower ($p < 0.05$) benzidine N-acetylation activity that the null cell line (Figure 2.9b).

At 20 µM substrate, 3,5-DMA N-acetylation in HighCYP1A2/ NAT2*4 cells was significantly higher ($p < 0.05$) than other cell lines. LowCYP1A2/NAT2*4 cells had significantly lower ($p < 0.05$) N-acetylation when compared to HighCYP1A2/NAT2*4 cells. 3,5-DMA N-acetylation with high CYP1A2 activity and NAT2 alleles NAT2*7B and NAT2*5B was significantly lower ($p < 0.05$) than in cell lines with same allele and lower CYP1A2 activity. When comparing cells transfected with only CYP1A2, N-acetylation was significantly lower ($p < 0.05$) when compared to the null cell line (Figure 2.10a). At 200 µM, no significant

differences (p>0.05) were observed when comparing cell lines that have the same NAT2 allele and high or low CYP1A2 activity. N-acetylation activity for CYP1A2 cell lines was significantly lower (p<0.05) than the null cell line (Figure 2.10b).

At an ABP concentration of 20 µM, ABP N-acetylation activities in GM4429 cells with high CYP1A2 activity and NAT2 alleles NAT2*4, NAT2*5B, and NAT2*7B were significantly higher (p<0.05) when compared to cells transfected with only CYP1A2. ABP N-acetylation was significantly lower (p>0.05) in cells transfected with NAT2*4 with low CYP1A2 activity when compared to HighCYP1A2/NAT2*4 cells. ABP N-acetylation was significantly lower (p<0.05) in NAT2*5B/HighCYP1A2 and CYP1A2 when compared to LowCYP1A2/NAT2*5B and null cell lines, respectively (Figure 2.11A).

At an ABP concentration of 200 µM, ABP N-acetylation was significantly lower (p<0.05) in GM4429 cells transfected with CYP1A2 only compared to the null cell line and in HighCYP1A2/NAT2*5B cells compared to LowCYP1A2/NAT2*5B cells. ABP N-acetylation was significantly lower (p<0.05) in cells transfected with CYP1A2 only when compared to cell transfected with NAT2.

N-hydroxy-ABP O-Acetylation, Cytotoxicity, HPRT Mutants, and dG-C8-ABP Adducts

There were no significant differences (p>0.05) in N-hydroxy-ABP O-acetyltransferase activity observed among the non-transfected and NAT2-transfected cell lines (Figure 2.12). Upon treating cells with ABP, as described in

the methods, cytotoxicity, *HPRT* mutants, and ABP-induced dG-C8-ABP adducts were not detected.
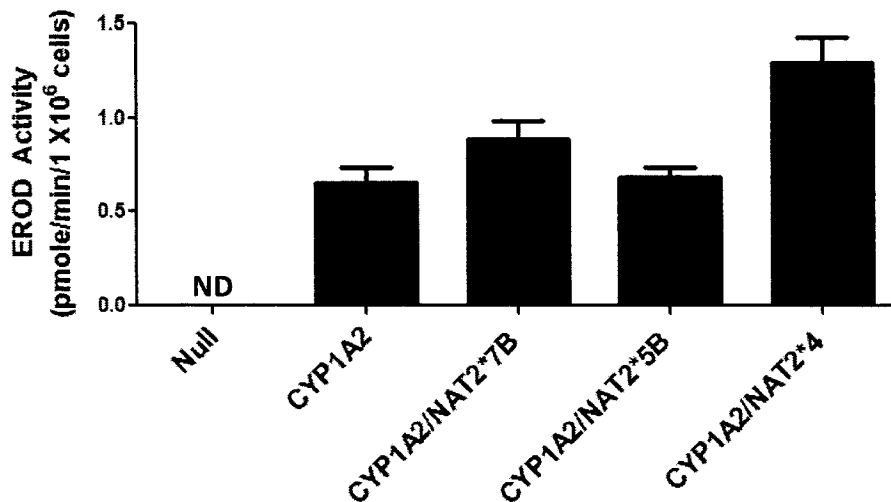
Figure 2.1 CYP1A2 EROD activity in NER-Deficient SV40-transformed GM4429 cells. Each bar represents mean ± SEM for 3 experiments determining 7-ethoxyresorufin-O-deethylase (EROD) activity (pmoles/min/1x10^6 cells) in NER-deficient SV40-transformed GM4429 cells stably transfected with human CYP1A2 and human NAT2 alleles. No significant difference in EROD activity was observed among transfected cells using one-way ANOVA analysis (p > 0.05) EROD activity in non-transfected cells was below the limit of detection (<0.05 pmoles/min/1x10^6 cells). ND, nondetectable
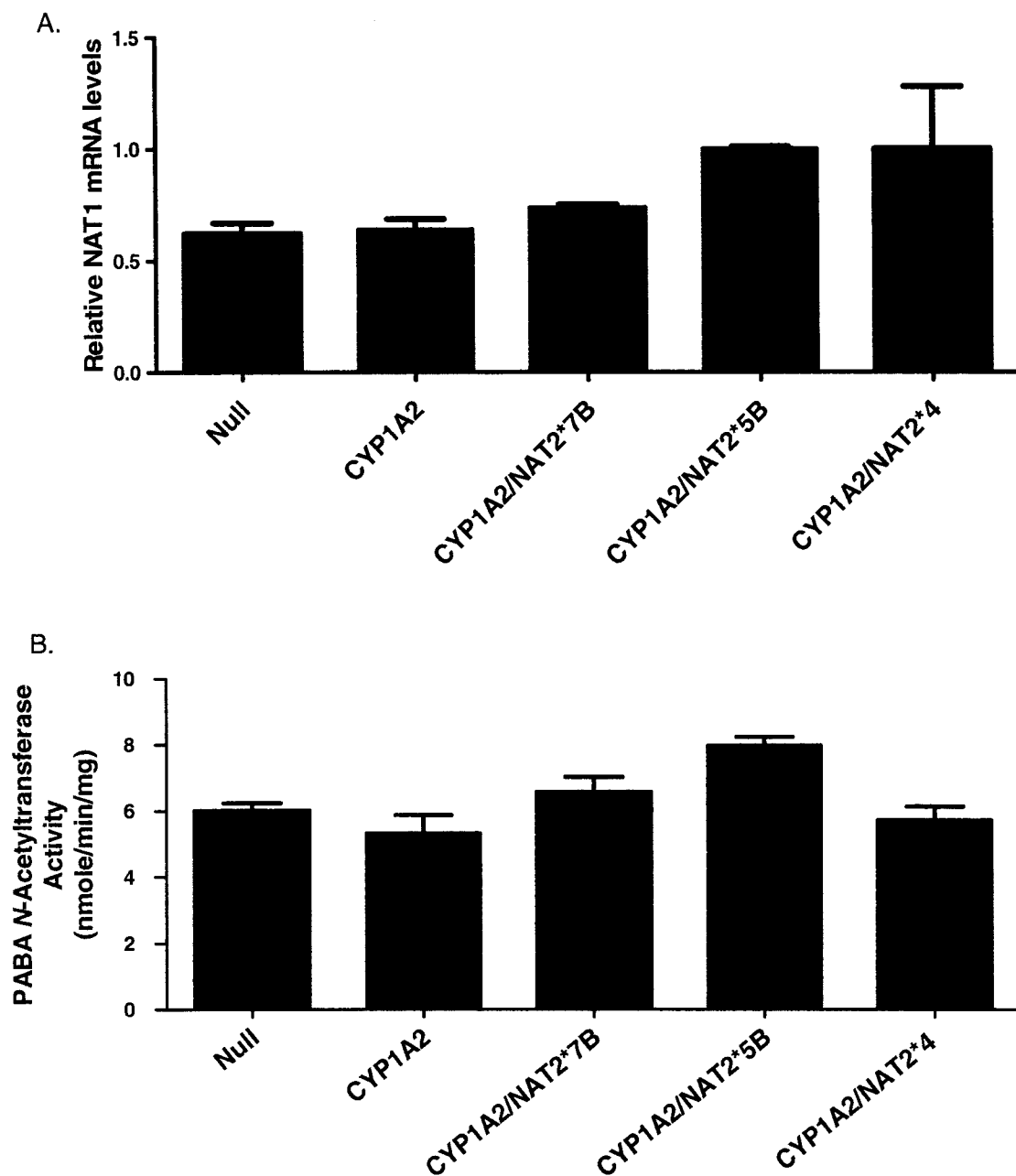
Figure 2.2 Relative NAT1 mRNA and PABA N-acetyltransferase activity in NER-deficient SV40 transformed GM4429 cells stably transfected with human CYP1A2 and human NAT2 alleles. No significant difference in relative NAT1 mRNA levels was observed among non-transfected and transfected cells using one-way ANOVA ($p > 0.05$)   No significant difference in PABA N-acetylation was observed among all GM4429 cells lines using one-way ANOVA ($p > 0.05$). Each bar represents mean $\pm$ SEM for 3 experiments.
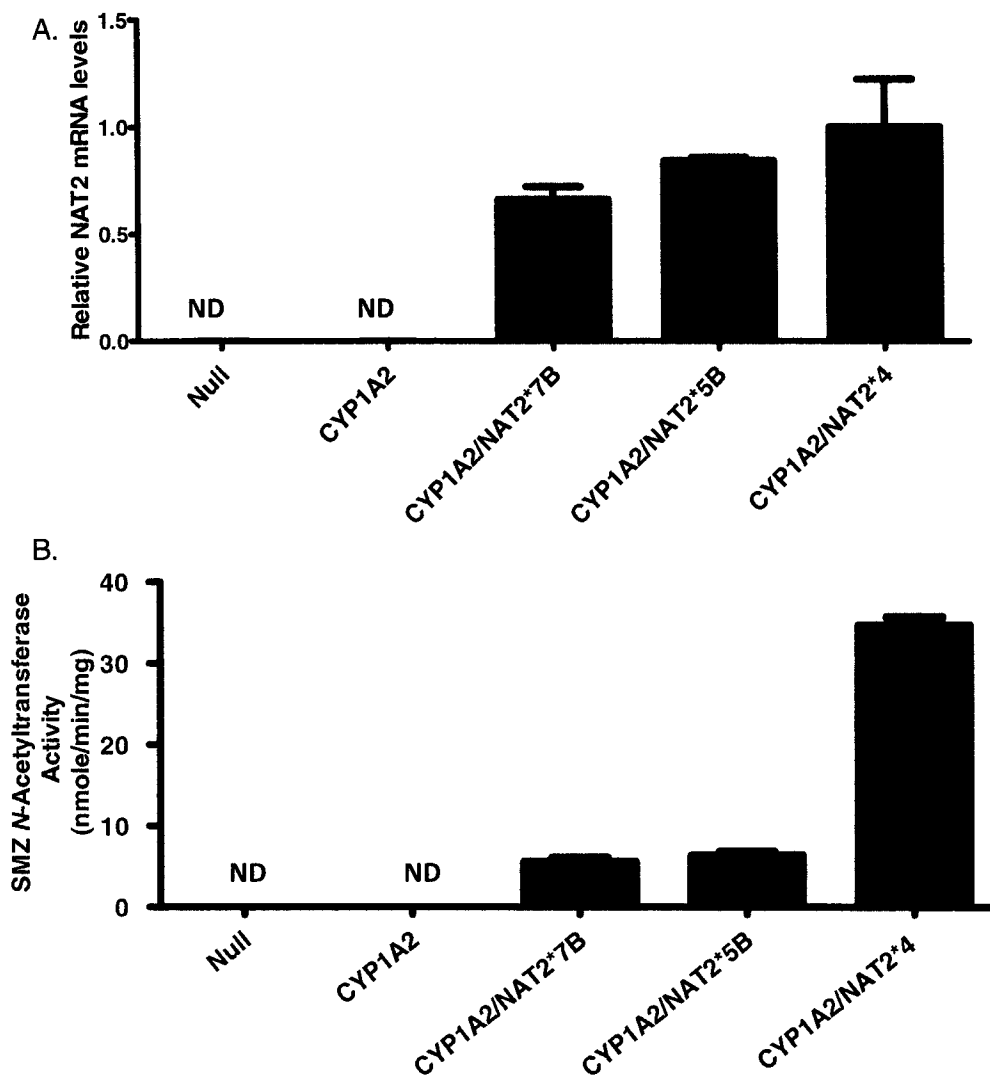
Figure 2.3 Relative NAT2 mRNA and SMZ N-acetyltransferase activity in NER-deficient SV40 transformed GM4429 cells stably transfected with human CYP1A2 and human NAT2 alleles. No significant difference in relative NAT2 mRNA levels was observed among transfected cells using one-way ANOVA (p > 0.05). All NAT-transfected cells had significantly higher SMZ N-acetylation activity than the non-transfected cells. Lysates collected from cells transfected with *NAT2*5B* and *NAT2*7B* showed significantly lower SMZ N-acetylation activity when compared to cell extracts transfected with the reference allele NAT2*4 using one-way ANOVA followed by Bonferroni posttest (p<0.001). SMZ N-acetyltransferase activity of non-transfected GM4429 cells was below the level of detection (<0.15nmoles/min/mg protein). Each bar represents mean ± SEM for 3 experiments determining SMZ NAT activity and NAT2 mRNA levels in NER-deficient SV40-transformed GM4429 cells stably transfected with human *CYP1A2* and human *NAT2* alleles.

	NAT1			NAT2			
Compound	$V_{max,app}$	$K_{m,app}$	$V_{max,app}/K_{m,app}$	$V_{max,app}$	$K_{m,app}$	$V_{max,app}/K_{m,app}$	Specificity Constant
	(nmoles·min⁻¹·mg⁻¹)	(µM)	(ml·min⁻¹·mg⁻¹)	(nmoles·min⁻¹·mg⁻¹)	(µM)	(ml·min⁻¹·mg⁻¹)	
PABA	11586 ± 258	984 ± 79.7	11.8 ± 1.9	ND			
Benzidine	8067 ± 488	953 ± 98.1	8.46 ±1.0	7.86 ± 0.28	95.7 ± 48.4	0.85 ± 0.0	9.95
3,4 -DMA	883 ± 48.6	667± 56.4	1.32 ± 0.14	29.8±1.75	66.9 ± 12.1	0.45 ± 0.19	2.93
AF	8617 ± 4120	3270 ± 195	2.63 ± 0.52	19.8±0.6720	20.5 ± 3.1	0.97 ± 0.1	2.71
ABP	159 ± 8.7	499.8 ± 56.6	0.32 ± 0.04	20.7 ± 0.10	23.7 ± 4.9	0.87 ± 0.2	0.37
3-EA	169 ± 67.4	1281 ± 79.3	0.13 ± 0.05	19.8±0.67	20.5 ± 3.07	0.97 ± 0.15	0.13
2,5-DMA	147 ± 56.3	10543 ± 4365	0.01 ± 0.004	7.85 ± 0.28	39.6 ± 5.6	0.20 ± 0.03	0.05
3,5- DMA	469 ± 251	2800 ± 1918	0.02 ± 0.01	23.9 ± 1.39	14.0 ± 3.84	1.70 ± 0.48	0.01
SMZ	ND			53.8 ± 5.9	34.7 ± 2.3	1.55 ± 0.2	
2,6-DMA	ND			ND			

Table 2.1 Michaelis-Menten constants towards human NAT1 and NAT2 recombinantly expressed in yeast. Results represent mean ± SEM for three experiments. N-acetylation of 2,6-DMA was not detectable. ND represents activity below the limit of detection, <0.15 nmole/min/mg.
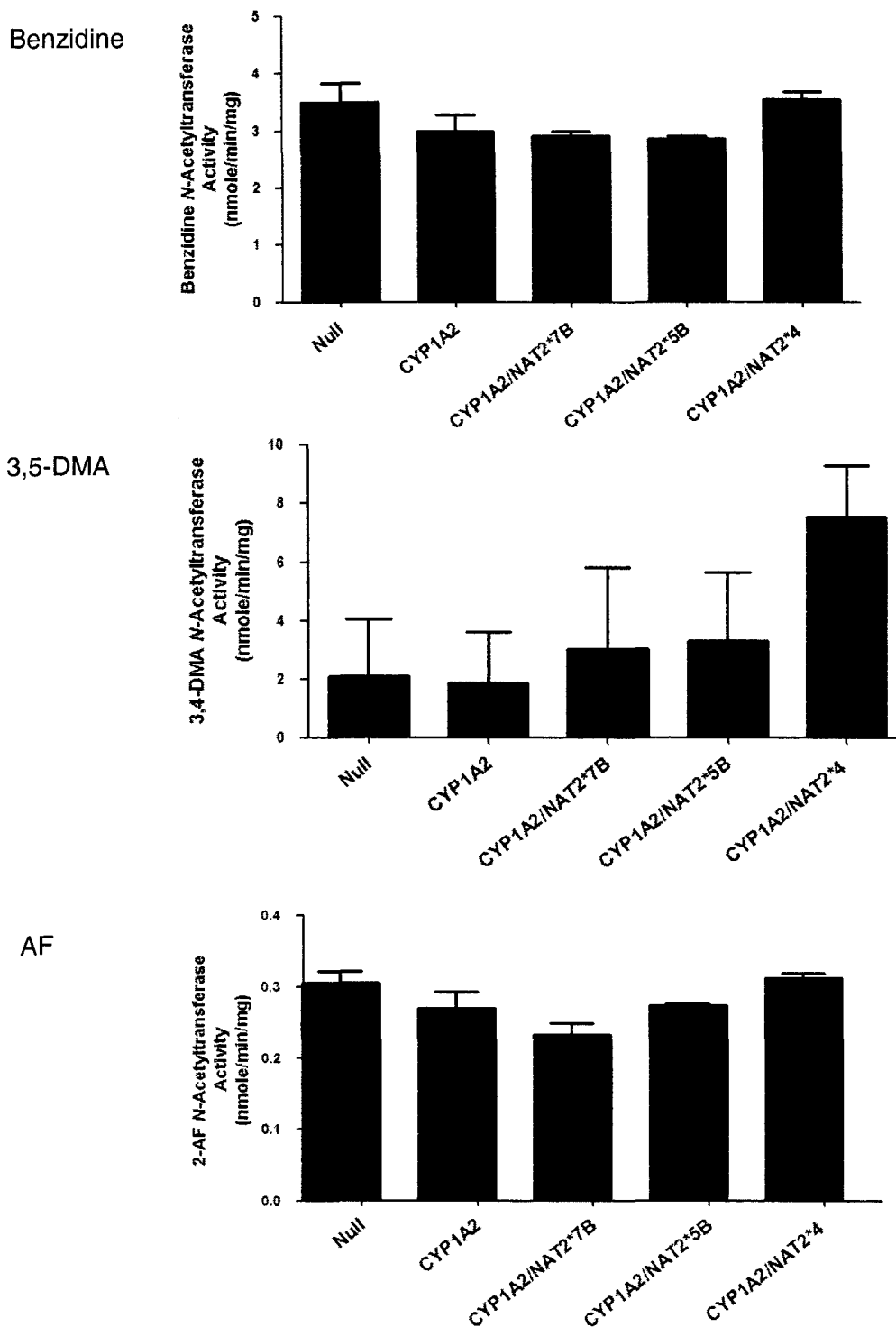
Figure 2.4 N-acetylation of NAT1 selective compounds in cell lysates of immortalized human fibroblasts stably transfected with human CYP1A2 and human NAT2 alleles. No significant difference in N-acetylation activity was observed among cell lines using one-way ANOVA ($p > 0.05$). Each bar represents mean ± SEM for 3 experiments.
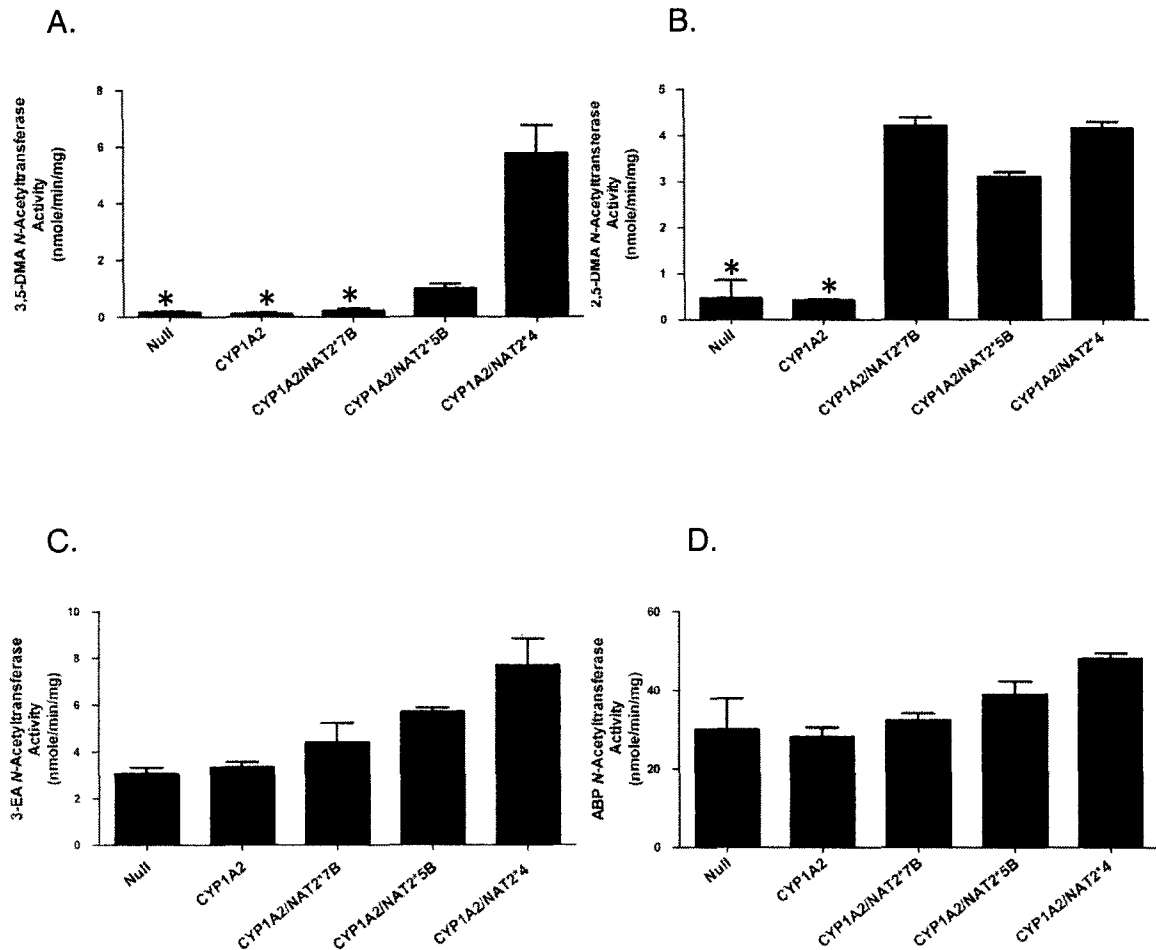
Figure 2.5 N-acetylation of NAT2 selective compounds in cell lysates of immortalized human fibroblasts. (**A.**) 3.5-DMA N-acetylation in non-transfected cells and cells transfected with NAT2*5B and NAT2*7B was significantly lower than cells expressing the reference allele NAT2*4 denoted by * P < 0.05 ; (**B.**) 2,5-DMA, (**C.**) 3-EA, and (**D.**) ABP N-acetylation in in non-transfected cells was significantly lower than cells expressing the reference allele NAT2*4 denoted by * P < 0.05 following one-way ANOVA. Each bar represents mean ± SEM for 3 experiments.
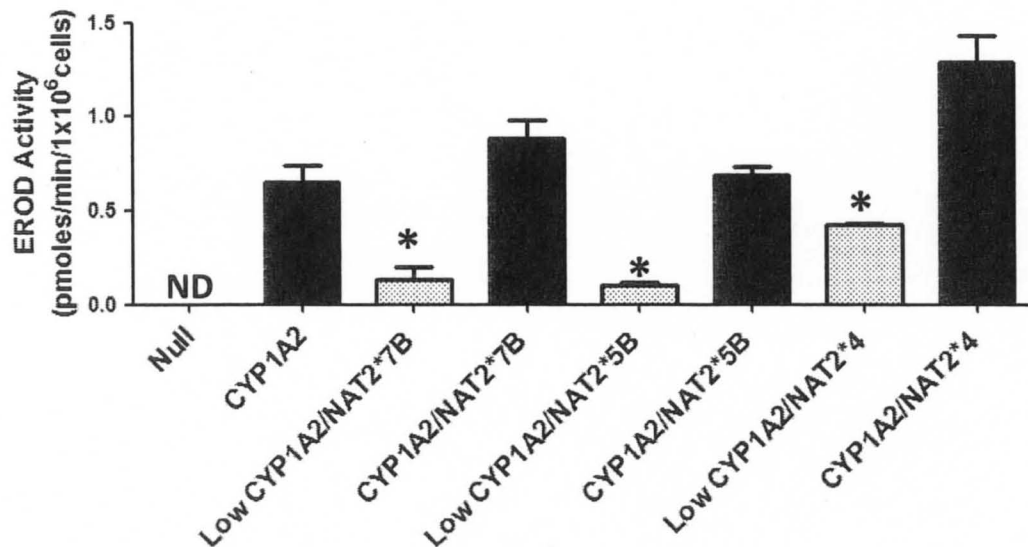
Figure 2.6 EROD activity in cells from selected immortalized human fibroblast clones. Each bar represents mean ± SEM for 3 experiments determining 7-ethoxyresorufin-O-deethylase (EROD) activity (pmoles/min/1×10^6 cells). Cell lines with low CYP1A2 activity had significantly lower enzymatic activity when compared to cells transfected with the same allele but high CYP1A2 activity as denoted by *$P<0.01$ using one-way ANOVA analysis followed by Bonferroni posttest. EROD activity in non-transfected cells was below the limit of detection (<0.05 pmoles/min/1×10^6 cells) as denoted by ND (not detected).
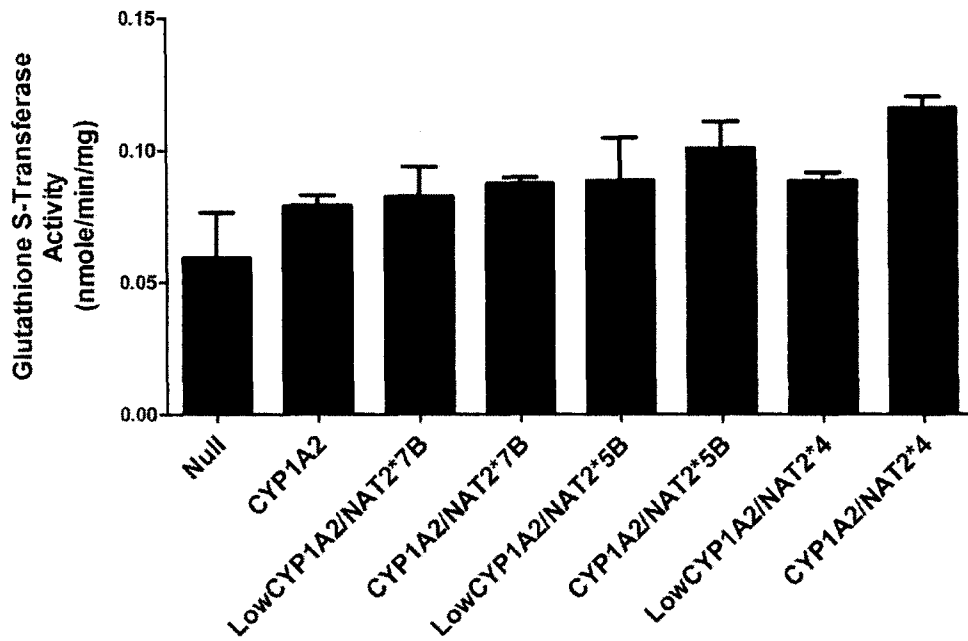
Figure 2.7 Glutathione S-Transferase activity in cell lysates of SV40-transformed human fibroblasts stably transfected with human CYP1A2 and human NAT2 alleles. No significant difference in GST activity was observed among all GM4429 cells lines using substrate1-chloro-2,4-dinitrobenzene (CDNB) as determined one-way ANOVA ($p > 0.05$). Each bar represents mean ± SEM for 3 experiments.
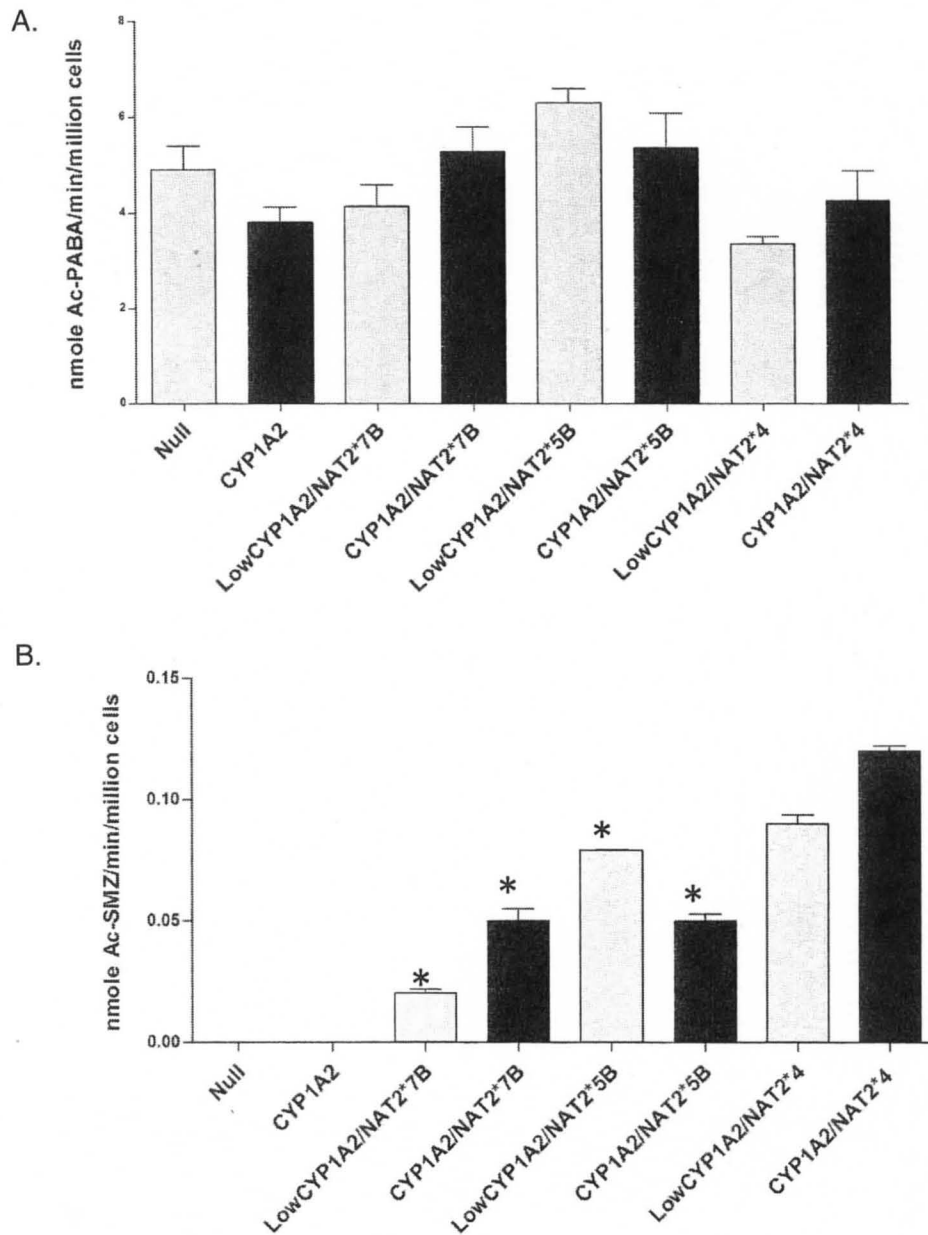
Figure 2.8 *In situ N*-acetylation of PABA (A.) and SMZ (B.) in cells from selected immortalized human fibroblast clones. No significant difference in PABA *N*-acetylation activity was observed among cell lines using one-way ANOVA analysis (p > 0.05). Non NAT2-transfected cells and NAT2 –transfected cells expressing *NAT2*5B* and *NAT2*7B* had significantly lower SMZ *N*-acetylation activity than the reference allele *NAT2*4* as denoted by * P<0.01 using one-way ANOVA followed by Bonferroni posttest. Each bar represents mean ± SEM for 3 experiments.
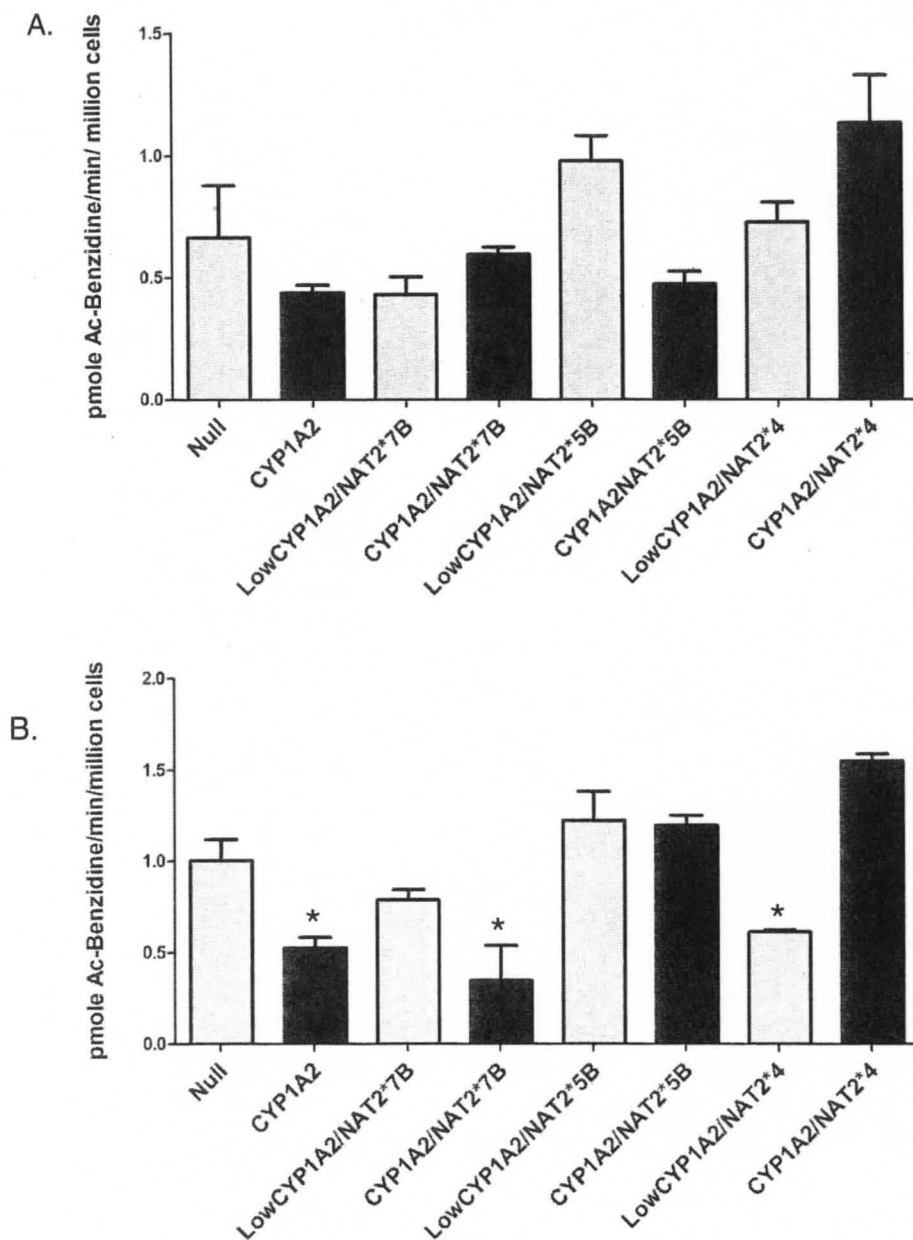
Figure 2.9 *In situ N*-acetylation of benzidine at 20 μM (A.) and 200 μM (B.) in cells from selected immortalized human fibroblast clones. No significant difference in benzidine *N*-acetylation activity was observed among cell lines at 20 μM using one-way ANOVA analysis (p > 0.05). Cell lines with CYP1A2-only, CYP1A2/*NAT2*5B*, and LowCYP1A2/*NAT2*4* had significantly lower benzidine *N*-acetylation activity at 200 μM than the reference allele CYP1A2/*NAT2*4* as denoted by * P<0.01 using one-way ANOVA followed by Bonferroni posttest. Each bar represents mean ± SEM for 3 experiments.
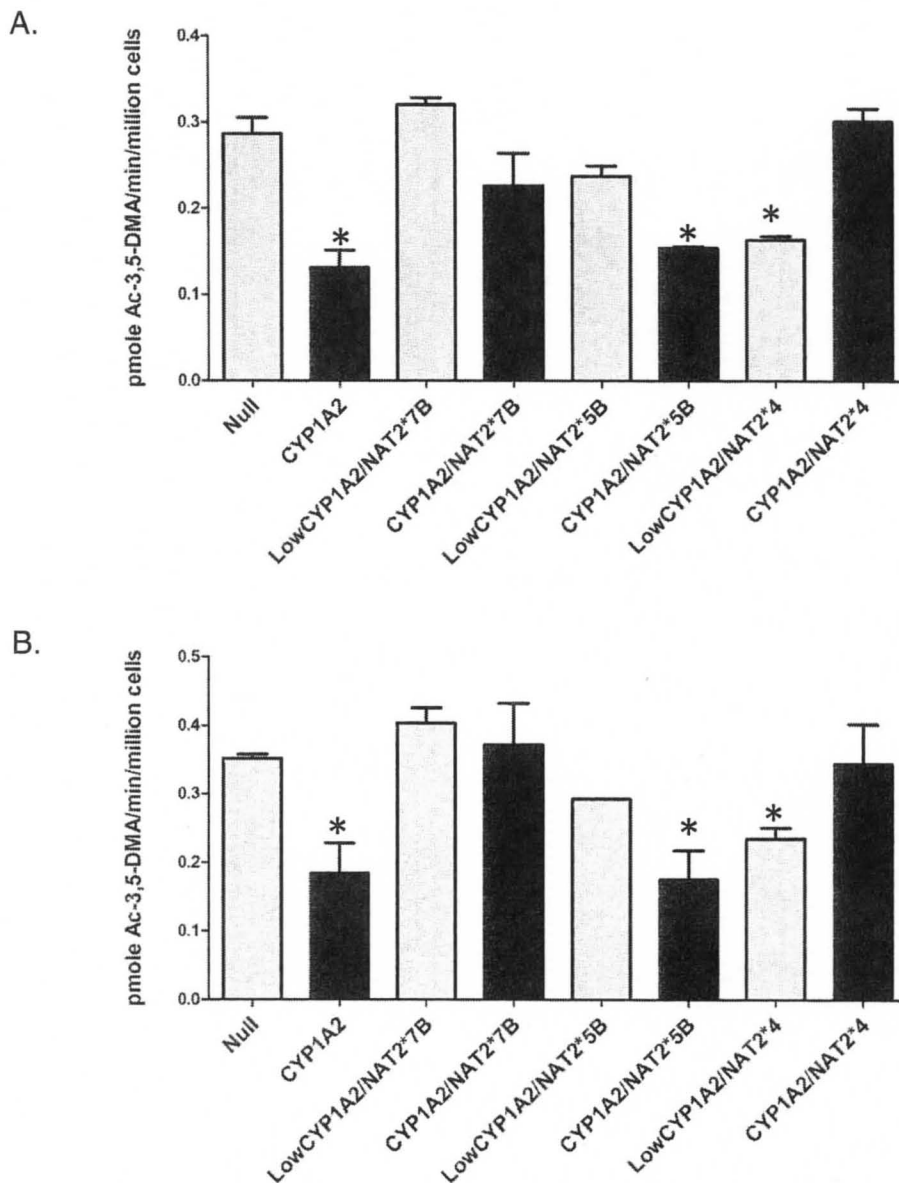
Figure 2.10 *In situ* N-acetylation of 3,5-DMA at 20 µM (A.) and 200 µM (B.) in cells from selected immortalized human fibroblast clones. Cell lines with CYP1A2-only, CYP1A2/*NAT2*5B*, and LowCYP1A2/*NAT2*4* had significantly lower 3,5-DMA N-acetylation activity than the reference allele CYP1A2/*NAT2*4* as denoted by * P<0.01 using one-way ANOVA followed by Bonferroni posttest. Each bar represents mean ± SEM for 3 experiments.

A.

B.
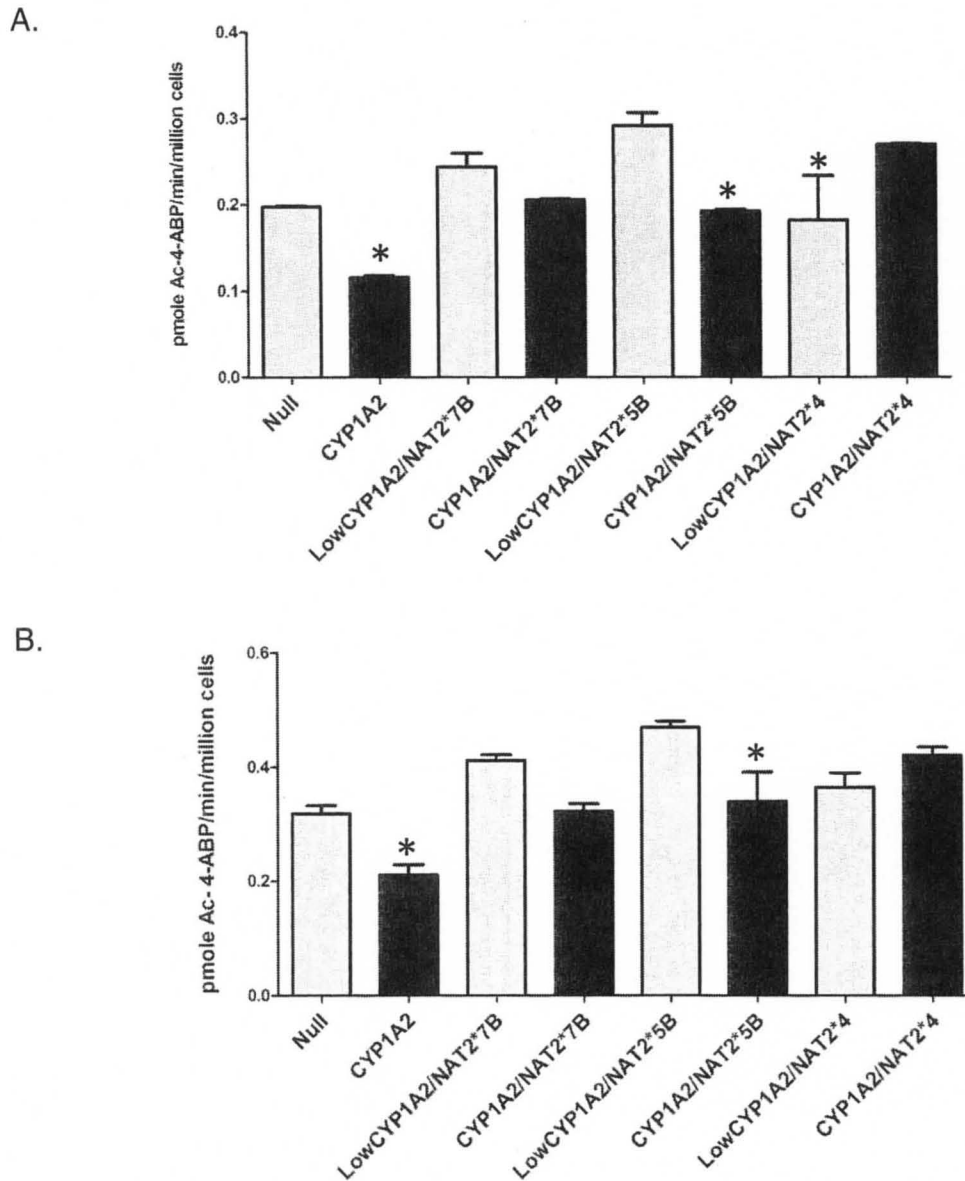
Figure 2.11 *In situ* *N*-acetylation of ABP at 20 μM (A.) and 200 μM (B.) in cells from selected immortalized human fibroblast clones. Cell lines with CYP1A2-only, CYP1A2/*NAT2*5B*, and LowCYP1A2/*NAT2*4* had significantly lower ABP *N*-acetylation activity at 20 μM than the reference allele *NAT2*4* as denoted by * P<0.01 using one-way ANOVA followed by Bonferroni posttest. Cell lines with CYP1A2-only and CYP1A2/*NAT2*5B* had significantly lower ABP *N*-acetylation activity at 200 μM than the reference allele CYP1A2/*NAT2*4* as denoted by * P<0.01 using one-way ANOVA followed by Bonferroni posttest. Each bar represents mean ± SEM for 3 experiments.
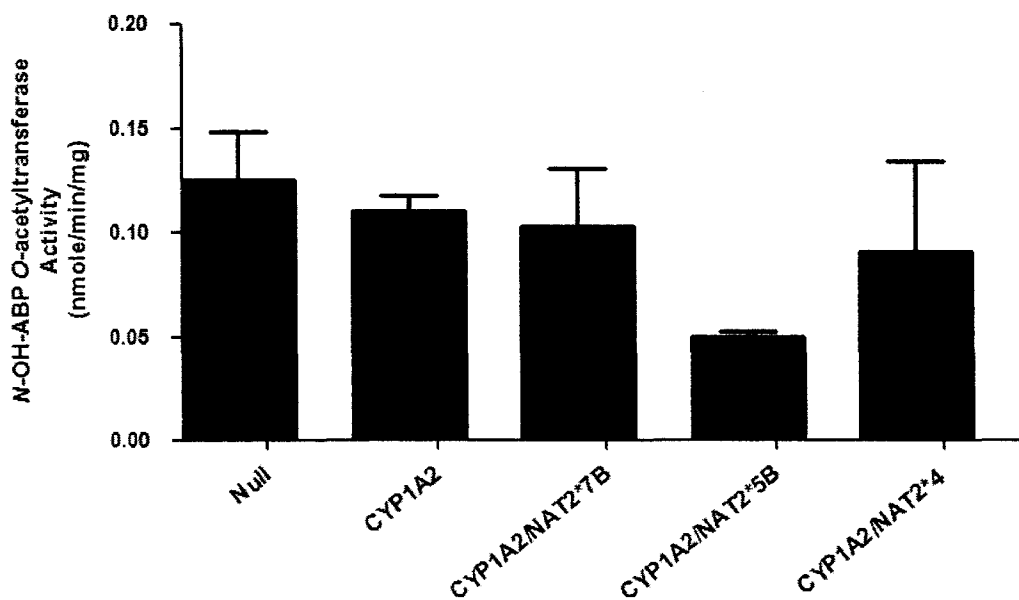
Figure 2.12 N-hydroxy-ABP O-acetyltransferase activity in immortalized human fibroblast that transfected with NAT2 alleles NAT2*4, NAT2*5B, and NAT2*7B. No significant difference in N-hydroxy-ABP O-acetyltransferase activity was observed among cell lines using one-way ANOVA analysis ($p > 0.05$). Each bar represents mean ± SEM for 3 experiments.

DISCUSSION

The use of NER-deficient immortalized human fibroblasts to study NAT functional genomics and carcinogen metabolism is an innovative addition to the previously used Chinese hamster ovary (CHO) cell (Metry et al., 2007), COS-1 cell (Zang et al., 2007), yeast (Fretland et al., 2001), and *E. Coli* (Hein et al., 1994) models. The use of this cell line provided an opportunity to study human CYP1A2, human NAT1, and human NAT2 phenotypic behavior which is important to better understand the relationship between risk and carcinogen metabolism. Studies have indicated that synergistic effects caused by gene-gene interactions increase risk to certain cancers (Cascorbi et al., 2001 and Sanderson et al., 2007). These findings support the use of cell lines expressing human NAT isozymes and human CYP1A2 for functional genomic studies of NAT and cancer risk.

In this study, we determined human NAT1 and NAT2 apparent intrinsic activities for the arylamine carcinogens benzidine, ABP, AF, 2,5-DMA, 3,4-DMA, 3,5-DMA, and 3-EA. We utilized these data to make comparisons of human NAT1 and NAT2 substrate affinities for these environmental carcinogens. Benzidine, 3,4-DMA, and AF were preferential human NAT1 substrates, while 3,5-DMA, 2,5-DMA, 3-EA, and ABP were preferential human NAT2 substrates. Liu et al. (2007) described similar analyses of the kinetic specificity constants for *N*-acetylation of environmental alkylanilines. In their studies, purified recombinant human NAT1 and NAT2 were expressed in *E. Coli* and used as a model to determine substrate selectivity for human NAT1 and NAT2. The Liu et al. (2007)

study show similar human NAT1 and NAT2 substrate specificity constants for monosubstituted and disubstituted alkylanilines.

The *N*-acetylation of 3,5-DMA was significantly lower in cells transfected with *NAT2*5B* or *NAT2*7B* allele compared with cells transfected with the reference allele *NAT2*4*. In the case of the most common *NAT2* alleles (*NAT2*4, NAT2*5B, and NAT2*7B*) our studies suggest that 3,5-DMA has a greater toxicological effect for slow NAT2 acetylators because of the significant decrease in *N*-acetylation causing more compound to be available for CYP-mediated activation.

*NAT1*10* is a variant haplotype with high allelic frequency that is associated with increased cancer risk (Hein et al. 2000). Previous studies conducted by Millner et al. (2012) showed that CHO cells transfected with *NAT1*10* have higher *N*- and *O*- acetyltransferase activity, mRNA and protein expression than cells transfected with the reference allele *NAT1*4*. Because *NAT1*10* is associated with increased *N*-acetyltransferase activity, our study findings suggest that environmental carcinogens, benzidine, 3,4-DMA, and AF, may be less toxic for the population of individuals that possess the *NAT1*10* allele. This is based on our study findings that indicate that that these substrates are preferentially *N*-acetylated by NAT1 and the ability of NAT1 10 to rapidly catalyze the detoxification *N*-acetylation reaction.

Our studies using human cell lines that endogenously express NAT1 and stably express human NAT2 and human CYP1A2 confirm results found in the previous study. Liu et al. (2007) also describes the use of NMR-based models to

analyze NAT binding site interactions of the aforementioned alkylanilines. The previous study using purified recombinantly expressed NATs was able to provide insight into substrate specificity by determining the contribution of alkylaniline substituents to NAT substrate selectivity. These data show that 2-alkyl groups decrease *N*-acetylation catalysis, especially that by NAT1. This trend can be seen in our current studies when comparing the NAT1 apparent maximum velocity for the alkylanilines. This finding could suggest why 2,6-DMA *N*-acetylation was below the limit of detection in both studies.

Although the previously described study done by Liu et al. (2007) found similar results, it did not utilize human cell lines to investigate the role of NAT carcinogen metabolism in the presence of CYP1A2. The present study adds considerable valuable to epidemiological studies that study genotype and risk alone because our results in human cells suggest that substrate selectivity and the interplay of various XMEs play an important role in carcinogen metabolism. *N*-acetylation of benzidine, ABP, and 3,5-DMA was determined in the presence of high and low CYP1A2 activity. We determined that ability of NAT to detoxify compounds in the presence of CYP1A2 is dependent on substrate concentration and substrate specificity. This study proposes that toxicological outcomes influenced by NAT detoxification are also determined by exposure levels and XME competition for available substrate. *N*-acetylation in combination with other catalysis by other XMEs appears to play an important role carcinogen metabolism and risk.

In several studies conducted in our laboratory, ABP-induced cytotoxicity, mutagenesis, and DNA-adducts were measured in CHO cells stably expressing human CYP450 and human NAT (Metry et al., 2007). Considerable levels of these toxicological outcomes were measurable following ABP exposure in CHO cells. In the current study, these toxicological outcomes were all below the limit of detection in our transfected human cell lines. This result suggests that additional human XME present in our cell lines may be acting to detoxify ABP, thus inhibiting the ABP-induced toxicological outcomes.

We determined GST activity in our cell lines by demonstrating the potential conjugation of ABP with glutathione. The lack of ABP- induced toxicological insult in our studies suggests that GST is involved in the detoxification of ABP. GSTs are very abundant cellular components, accounting for up to 10 percent of the total cellular protein (Noguti et al., 2012). This finding is important when building a comprehensive understanding of the bioactivation and detoxification of environmental carcinogens by XMEs.

In summary, human NAT1 and NAT2 are both capable of catalyzing the N-acetylation of benzidine, ABP, AF, 2, 5-DMA, 3, 4-DMA, 3, 5-DMA, and 3-EA. These isozymes play an important role in environmental carcinogen metabolism. The affinity for these compounds as well as the rate at which these compounds are N-acetylated by NAT differ for each isozyme. This study is the first to demonstrate the use of human fibroblasts that express human NAT1, human NAT2 haplotypes, and human CYP1A2. Future studies will involve characterization of the effects of modulated human GST activity in combination

with varying human NAT and human CYP1A2 activity on toxicological outcomes such as mutagenesis and DNA adducts. There are multiple interactions that influence the overall biotransformation of environmental carcinogens. We have illustrated in this study that the complexities of these competing pathways are important consideration when determining the role that NAT plays in carcinogen metabolism.

CHAPTER III

IDENTIFICATION AND CHARACTERIZATION OF NOVEL HUMAN ARYLAMINE N-ACETYLTRANSFERASE SMALL MOLECULE INHIBITORS

INTRODUCTION

Many environmental arylamines play an important role in the etiology of cancer and require metabolic activation by acetylation. Arylamine *N*-acetyltransferases (NAT), phase II xenobiotic metabolizing enzymes, catalyze the *N*-acetylation or *O*-acetylation of arylamine carcinogens. *O*-acetylation, which is preceded by cytochrome P450 *N*-hydroxylation, results in nitrenium ions that covalently bond with nucleophilic groups on DNA forming adducts. If unrepaired, these adducts can lead to mutagenesis and initiate cancer. Humans possess two *NAT* genes, *NAT1* and *NAT2*, which encode similar enzymes that have distinct tissue distribution and substrate specificities. NAT1 and NAT2 have been closely associated with several types of cancer because of their role in the metabolism of arylamine carcinogens.

NAT1 in particular has been associated with several cancers. Molecular epidemiology studies report that NAT1 expression and genetic polymorphisms are associated with individual risk to urinary bladder, colorectal, lung, and breast cancer. Studies suggest that NAT1 plays an important role in cell growth and

survival, as well as in cell proliferation and invasion, which are hallmarks of metastatic cancer.

Collectively, these data implicate NAT1 function in cancer progression and malignancy, suggesting that the use of NAT1 as a molecular target may be an effective approach for cancer therapy. Several studies have explored the use of small molecule inhibitors, providing proof of principle that NAT can be effectively inhibited by small molecules (Westwood et al., 2010), but none has successfully developed a novel small molecule inhibitor that is efficacious, potent, and nontoxic.

In order to elucidate ways to reduce or ablate toxicological risk caused by arylamine carcinogen metabolism, we explored the identification and use of small molecule inhibitors. Studies provide evidence that NAT inhibitors have been beneficial in investigating the catalytic mechanism of NATs as these enzymes are emerging as molecular targets (Russell et al., 2009). The purpose of this study is to utilize NAT as a molecular target for the development of small molecule inhibitors for cancer prevention. We utilized *in silico* screening of 17 million compounds to identify those that interact with NAT active sites. The top 150 compounds were scored and ranked based on their active site association. Sixty of these compounds were tested for their ability to inhibit recombinant human NAT1.

In the present study, we have identified an effective small molecule inhibitor that decreases NAT1 activity in yeast and Chinese hamster ovary cells that express recombinant human NAT1. In future studies we anticipate that NAT

inhibition by our small molecule inhibitor will decrease experimental cancer initiation and progression.

MATERIALS AND METHODS

Computational Screening for Small Molecule Inhibitors

Previously reported high resolution crystal structures of human NAT1 and NAT2 (Wu et al., 1997) were used as target structures to identify potential compounds with NAT active site association. In collaboration with Dr. John Trent, the human NAT protein structures obtained from the Protein Data Bank (PDB) under the codes 2PQT (NAT1) and 2PFR (NAT2) were used to complete the screening of the ZINC library containing approximately 17 million compounds. The computational screening program Surflex-Dock 2.3 was used to perform protein-ligand docking studies that generated a ranked list of candidates. This docking software is capable of ranking the inhibitor candidates by reporting approximate binding affinity using a computational parameterized function. Compounds with high approximate binding affinity were purchased and investigated for their ability to inhibit NAT activity.

In vitro Screening of N- Acetyltransferase Inhibition

Initial screening of compounds for their NAT inhibitory properties was completed using recombinant human NAT1 or NAT2 stably expressed in yeast (*Schizosaccharomyces pombe)* as previously described (Fretland et al., 2001). Individual reactions were set up using 50 µL of diluted yeast lysate incubated for 10 minutes at 37°C in the presence of 300 µM NAT1 (p-aminobenzoic acid) or NAT2 (sulphamethazine) selective substrate, 1 mM acetyl coenzyme A, and 0.1 mg/mL candidate inhibitor. Reactions were terminated using 10% volume of 1 M

acetic acid. Control reactions replaced the inhibitor with the vehicle DMSO. Following centrifugation at 15,000 x g for 10 minutes, the supernatant was collected and analyzed by high performance liquid chromatography (HPLC, Beckman System Gold) as previously described (Chapter II).

Cell Culture and Preparation of Cell Lysate

UV5-Chinese hamster ovary (CHO) cells (CRL-1865) were obtained from American Type Culture Collection (ATCC). These cells, previously transfected with human NAT1(Millner et al., 2012), were cultured at 37°C in 5% CO_2 in alpha-modified minimal essential medium (α-MEM, Lonza, Walkersville, MD) supplemented with 10% fetal bovine serum (Hyclone, Logan, UT), 100 units/mL penicillin (Lonza), 100 µg/mL streptomycin (Lonza), 2 mM L-glutamine (Lonza). These cells were allowed to grow to confluency in 6-well cell culture plates 24 h before treatment.

NAT1 In Vitro and In Situ Inhibition Assays

In vitro inhibition of NAT1 activity was assayed using 50 µL of cell lysate incubated with 300 µM PABA, 1 mM acetyl coenzyme A, and various concentrations of Compound 10 (0 – 100 µM) for 10 minutes at 37°C. Reactions were terminated by the addition of 10% volume 1M acetic acid. Following centrifugation at 15,000 x g for 10 minutes, the supernatant was collected and analyzed by high performance liquid chromatography using a method previously described (Chapter II). For *in situ* studies, 1 x 10^6 cells were seeded and

incubated with 300 μM PABA and various concentrations (0-1000 μM) of Compound 10 for 24h. The culture medium was collected and N–acetyl-PABA was quantified by HPLC.

In vitro IC$_{50}$ values

IC$_{50}$ values of active compounds were determined by nonlinear regression using Prism 5 (GraphPad Software Inc., La Jolla, CA). Inhibition kinetics were studied in yeast at inhibitor concentrations of 0 - 100 μM in the presence of 10 μM NAT substrates ABP, PABA, or SMZ and 100 μM acetyl coenzyme A. Acetylated products were quantified using HPLC.

Determination of Compound 10 Kinetics

CHO cells were treated with α-MEM supplemented with 10 μM PABA or ABP, and various concentrations of Compound 10 (1-500 μM). After 2 h treatment with various concentrations of Compound 10, NAT1 inhibition was determined by collecting 100 μL of medium and quantifying N – acetyl-PABA and N-acetyl- ABP by HPLC as described above. The inhibition type of Compound 10 was determined using an Eadie-Hofstee plot prepared by plotting V/S against V, and the Lineweaver-Burk plot prepared by plotting 1/S against 1/V.

Statistical Analysis

Experiments were performed in triplicate. The data are reported as mean ± SEM. Statistical significance was assessed using one-way analysis of variance (ANOVA) for multiple comparisons and Student's t test for single comparisons using Prism 5 (GraphPad, La Jolla, CA).

RESULTS

In this study, the protein structures of human arylamine *N*-acetyltransferases were used to conduct protein-ligand docking studies. Our initial approach in the identification of potential small molecule inhibitors of NATs was to perform protein-ligand docking studies using Surflex-Dock 2.3 to generate a ranked list of candidates. This program utilizes a docking algorithm that positions ligands into the binding site of our enzyme of interest. Surflex-Dock 2.3 is capable of ranking the inhibitor candidates by reporting approximate binding affinity (Kd) using a parameterized function.

The docking of ligands in the catalytic site of NAT protein was performed using Surflex-Dock software. Using the software, 150 compounds were identified as potential inhibitors of NAT enzymatic activity. The candidate inhibitors were prioritized based on their Surflex-Dock approximated binding affinity. Sixty of the top ranking compounds were purchased and experimentally tested for their ability to inhibit NAT activity. The percent inhibitions of all compounds were determined *in vitro* in yeast lysates that express recombinant human NAT1 or NAT2. This was determined using the substrates PABA, selective for NAT1, or SMZ, selective for NAT2. From these data, we determined NAT selectivity for each inhibitor. Compound specificities were determined by dividing the percent NAT1 inhibition by the percent NAT2 inhibition. Compounds that had a calculated NAT selectivity of 1 or above were deemed NAT1 selective. The results obtained from the experimental screening are shown in Table 3.1.

We selected lead compounds 1,3,5-Triazine-2,4-diamine, 6-[3,5-dimethyl-1-piperidinyl)methyl]-*N*-(4-ethoxyphenyl) (2), 9,10-dihydro-9,10-dioxo-1,2-anthracenediyl diethyl ester (10), 2-[(3-hydroxyphenyl)methylene] (11), and 4,4'-methylenebis[*N*-(1,3-benzodioxol-5-ylmethyl) (16) that exhibited more than 50% inhibition at concentrations at or below 1 mg/mL. The protein-ligand structures for the lead compounds are depicted in Figure 3.1. Compound 2 inhibited both NAT1 and NAT2 with *in vitro* IC_{50} values of >2 mM and 176 µM, respectively. Compound 11 inhibited NAT1 and NAT2 with *in vitro* IC_{50} values of 191 and 131 µM, respectively. Compound 16 inhibited NAT1 and NAT2 with *in vitro* IC_{50} values of 202 µM and >2mM, respectively. Compound 10 was the most potent inhibitor, in that it inhibited NAT1 and NAT2 with *in vitro* IC_{50} values of 0.75 and 82.2 µM, respectively. The *in situ* IC_{50} values of our lead compounds were determined in UV-5 CHO cells that express recombinant human NAT1. These values were 300, 118, and 211 µM, and >2mM for Compounds 2, 10, 11, and 16 respectively. These data show that Compound 10 is the most potent inhibitor using *in vitro* and *in situ* inhibition assays. We note that Compound 10 is selective against NAT1 relative to NAT2. Table 3.2 shows the structures of the lead compounds and their experimental IC_{50} values.

The arylamine ABP is a constituent of tobacco smoke, a well-characterized environmental carcinogen. The *N*-hydroxylated ABP intermediates are able to covalently interact with DNA to form adducts that have the potential to initiate cancer. ABP is biotransformed by both NAT1 and NAT2. We determined the ability of Compound 10 to inhibit the *in vitro* acetylation of ABP by NAT1 and

NAT2 in lysates of yeast that express recombinant human NAT1 or NAT2. The IC_{50} values were determined to be 0.95 and 41.3 µM for NAT1 and NAT2, respectively (Figures 3.2 and 3.3).

Further studies were completed using the most potent inhibitor, compound 10, to determine its ability to inhibit N-acetylation of ABP at various concentrations in UV5-Chinese hamster ovary (CHO) cells. Compound 10 was able to inhibit NAT1 in situ N-acetylation of ABP in UV5-CHO cells that stably express recombinant human NAT1. The IC_{50} value towards the inhibition of N-acetylation of ABP was 81.6 µM. These data are shown in addition to the inhibition of PABA N-acetylation at various concentrations in Figure 3.2.

In order to evaluate the kinetic characteristics of compound 10 inhibition, UV5-CHO cells were treated with complete media supplemented with substrate and various concentrations of inhibitor. These kinetic data were used to construct Eadie-Hofstee and Lineweaver-Burke plots (Figure 3.3). These studies demonstrated noncompetitive binding, which may be indicative of tight binding or irreversible inhibition. Tight binding is speculated due to the nature in which the inhibitors were identified, active site association.

Two available structural analogs 1-(9,10-dihydro-8-hydroxy-9,10-dioxo-1-anthracenyl)4-ethyl ester (analog 1) and 9,10-dihydro-9,10-dioxo-1,8-anthracenediyl diethyl ester (analog 2) of Compound 10 were tested for their ability to inhibit NAT1. The in situ IC_{50} values of these analogs were determined to be 384 and 147 µM, respectively. The structures and IC_{50} values of analogs 1 and 2 are shown in Table 3.3.

To characterize the identified inhibitors we utilized the simulation software ADMET Predictor (Simulations Plus) to predict QSAR descriptors of our lead compounds. The physiochemical properties of the lead compounds and analogs are presented in Table 3.4. All compounds, except Compound 16, satisfied Lipinski's rule-of-five. This rule is based on the World Drug Index Database and is used to evaluate the compounds potential to become a drug (Lipinski et al., 2000). This evaluation is based on properties of ~90% of drugs on the market that have a (1) a molecular weight less than 500, (2) a partition coefficient that is less than 5, (3) less than 5 hydrogen bond donors (sum of O-H and N-H), and (3) less than 10 hydrogen-bond acceptor (sum of N and O atoms). Compound 16 did not satisfy Lipinski's rule-of-five due to a molecular weight greater than 500. We also utilized the ADMET predictor software to predict the cytochrome P450 intrinsic clearance constants of the lead compounds and Compound 10 structural analogs. This program predicts the intrinsic clearance for the major CYPs that are responsible for ~90% of CYP-mediated reactions. These isoforms include CYP1A2, CYP2C19, CYP2C9, CYP2D6, and CYP3A4. These data are shown in Table 3.5. Our lead compound, 10, is predicted to have no violations of ADMET properties; therefore we have identified an inhibitor of human arylamine N-acetyltransferase that can be used for further biological testing to better understand the role that NAT1 plays in cancer progression.

Compound	Targeted Isozyme	Priority number	% Inhibition of PABA NAT Activity (NAT1)	% Inhibition of SMZ NAT Activity (NAT2)	NAT1 Specificity (NAT1/NAT2)
1	NAT2	6	0	4	0
2	NAT2	9	7	49	0.14
4	NAT1	14	0	3	0
5	NAT1	19	30	0	
6	NAT2	7	0	7	0
7	NAT2	11	25	0	
8	NAT1	3	0	0	
9	NAT1	20	14	7	2.00
10	NAT1	23	100	100	1.00
11	NAT1	40	95	88	1.08
12	NAT1	67	8	23	0.35
13	NAT1		3	0	
14	NAT1		7	0	
15	NAT2	24	5	9	0.56
16	NAT2	23	75	5	15.00
17	NAT1	27	0	0	
18	NAT2	25	0	0	
19	NAT1	47	16	2	8.00
20	NAT2	28	16	2	8.00
21	NAT1	50	2	9	0.22
23	NAT2	26	5	21	0.24
24	NAT2	27	15	22	0.68
25	NAT2	30	2	37	0.05
26	NAT1	26	31	0	
27	NAT2	46	0	0	
28	NAT2	57	0	26	0
30	NAT1	49	0	7	0
31	NAT2	52	27	14	1.93
32	NAT1	54	43	30	1.43
33	NAT2	53	7	0	
34	NAT2	33	14	10	1.40
35	NAT2	22	0	2	0
36	NAT2	41	0	0	
37	NAT2	32	17	4	4.25
38	NAT2	60	21	13	1.62
39	NAT2	67	5	0	
40	NAT2	58	3	0	
41	NAT2	56	0	2	0
42	NAT2	49	14	0	
43	NAT2	55	0	27	0
44	NAT2	68	13	10	1.30

Compound	Targeted Isozyme	Priority Number	% Inhibition of PABA NAT Activity (NAT1)	% Inhibition of SMZ NAT Activity (NAT2)	NAT1 Specificity (NAT1/NAT2)
45	NAT2	51	20	0	
46	NAT2	38	21	15	1.40
47	NAT2	44	5	14	0.36
48	NAT1	33	17	54	0.31
49	NAT1	22	11	60	0.18
50	NAT1	24	33	29	1.14
51	NAT1	68	0	23	0
52	NAT1	14	11	20	0.55
53	NAT1	63	24	12	2.00
54	NAT1	53	48	13	3.69

Table 3.1 *In vitro* screening against human NAT1 and NAT2 recombinantly expressed in yeast. Priority numbers were assigned based on computational screening approximated binding affinities.
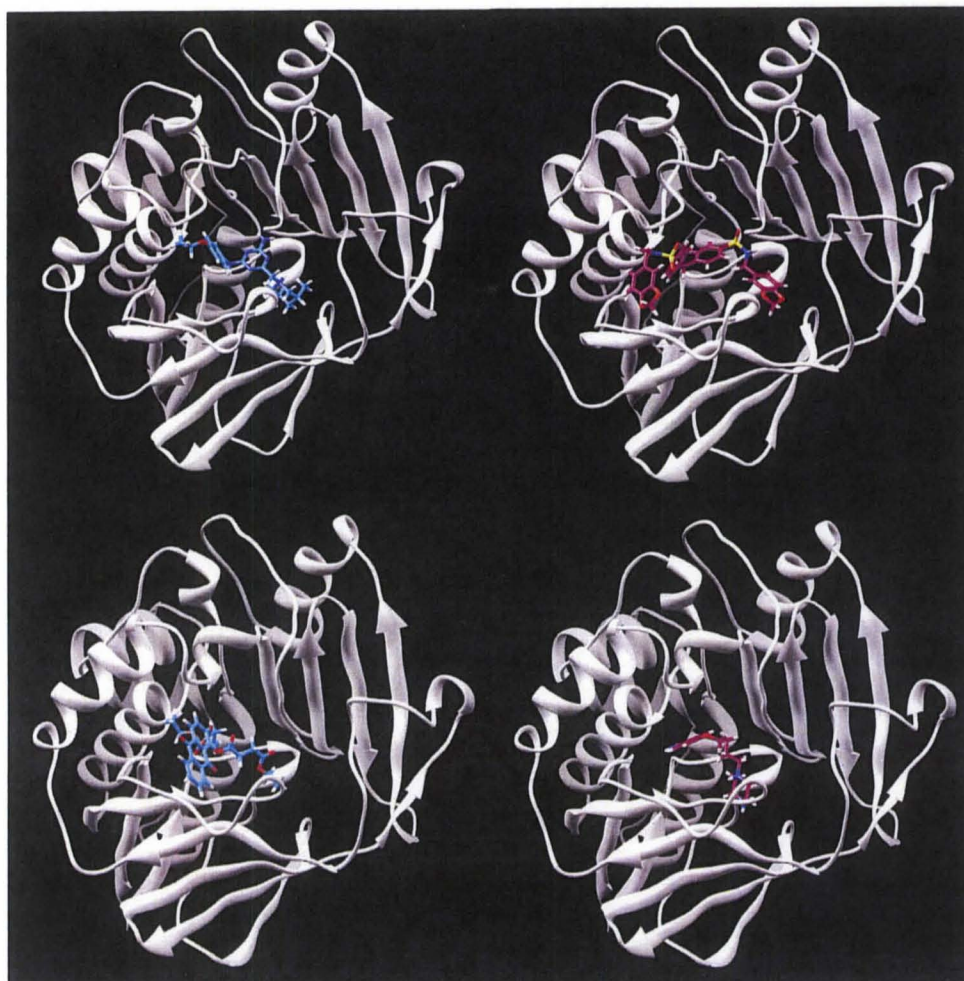
Figure 3.1 Protein-ligand poses for lead compounds **2**, **10**, **11**, and **16** (left to right) using Surflex-Dock 2.3.

Compound	Structure	In vitro NAT1 IC$_{50}$ (μM)	In vitro NAT2 IC$_{50}$ (μM)	NAT2 IC$_{50}$/ NAT1 IC$_{50}$	In situ NAT1 IC$_{50}$ (μM)
2		>2 mM	176 ± 24.3	0.08	300±20.4
10		0.75 ± 0.2	82.2 ±12.9	109.6	118±19.3
11		191 ± 33.9	131 ± 15.7	0.69	211±30.8
16		202 ± 34.2	>2 mM	9.90	>2 mM

Table 3.2 Structures of lead compounds and the experimental IC$_{50}$ values. The IC$_{50}$ values of the most efficacious inhibitors (compounds **2, 10, 11** and **16**) were determined *in vitro* against human NAT1 (PABA) and NAT2 (SMZ) recombinantly expressed in yeast. The *in situ* IC$_{50}$ values were determined in UV5-CHO cells that stably express recombinant NAT1.
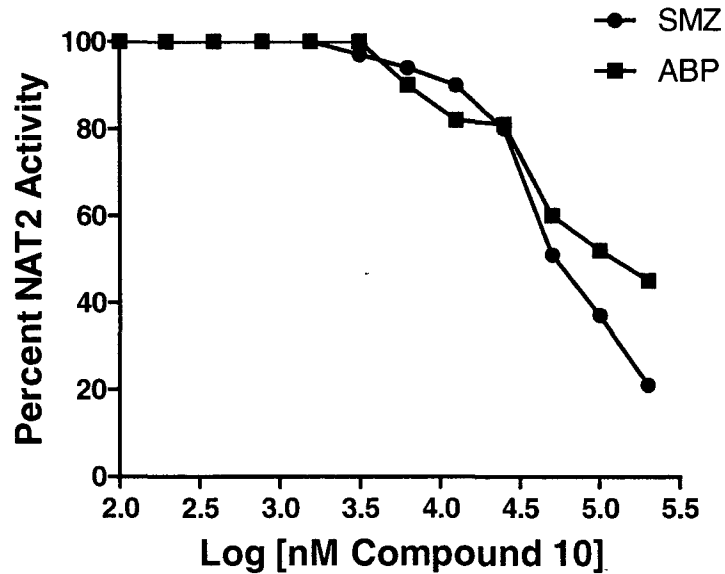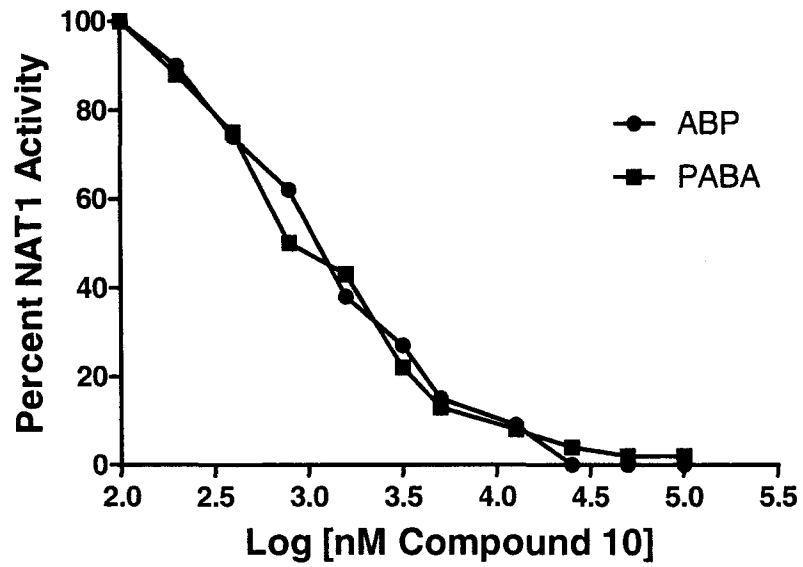
Figure 3.2 *In vitro* NAT1 and NAT2 activity was determined using 100 μM acetyl coenzyme A and 10 μM 4-aminobiphenyl (ABP), p-aminobenzoic acid (PABA), or sulfamethazine (SMZ) with varying concentrations of Compound 10 (0 – 100 μM) in yeast lysates that express recombinant human NAT1.

A.
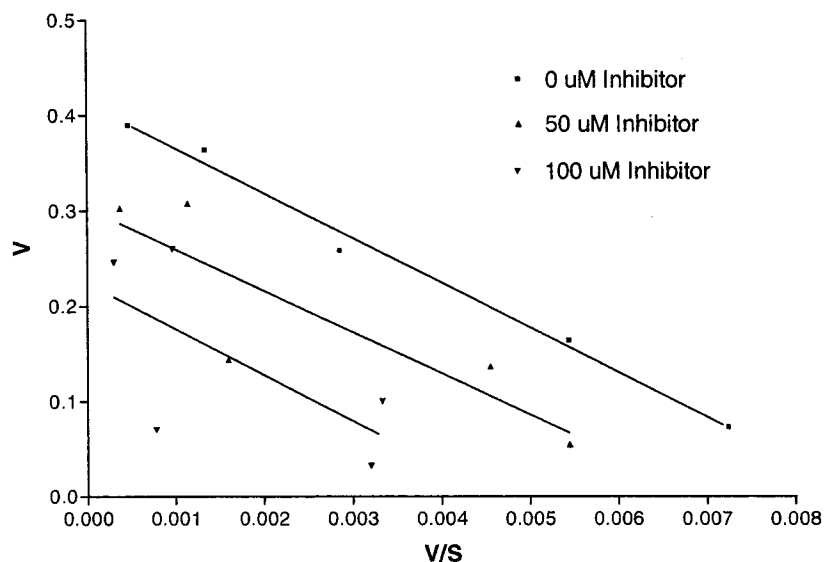
B.
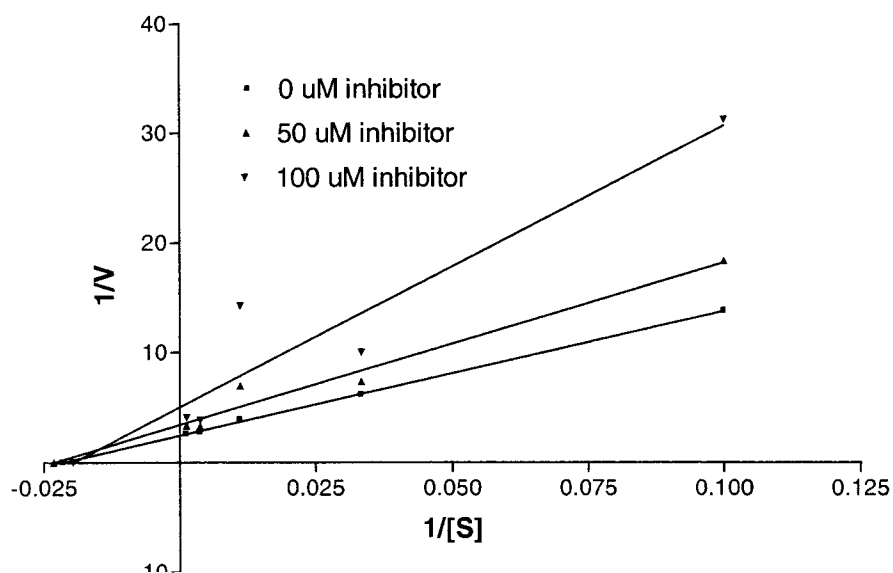
Figure 3.3 Kinetic characteristics of Compound 10 inhibition. Seeded CHO cells were treated with complete α-MEM supplemented with 10 μM PABA substrate (S), and various concentrations of Compound 10 (1 – 500 μM). After 2 h treatment with various concentrations of Compound 10, NAT1 inhibition was determined by collecting 100 μL of media and quantifying *N* – acetyl-PABA by HPLC. Eadie-Hofstee (A.) and Lineweaver-Burke(B.) plots showing noncompetitive inhibition and are indicative of tight-binding. Velocity (V) is in units of nmole/min.
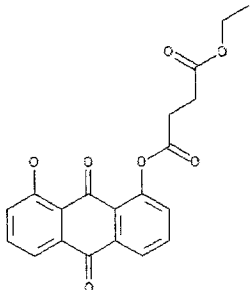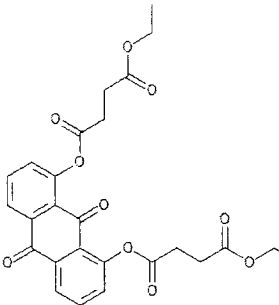
Entry No.	Compound	In vitro NAT1 IC$_{50}$ (μM)	In vitro NAT2 IC$_{50}$ (μM)	In situ NAT1 IC$_{50}$ (μM)
Analog 1		171±4.7	>2mM	384±12.2
Analog 2		94±6.8	>2 mM	147±9.4

Table 3.3 Compound 10 Analog 1 and Analog 2 structures and experimental IC$_{50}$ values determined *in vitro* in yeast lysate against human NAT1 (PABA) and NAT2 (SMZ), and *in situ* in UV5-CHO cells that stably express recombinant NAT1.

Compound	2	10	11	16	Analog 1	Analog 2
MlogP	3.29	0.91	0.84	2.05	1.69	0.91
S+logD	3.85	2.74	1.64	3.84	2.95	3.06
S+Vd (L/kg)	3.42	1.03	1.05	0.68	0.58	0.93
Diffusion Coefficient	0.7	0.65	1.25	0.6	0.8	0.65
Lipinski Rule of Five	0	0	0	1(MW)	0	0

Table 3.4 ADMET Predictor Calculated QSAR descriptors of lead compounds and Compound 10 analogs. MlogP is the Moriguch model of octanol-water partition coefficient. S+logP is the Simulations Plus model octanol-water distribution coefficient. S+Vd is the Simulations Plus model pharmacokinetic volume of distribution. The molecular diffusion coefficient is predicted for water with units of $cm^2/s \times 10^5$. A 0 indicates that the compound does not dissatisfy any of the Lipinski rules. The number 1 indicates that Compound 11 dissatisfies 1 rule for molecular weight (MW).

Compound	2	10	11	16	Analog 1	Analog 2
CYP1A2	35.6	0.18	0.074	0.12	0.35	0.23
CYP2C19	0.64	0.002	0.002	0.04	0.09	0.04
CYP2C9	0.02	0.04	0.05	69.2	3.5	0.86
CYP2D6	3.0	0.01	0.01	0.02	0.01	0.01
CYP3A4	1.52	1.49	0.17	1.77	0.045	1.62

Table 3.5 ADMET Predictor predicted CYP intrinsic clearance constants (ml/min/kg) of lead compounds and Compound 10 analogs.

DISCUSSION

Here, we report the identification and characterization of novel small molecule inhibitors of the molecular target NAT1. The most important conclusion of this study is that structure-based computational screening was used to identify effective inhibitors of NAT1. The data provided in this study reveal that compound 10 is an effective and potent inhibitor of human NAT1. Compound 10 appears to be the most suitable compound for further inhibitor development and for studies that determine the effects of NAT1 inhibition on cancer progression. We wish to note that this study shows proof-of-concept that virtual screening methods are a viable approach to identifying novel inhibitors of enzymes that play a role in carcinogen metabolism.

Although this was a relatively small-scale study with only 60 compounds tested, 4 new lead compounds were discovered. We can utilize these compounds to gain a better understanding of the role that human arylamine NAT1 plays in cancer progression. Compound 10 was less effective in whole cell assays, possibly due to lower bioavailability due to poor absorption.

In this study, we identified and tested structural analogs of compound 10 that were not as effective in inhibiting NAT1 activity. We speculate that the structural analogs lack the inhibition ability of 10 because the positioning of binding moieties are not optimally positioned to interact with the three key amino acids in the active site loop. Further investigation is needed to validate these speculations.

In conclusion, the present study further suggest that NAT1 can be used as a molecular target and it identifies a novel small molecule inhibitor that may prove to be most promising as an anticancer therapeutic. While known NAT1 inhibitors, such as tamoxifen, have provided insight into the role of NAT1 in carcinogen metabolism, small molecule inhibitors have established a new era in the use of NAT1 as a molecular target for cancer drug development.

CHAPTER IV

INHIBITION OF HUMAN ARYLAMINE N-ACETYLTRANSFERASE I
DECREASES EXPERIMENTAL CANCER INITIATION AND PROGRESSION

INTRODUCTION

In order to elucidate ways to reduce or to ablate toxicological risk caused by arylamine carcinogen metabolism, we explored the identification and use of a small molecule inhibitor. Studies provide evidence that NAT inhibitors have been useful in investigating the catalytic mechanism of NATs as these enzymes are emerging as molecular targets (Russell et al., 2009). Other studies explore NAT inhibitors as a means to alter biotransformation by NAT, consequently providing potential differences in toxicological consequences (Dairou et al., 2009).

Our study introduces the use of novel and effective inhibitors of NAT1 to reduce experimental cancer initiation and progression. Recent studies provide evidence that NAT1 knock-down affects cell growth and morphology, suggesting that NAT1 may function beyond a Phase II drug metabolizing enzyme, further raising the potential of NAT1 as a therapeutic molecular target (Tiang et al., 2011). Collectively, these data implicate NAT1 function in cancer progression and malignancy suggesting that the use of NAT1 as a molecular target may be an effective approach for cancer therapy. In Chapter III, we identified a small

molecule inhibitor that decreases NAT1 activity in yeast and Chinese hamster ovary cells that recombinantly express human NAT1.

Studies have shown that NAT1 is highly expressed in breast tumors as compared to normal tissue, being especially elevated in invasive ductal and lobular breast carcinomas (Russell et al., 2009). Other studies suggest that NAT1 plays an important role in cell growth and survival, as well as in cell proliferation and cell invasion, which are hallmarks of metastatic cancer (Tiang et al., 2010). In this chapter, we use the small molecule inhibitor, Compound 10, to decrease NAT1 activity in human breast cancer cell lines, MDA-MB-231 (post epithelial to mesenchymal transition) and MCF-7 (luminal), in order to study the effects of NAT1 inhibition on carcinogen metabolism and cancer progression in two different breast adenocarcinoma cell lines.

MATERIALS AND METHODS

Cell Culture and Preparation of Cell Lysates

MDA-MB-231 (HTB-26) and MCF-7 (HTB-22) human breast adenocarcinoma cells were obtained from American Type Culture Collection (ATCC). Cells were cultured in Dulbecco's Modified Eagle Medium (DMEM , Lonza, Walkersville, MD) supplemented with 10% fetal bovine serum (Hyclone, Logan, UT), 100 units/mL penicillin (Lonza), and 100 µg/mL streptomycin (Lonza). Non-tumorigenic human breast epithelial cells (MCF-10A) were a gift from Mrs. Sheila Thomas (University of Louisville, James Graham Brown Cancer Center). Cells were cultured in Mammary Epithelium Basal Medium (MEBM, Lonza, Walkersville, MD) supplemented with bovine pituitary extract (2 mL / 500 mL MEBM, Lonza), epidermal growth factor (0.5 mL / 500 mL MEBM, Lonza), insulin (0.5 mL / 500 mL MEBM, Lonza), transferrin (0.5 mL / 500 mL MEBM, Lonza), hydrocortisone (0.5 mL / 500 mL MEBM, Lonza), epinephrine (0.5 mL, 500 mL MEMB Lonza), and gentamicin (0.5 mL / 500 mL MEBM, Lonza). Cells were maintained at 37°C in 5% CO_2. MDA-MB-231 and MCF-7 cells were trypsinized with 0.25% Trypsin-EDTA (Gibco). MCF-10A cells were trypsinized with 1X TrypLE™ Express (Gibco). To prepare cell lysates, cells were washed with cold PBS and resuspended in homogenization buffer (20 mM $NaPO_4$ at pH 7.4, 1 mM EDTA , 2 µg/mL aprotinin, 0.1 mM phenylmethanesulfonyl fluoride (PMSF), 2 mM pepstatin A, 1 mM dithiothreitol, and 0.2% Triton X-100) on ice. Homogenates were centrifuged at 15,000 x g for 10 min at 4°C. Total protein

concentrations in supernatants were determined by the Bradford method (Bradford, 1976).

Drug Treatment

Compound 10 was dissolved in DMSO for each experiment. Stock solutions were stored at -20°C and used for further dilution in culture medium to obtain desired concentrations. The final solvent concentration was 0.5% v/v of DMSO. Control cultures of cells for each experiment were grown in culture medium with DMSO used as control.

Inhibition of NAT1 In Situ

Cells were grown to confluence and treated with media supplemented with 10 μM ABP or PABA with varying concentrations of Compound 10 (0 - 1000 μM) for 4h at 37°C. The culture media were collected and 1/10 volume of 1M acetic acid was added. The mixture was centrifuged at 13 000 g for 10 min. The supernatant was analyzed by reverse phase HPLC and N-acetyl-PABA or ABP products were quantitated as described in Chapter II.

Cell Viability and Proliferation Assay

The effect of Compound 10 on cell viability and cell proliferation was assayed using the AlamarBlue (Invitrogen, Eugene, OR) fluorescence assay. MDA-MB-231 and MCF-10A cells were seeded in 96-well plates and incubated for 24 h. The cells were then treated with varying concentrations of Compound

10 in their respective culture medium. AlamarBlue, resazurin, is a nontoxic non-fluorescent indicator dye that is converted to highly red fluorescent resorufin via reduction in living cells. AlamarBlue was added 1 h prior to the desired time point in an amount equal to 1/10 of the culture volume, and the plates were further incubated at 37°C. The amount of AlamarBlue reduction was measured using a fluorometric plate reader (excitation wavelength of 570 nm and emission of 580 nm). Data are reported as the mean ± SEM fluorescence intensity versus Compound 10 concentration for 4 separate experiments.

Measurement of O-Acetyltransferase Activity

N-hydroxy-4-aminobiphenyl (N-OH-ABP) O-acetyltransferase activity was evaluated in MDA-MB-231 cell lysate using reverse phase HPLC as described by Hein et al., (2006). Reaction mixtures containing 100 µg total protein, 1 mg/mL deoxyguanosine (dG), 100 µM N-OH-ABP, 1 mM acetyl coenzyme A, and Compound 10 (0-100 µM) were incubated at 37°C for 10 min. Reactions were stopped with the addition of 100 µL of water saturated ethyl acetate and centrifuged for 10 minutes at 13, 000 g. The organic phase was removed, evaporated to dryness, and re-suspended in 100 µM of 10% acetonitrile. HPLC separation was achieved using a gradient of 80:20 sodium perchlorate (pH 2.5): acetonitrile over 3 minutes to 50:50 sodium perchlorate (pH 2.5)/acetonitrile and dG-C8-ABP adducts were detected at a wavelength of 300 nm.

DNA Isolation and dG-C8-ABP Quantitation

DNA was isolated as previously described by Bendaly et. al. 2009. Cells were incubated in alpha-MEM media containing 12.5, 40, and 200 µM ABP and various concentrations of Compound 10 (0-250 µM). After cells reached approximately 90% confluency, cells were harvested. The cells were centrifuged for 5 min at 13, 000g, and the cell pellet was resuspended in homogenization buffer, 0.1 volume of 10% SDS, and 0.1 volume of Proteinase K and incubated overnight at 37° C. The DNA was extracted using phenol/choloroform:isomyl alcohol and precipitated with isopropanol. The pellet was dried and resuspended in 500 µL of DNA adduct buffer (5 mM Tris pH 7.4, 1 mM $CaCl_2$, 1 mM $ZnCl_2$, and 10 mM $MgCl_2$). The DNA was quantitated by spectrophotometry, A_{260}.

Evaluation of Cell Invasion

To determine the effects of Compound 10 on invasive potential of MDA-MD-231 cells, we utilized the CytoSelectTM 24-well cell invasion assay, colorimetric format (Cell Biolabs Inc., San Diego, CA). The assay was completed according to the manufacturer's protocol. Cells (300,000) were seeded and allowed to invade towards culture media containing 10% FBS for 24 h in the presence of various concentrations (0, 31.25, 62.5, and 125 µM) of Compound 10. Cells on the bottom of the polycarbonate membrane were stained, extracted, and the absorbance was quantified at 560 nm. Cell invasion was plotted as the percentage of controls (DMSO).

Flow Cytometric Analysis of Cell Cycle

For cell cycle analysis MDA-MB-231 cells were treated with Compound 10 (0 – 250 μM) in culture media for 144h. Cells were harvested by trypsinization and fixed in 70% ethanol at 4°C overnight. Fixed cells were collected by centrifugation and washed with cold PBS. Cells were then stained with 0.1 mg/mL propidium iodide in 0.6% Triton-X in the presence of RNase A (100U/mL final, Sigma) for 1 h in the dark at room temperature. Cell cycle analysis was performed on a FACSCalibur according to manufacturer's protocol (BD Biosciences). A minimum of 20,000 cells were analyzed per sample. Data were collected and analyzed using FlowJo Software (Ashland, OR).

Real-time-PCR for RT^2 Profiler PCR Array

MCF-7 cells were cultured in medium treated with Compound 10 (0 and 125 μM) for 24 h. Cells were harvested by trypsinization and total RNA was isolated using the RNeasy kit (Qiagen) followed by removal of contaminating DNA by treatment with TurboDNase Free (Ambion, Austin, TX). Synthesis of first strand cDNA was performed using Genomic DNA Elimination Mixture provided by the Human Breast Cancer RT^2 Profiler PCR Human Breast Cancer Array (SA Biosciences) according to manufacturer's protocol. This real-time PCR array profiles the expression of 84 key genes commonly involved in biological processes during breast carcinogenesis and in breast cancer cell lines. The PCR components (2x RT^2 SYBER Green Mastermix, cDNA synthesis reaction, and RNase-free water) were dispensed into the RT^2 Profiler PCR Array and applied to the Applied

Biosystems StepOnePlus Real-Time PCR System (Applied Biosystems). Differences in mRNA levels were determined in comparison to the control (DMSO). Fold-change values greater than one indicated a positive- or an up-regulation, and the fold-regulation is equal to the fold-change. Fold-change values less than one indicated a negative or down-regulation, and the fold-regulation is the negative inverse of the fold-change.

Mitotic Indices

MDA-MB-231 cells were treated with Compound 10 (0, 62.5, and 250 µM) for 24, 48, 72, and 144h. Cells were harvested and prepared for mitotic index as previously described by States et. al 2002. Briefly, cells were resuspended in serum-free 0.4% KCl for 10 min at 37°C. Fixative solution (methanol:acetic acid, 3:1,v/v) as added at 2% total volume. Cells were fixed at room temperature for 20 min. Cells were then dropped onto slides and allowed to air dry. Slides were then stained with Wright-Giema, allowed to dry, and examined under a microscope.

Western Blotting

The effect of Compound 10 on NAT1, Cyclin B1, and Cyclin D1 protein expression in UV5-CHO or MDA-MB-231 cells was evaluated by western blot. Cells were cultured at 37°C in 5% CO_2 in alpha-modified minimal essential medium (α-MEM, Lonza, Walkersville, MD) supplemented with 10% fetal bovine serum (Hyclone, Logan, UT), 100 U/mL penicillin (Lonza), 100 µg/mL streptomycin (Lonza), and 2 mM L-glutamine (Lonza) and treated with

Compound 10 (0, 62.5, and 250 µM) for 96 h. After which, cells were harvested by trysinization and lysates were prepared as previously described above. Approximately 20 µg of cell lysate were mixed with 1:1 5% β-mercaptoethanol in Laemmli buffer (Bio-Rad), boiled for 5 min, and resolved by 12% SDS-PAGE gel. The proteins were transferred by semi-dry electroblotting to polyvinylidene fluoride (PVDF) membrane. The membranes were probed with the primary mouse monoclonal IgG G5 (NAT1, 1:2000, Santa Cruz Biotechnology), SC245 (cyclin B1, 1:2000, Santa Cruz Biotechnology), or Cyclin D1 (cyclin D1, 1:2000, Santa Cruz Biotechnology), and with horse radish peroxidase (HRP) - conjugated secondary goat anti-mouse IgM antibody (Santa Cruz Biotechnology). West Pico Chemiluminescent substrate (Pierce) was used for signal detection and densitometric analysis was performed using Quantity One Software (Bio-rad laboratories, Hercules, CA) .

Statistical Analysis

Statistical differences were assessed using one-way analysis of variance (ANOVA) for multiple comparisons or an unpaired Student's t test for single comparisons using Prism 5 (GraphPad, La Jolla, CA).

Compound 10 decreases endogenous NAT1 activity and ABP-induced DNA adducts

MDA-MB-231 and MCF-7 human breast adenocarcinoma cells were incubated with several concentrations of compound 10 in the presence of NAT1 substrates PABA and ABP. As illustrated in Figure 4.1, compound 10 inhibited endogenous ABP and PABA *N*-acetylation activity in both human breast cancer cell lines in a dose dependent manner. In MDA-MB-231 cells compound 10 at the highest concentration, 250 µM, completely inhibited ABP *N*-acetylation. Similar effects were seen in both cell lines.

We postulated that a decrease in *N*-acetylation through inhibition of NAT1 would result in a decrease in toxicological outcomes associated with NAT1 metabolism. In order to test this hypothesis we evaluated the effect of Compound 10 on the *N*-hydroxy-ABP *O*-acetylation and ABP-induced dG-C8-ABP adduct formation. We utilized MDA-MB-231 cells to determine if Compound 10 inhibition would cause a decrease in endogenous *O*-acetylation activity. As illustrated in Figure 4.2, Compound 10 decreased *N*-hydroxy-ABP *O*-acetyltransferase activity in a dose-dependent manner. Coupled with cytochrome P450 hydroxylation, *O*-acetylation of *N*-hydroxylated amines contributes toward the activation of carcinogenic amines such as ABP. These *N*-acetoxy compounds, such as *N*-acetoxy-ABP, will form arylnitrenium ions resulting in DNA adducts. If these adducts are not repaired through cellular DNA repair mechanisms, mutations will occur that initiate cancer progression. To further explore the ability of NAT1

inhibition to decrease adduct formation we treated both UV5-CHO and MDA-MB-231 cells with ABP in the presence of Compound 10. Compound 10 decreased the formation of ABP-induced dG-C8-ABP adducts in UV5- CHO cells stably expressing *CYP1A1* and *NAT1*4* (Figure 4.3a). Compound 10 was not as effective in decreasing ABP-induced adducts in the MDA-MB-231 cells (Figure 4.3b). We speculate that this is because, unlike UV5-CHO cells, MDA-MB-231 cells are able to repair DNA adducts. Together these data confirm that Compound 10 is able to inhibit endogenous NAT1 *N*-acetylation and *O*-acetylation activity, consequently reducing ABP activation and ABP-induced dG-C8-ABP DNA adduct formation in UV5-CHO and human adenocarcinoma breast cells.

Compound 10 inhibits cell proliferation in a highly metastatic human breast cancer cell line

To further elucidate the role of NAT1 in cell proliferation, we examined the effect of NAT1 inhibition by Compound 10 on cell proliferation. Initially, we tested the effect of Compound 10 on cell viability in order to address any concern that a decrease in NAT1 activity was caused by Compound 10 toxicity. Cell viability was measured by the AlamarBlue fluorescence assay. This nontoxic dye detects functional oxidative phosphorylation in order to determine the number of viable adherent and floating cells which is indicated by fluorescence intensity.

We evaluated Compound 10 toxicity in MDA-MB-231 cultured in medium treated with various concentrations of Compound 10 for 4, 24, 48, 72, and 144 h.

Fluorescence intensity was measured at time points 4 - 48 h to determine effects of Compound 10 on cell viability. These time points correspond to the periods at which NAT1 activity inhibition experiments were conducted (4 h) and are within doubling times for these cells. Compound 10 did not decrease cell viability of MDA-MB-231 (Figure 4.4a) or MCF-7 (Figure 4.4b) cells at these time points. Fluorescence intensity increases at these time points indicate that Compound 10 did not affect cell viability. These cell viability data were also utilized to determine if Compound 10 inhibition affects cell proliferation. Figure 4.4 also illustrates that at time points 72 and 144h, there is a dose-dependent decrease in cell proliferation. This was determined by the decrease in fluorescence intensity which is indicative of a decrease in cell number. These data demonstrate that while Compound 10 is not toxic to MDA-MB-231 cells, at longer time points (above 72 h) cell proliferation is disrupted.

One major concern when developing a therapeutic inhibitor is the effect the compound will have on non-tumorigenic cells at later time points. Therefore, we also tested the ability of Compound 10 to decrease cell viability and proliferation in a non-tumorigenic cell line, MCF-10A. As seen in Figure 4.4, a similar pattern was observed in the non-tumorigenic cells (MCF-10A) as in the tumorigenic cells (MDA-MB-231). Cell viability of MCF-10A cells was not affected as indicated by fluorescence intensity at early time points. However, as seen in MDA-MB-231 cells, a decrease in cell proliferation was observed in the non-tumorigenic cell line. A comparison between the tumorigenic and non-tumorigenic cell lines was established to determine selectivity of Compound 10

for tumorigenic cells. This was achieved by calculating the corresponding IC_{50} for cell proliferation at 72 h in MCF-10A and MDA-MB-231 which resulted to be 113 and 32 µM respectively. We also calculated the *in situ* therapeutic index (TI) = IC_{50} non-tumorigenic cells/ IC_{50} tumorigenic cells. The TI for Compound 10 is 3.4, which shows moderately low toxicity towards non-tumorigenic human breast epithelial cells. These data show that inhibition of NAT1 activity by Compound 10 disrupts cell proliferation in tumorigenic and non-tumorigenic human breast cell lines. These data support previous findings that suggest that NAT1 plays an important role in cell proliferation, and consequently is a molecular target for cancer therapy.

Compound 10 treatment suppresses cell invasion

Cell invasion is considered one of the hallmarks of progression in metastatic cancers. Cell migration is an important facilitator of cell invasion because once cells gain the ability to migrate to distal organs and tissues, cell invasion can ensue. Our studies have shown that Compound 10 can suppress the migration of MDA-MB-231(Figure 4.5) and MCF-7 (Figure 4.6) cells in a dose-dependent manner. Cells treated with a non-cytotoxic dose of Compound 10 for 24 h demonstrated a decrease in cell migration. These results suggest that Compound 10 can decrease cell invasion of metastatic breast cancer cells. Although we have shown that Compound 10 can decrease the invasion potential of these human breast cancer cells, the exact mechanism is unknown.

Effect of Compound 10 on NAT1 Levels

In order to investigate the possibility of the decrease in NAT1 activity in cultured cells being a result of a decrease in NAT1 protein, we evaluated the expression of NAT1 protein after Compound 10 treatment. UV5-CHO cells were incubated at 37°C for 3 d in the presence of 0, 62.5, and 250 μM Compound 10. These data (Figure 4.8A) show that Compound 10 does not affect NAT1 protein expression in cultured cells.

Effects of Compound 10 on cell cycle progression

We evaluated the effects of Compound 10 on cell cycle progression by measuring mitotic indices of human breast cancer cells treated for 24, 72, and 144 h. The mitotic index of treated cells increased in a dose- and time-dependent manner (Figure 7). We used western blot analysis to evaluate the protein expression of cell cycle cyclins B1 and D1. Cyclin B1 expression significantly ($p<0.05$) increased with increasing dose, while Cyclin D1 protein expression remained the same (Figure 4.8).

Compound 10 causes differential expression of genes involved in human breast carcinogenesis

We investigated the potential mechanism of action of Compound 10 by evaluating gene expression changes using PCR array. There were 11 genes

that were up-regulated upon Compound 10 treatment and 13 genes that were down-regulated compared to the vehicle treated control (Table 4.1).
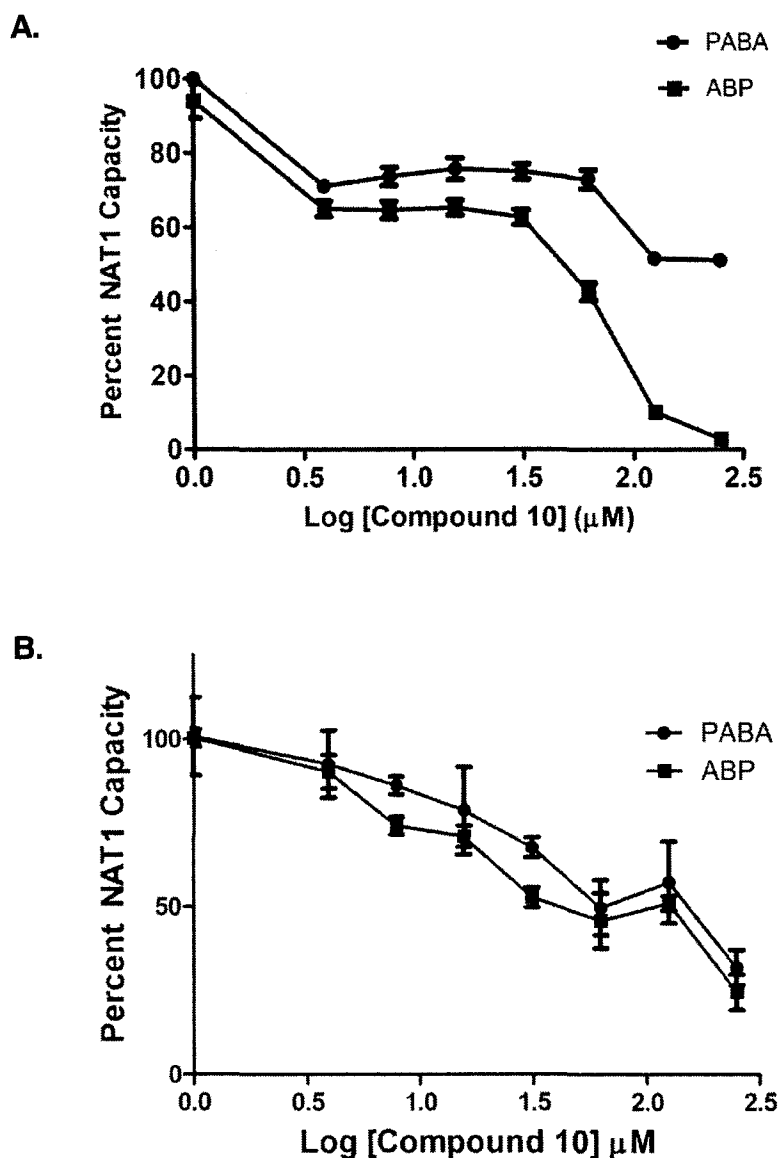
Figure 4.1 Inhibition of *in situ* NAT1 capacity in human breast adenocarcinoma MDA-MB-231 **(a)** and MCF-7 **(b)** cells that express endogenous NAT1. These cells were treated with media supplemented with 10 μM ABP or PABA with varying concentrations of Compound 10 (0 – 250 μM). Reaction products were collected and analyzed using high-performance liquid chromatography (HPLC) to determine the amount of acetylated product. Each point represents mean ± SEM for 3 experiments.
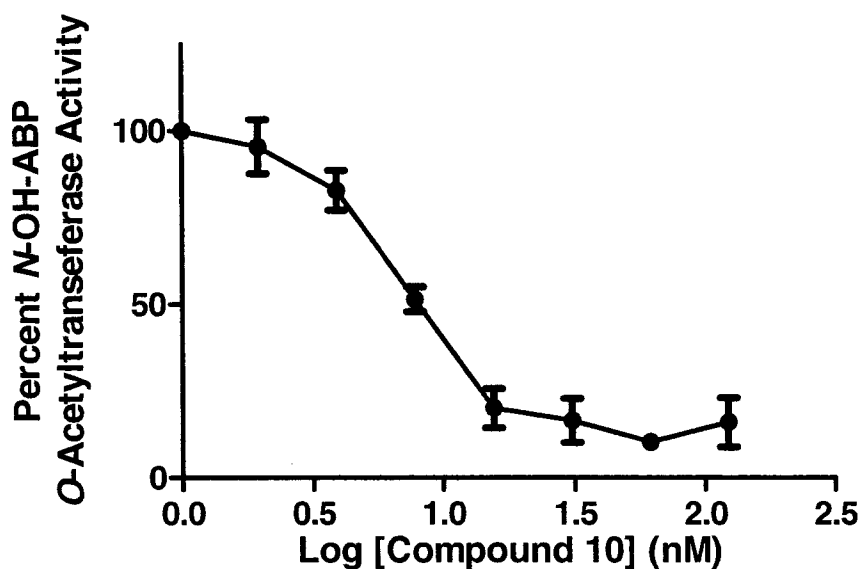
Figure 4.2. Compound 10 inhibition of N-OH-ABP O-acetyltransferase activity in human breast adenocarcinoma cells (MDA-MB-231) that express endogenous NAT1. Assays containing 50 µg protein, 100 µM N-OH-ABP, 1 mM acetyl coenzyme A, 1mg/mL deoxyguanosine, and Compound 10 (0 -100 µM) were incubated for 10 min. at 37°C. Reactions were stopped with the addition of 100 µL of water saturated ethyl acetate and centrifuged at 13,000xg for 10 min. The organic phase was removed, evaporated to dryness, dissolved in 100 µL of 10% acetonitrile, and injected onto the HPLC. Each point represents mean ±SEM for 3 experiments.
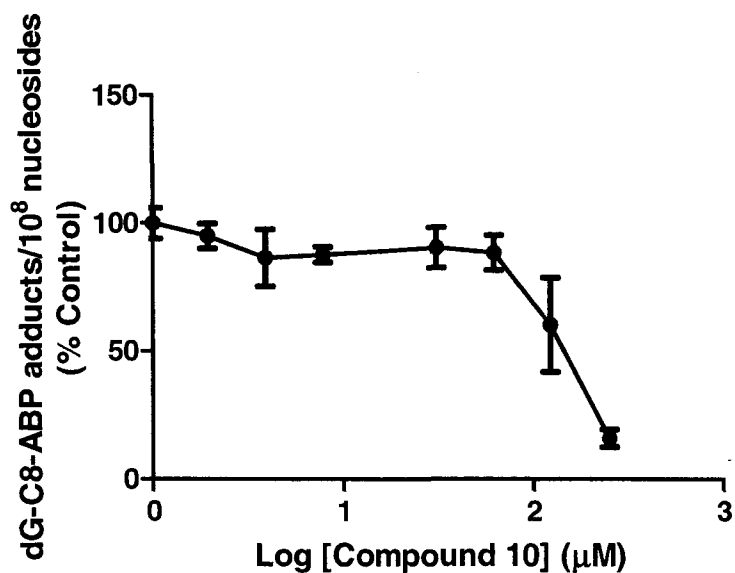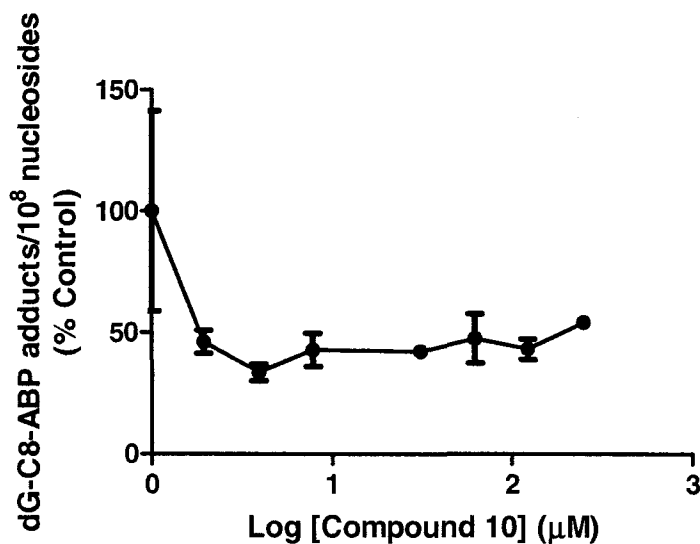
Figure 4.3 Percent ABP-induced dG-C8-ABP adduct formation in **(A.) UV5-CHO** cells stably expressing *CYP1A1* and *NAT1*4* and **(B.) MDA-MB-231** cells that express endogenous *NAT1*4*. ABP-induced dG-C8-ABP adducts/10^8 nucleosides were quantitated by mass spectrometry after cells were treated with Compound 10 for 24h. Adduct formation was plotted as the percentage of untreated cells (control). Each point represents the mean ± SEM for three determinations.
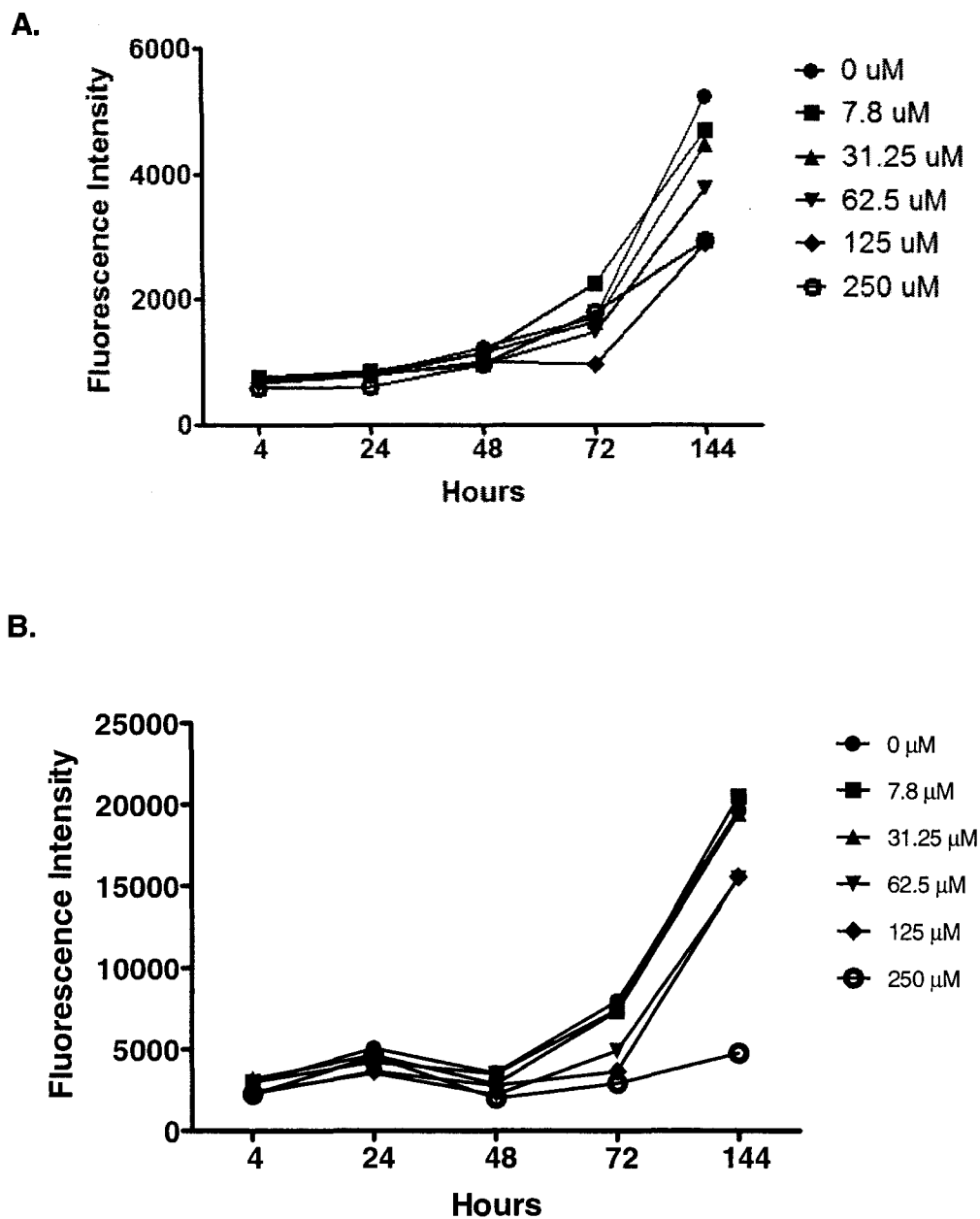
Figure 4.4 Determination of Compound 10 effect on cell viability and cell proliferation using AlamarBlue® fluorescence assay in **(A.) tumorigenic MDA-MB-231** and **(B.) non-tumorigenic MCF-10A cells**. Cells were plated and treated with Compound 10 at various concentrations (0- 250 µM) for up to 144h. AlamarBlue® was added in an amount equal to 10% (v/v) volume directly to the cells in culture media 1 h prior to the desired time point. The fluorescence was read using a fluorescence excitation wavelength of 570 nm and emission of 580 nm. Each point represents the mean ± SEM from 4 experiments.

A.

B. 100% (0 µM) **C.** 72% (125 µM)
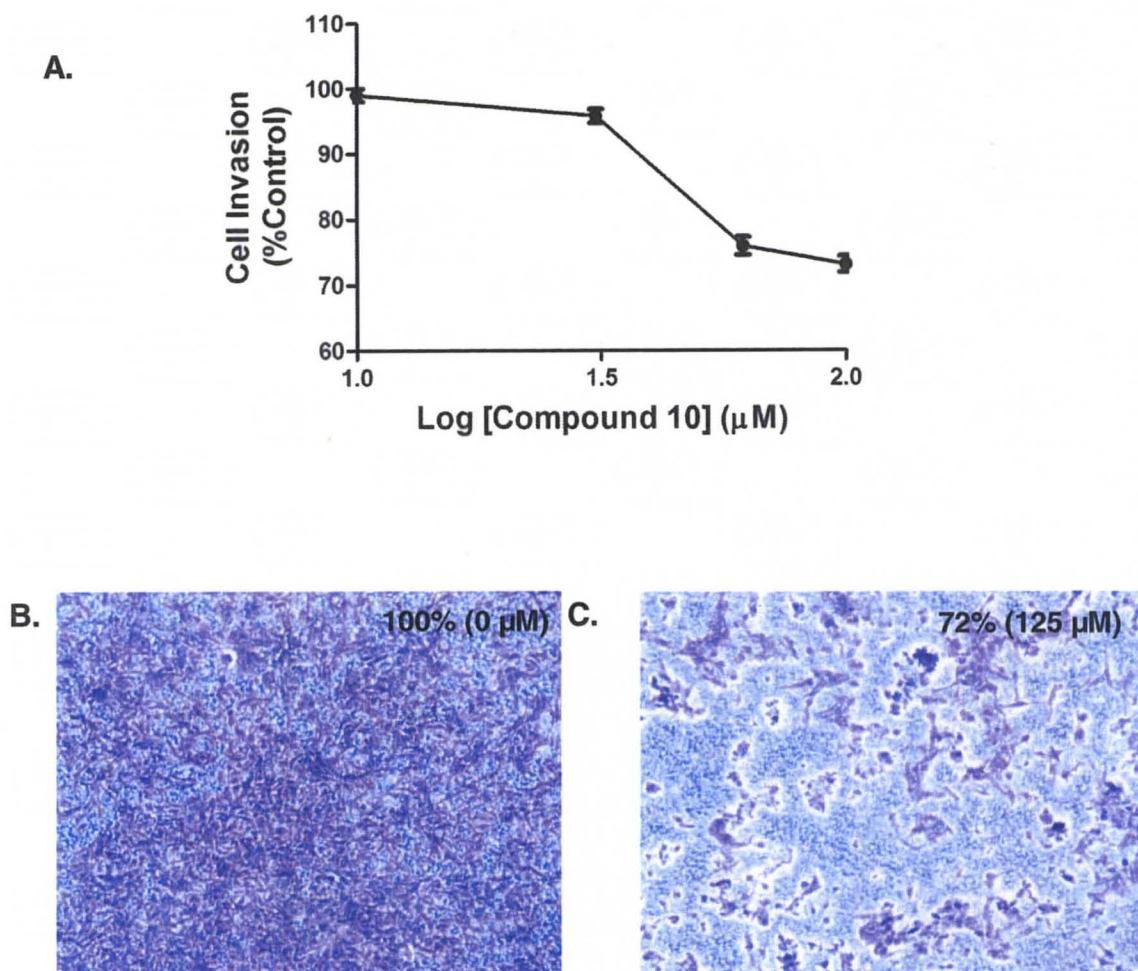
Figure 4.5 A. Inhibition of cell invasion by Compound **10** in MDA-MB-231 cells. 300,000 cells were seeded and allowed to invade towards culture media containing 10% FBS for 24 h in the presence of various concentrations (0, 31.25, 62.5, and 125 µM) of Compound **10**. Cells on the bottom of the polycarbonate membrane were stained, extracted, and the absorbance was quantified at 560 nm. Cell invasion was plotted as the percentage of untreated cells (control). Each point represents the mean ± SEM for 3 experiments. **Figures 4.5B – C.** Representative photographs of invasive cells from cell invasion assay at Compound **10** concentrations of 0 µM and 125 µM, respectively.
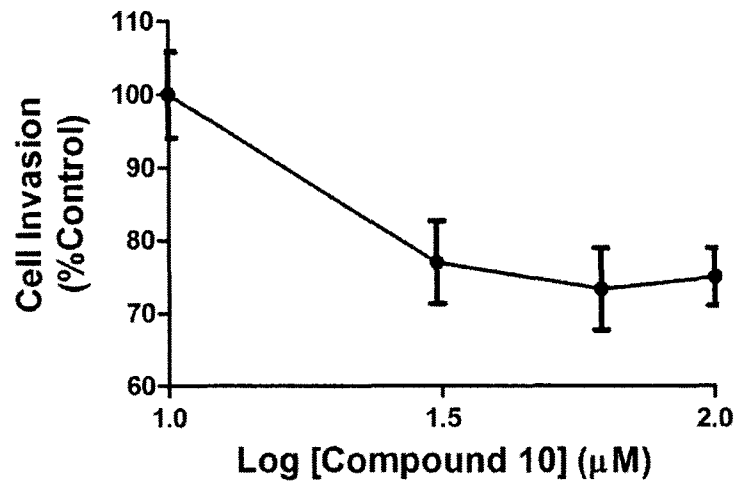
Figure 4.6 Inhibition of cell invasion by Compound **10** in MCF-7 cells. Cells were seeded and allowed to invade towards culture media containing 10% FBS for 24 h in the presence of various concentrations (0, 31.25, 62.5, and 125 μM) of Compound **10**. Cells on the bottom of the polycarbonate membrane were stained, extracted, and the absorbance was quantified at 560 nm. Cell invasion was plotted as the percentage of untreated cells (control). Each point represents the mean ± SEM for 3 experiments.
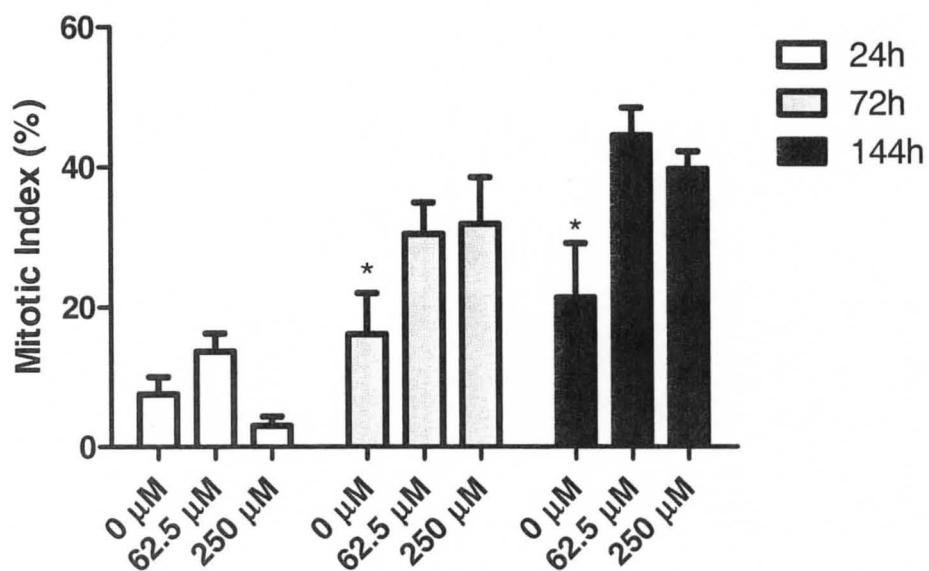
Figure 4.7 Mitotic index of MDA-MB-231 treated with compound 10. Cells were treated for 24, 72, and 144h with 0, 62.5, and 250 µM compound 10 and resuspended in serum-free media with 0.4% KCl, Fixed in methanol:acetic acid, 3:1,v/v, dropped onto slides and allowed to air. Slides were stained with Wright-Giema, allowed to dry, and examine under a microscope. A total of 200 cells were counted per slide. Mitotic index was significantly (p< 0.05) lower at 0 µM than at 72 and 144 h timepoints when compared to 62.5 and 250 µM at the same time points. Each bar represents mean ± SEM for 3 slides.
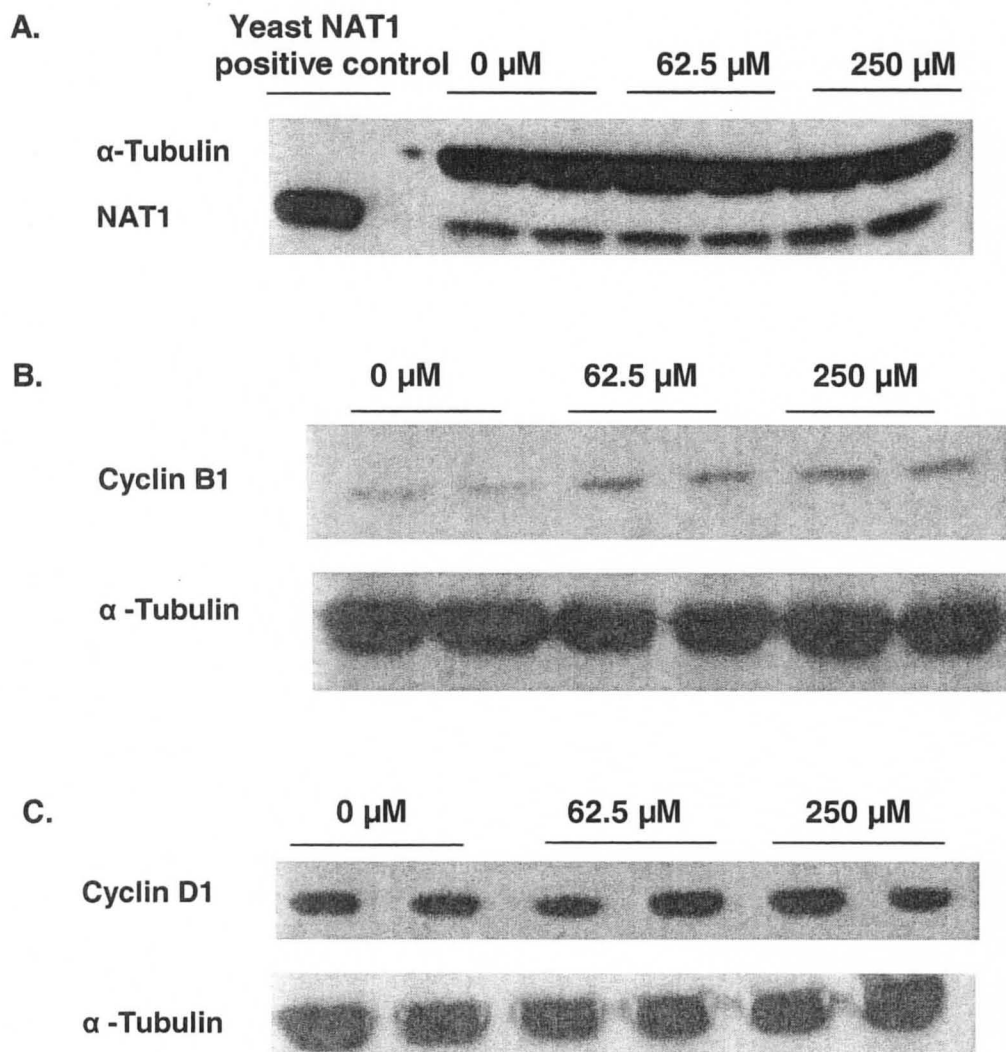
Figure 4.8 Western blot analysis of NAT1, Cyclin B1, and Cyclin D1 protein expression following Compound 10 treatment. UV5-CHO (NAT1 protein expression) or MDA-MD-231(Cyclin B1 and D1) cells were treated with 0, 62.5, and 250 µM compound 10 for 4 days. Cellular lysate proteins were resolved by SDS-PAGE, transferred to PVDF membranes, and probed for NAT1, Cyclin B1, or Cyclin D1.

A.

Gene Name	Fold Up-regulation
Mitogen-activated protein kinase 3	2.0654
Snail homolog 2 (Drosophilia)	2.1834
Cyclin A1	2.3178
Retinoblastoma 1	2.4152
Rass association domain family member 1	2.4531
MutL homolog 1, colon cancer, nonpolyposis type 2	2.4887
Hypermethylated in cancer 1	3.1823
ATP- binding cassette, sub-family B	3.566
Keratin 5	5.2782
Matrix metallopeptidase 2	6.1539
Cyclin E1	7.9511

B.

Gene Name	Fold Down-regulation
Glutathione S -transferase	-1.5425
Baculoviral IAP repeat containing 5	-1.5335
GLI family zinc finger 1	-1.5089
X-box binding protein 1	-1.416
Cyclin D2	-1.3628
Slit homolog (Drosophila)	-1.3425
ADAM metallopeptidase domain 23	-1.3361
Breast cancer 2, early onset	-1.2611
Solute carrier family 39(zinc transporter), member	-1.2402
Interleukin 6 (interferon, beta 2)	-1.1377
Cyclin-dependent kinase inhibitor 2A	-1.1158
Cystastin E/M	-1.0643
Nuclear receptor subfamily 3, group C, member 1	-1.0622

Table 4.1 Gene expression fold changes in MCF-7 cells treated with Compound 10 (0 and 125 µM) for 24h. Total RNA was harvested and reverse-transcribed for subsequent real–time PCR analysis assaying the expression of a series of 84 genes linked to human breast cancer progression. Genes showing significant increase (A.) and decrease (B.) in fold change compared to untreated cells (the control) are listed. Genes that did not show differential expression after treatment are not shown.

DISCUSSION

Studies have implicated arylamine NAT1 in tumor and cancer progression (Tiang et al., 2010). Its expression has been associated with the incidence of many cancers such as breast, lung, and bladder cancers. Accordingly, NAT1 is a proposed molecular target for cancer therapy. In the current study, we report that our lead compound ethyl[1-(3-ethoxycarbonylpropanoyloxy)-10-dioxo-2-anthryl-butanedioate (Compound 10) is a novel small molecule inhibitor of NAT1 that suppresses experimental cancer initiation and progression. Compound 10 displayed an *in vitro* and *in situ* IC_{50} that demonstrates greater potency when compared to previously reported NAT inhibitors, such as tamoxifen (IC_{50} = 57 µM) (Kawamura et al., 2008) . A decrease in *O*-acetylated product with NAT inhibition suggests that this inhibitor decreases carcinogen activation in human breast cancer cells. These data are important in that they provide further evidence that NAT is becoming increasingly important as a novel therapeutic target.

We recognize that in order to strengthen this study, NAT1 binding assays using differential scanning calorimetry are important. Precise experimental methods to determine ligand-binding affinity are needed to enhance drug discovery (de Azevedo et al., 2008). However, isolated NAT1 is very unstable (Husain et al., 2007) making these experiments very difficult to perform. A prior study showed that Compound 10 as a chemotherapeutic agent to reduce the growth of transplanted tumors in mice (Gal et al., 1952). Our study is the first to provide insight on the mechanism of action for this compound.

We have utilized PCR arrays to show that NAT1 activity may be related to cell signaling pathways that are important in human breast cancers. These data will allow us to explore these cell signaling pathways in order to better understand the mechanistic role of NAT1 in cancer progression. Our studies suggest that NAT1 plays an important role in cell cycle progression. These data show an increase of mitotic indices and mitosis-related cyclin B1 upon Compound 10 treatment. These results provide insight to the role that NAT1 plays in cancer progression. Until recently, the role of NAT1 in cancer progression was attributed only to its role in arylamine carcinogen metabolism. Here not only do we support recent findings that implicate NAT1 in cell growth and proliferation, but we suggest a potential role that NAT1 may play a role in regulating cell cycle progression. Future studies include investigation into the use of chemopreventive natural products in combination with Compound 10 to enhance the chemopreventive effects of our lead inhibitor. We are also exploring the use of differential scanning calorimetry to confirm ligand-protein binding.

Cancer is a major public health concern in the United States. The American Journal for Clinicians estimates that in 2012 there will be an estimated 1.6 million new cases of cancer. Although, the rate of cancer in both men and women has declined, progress needs to be made in reducing incidence and mortality rates. Therefore further progress in new discoveries in cancer prevention, early detection, and treatment is important . In conclusion, these data

suggest that NAT can be used as a molecular target for the treatment of cancers related to NAT1 expression and the activation of environmental carcinogens.

CHAPTER V

SUMMARY AND CONCLUSIONS

This dissertation project used computational and experimental methods to provide an in depth understanding of the role that human arylamine *N*-acetyltransferase plays in carcinogen metabolism and cancer progression. These studies provide clarity and future direction for functional genomic and epidemiological studies that seek to explain relationships between carcinogen exposure, metabolism, and cancer susceptibility. In this study, we have made progress towards understanding the mechanistic role that NAT1 plays in cell proliferation and cell cycle, and therefore cancer progression.

Functional genomic studies in human fibroblasts

In Chapter 1, we described the successful construction and use of NER-deficient immortalized human fibroblast cell lines in order to better understand the role of human NAT1 and NAT2 in carcinogen metabolism and substrate selectivity. Our model allowed us to provide insight into functional genomic studies that seek to clarify relationships between human NAT1, human NAT2, and human CYP1A2. The data obtained in this study show that arylamine NAT compound selectivity influences disposition and detoxification of well-

characterized and putative arylamine carcinogens that are persistent in the environment. Furthermore, this study suggests that known genetic polymorphisms in enzymes that metabolize environmental carcinogens may be more biologically relevant to substrates that show selectivity for such enzymes. For example, our studies show that known NAT2 genetic polymorphisms should be most biologically relevant for the putative carcinogen 3,5-DMA. These findings can be used to predict overall inter-individual risk of carcinogenesis based on haplotype and exposure.

The phase I XMEs CYP450s can lead to the activation of procarcinogens to electrophilic intermediates that cause DNA damage and toxicity. Studies suggest that CYP levels not only affect tumor initiation, but signal transduction pathways, which alter cell cycle, tumor promotion, and tumor progression (Nebert et. al., 2006). In this study, we sought to determine the effects of varying CYP-mediated activation on NAT detoxification. Although our model mimics the classical interaction of environmental carcinogens and phase I and phase II XMEs, our data were inconclusive suggesting that our model is too simplistic and more work needs to be completed to understand the complex interplay between phase I and phase II enzymes that work in concert.

Our laboratory has reported in several studies substantial levels of cytotoxicity, mutagenesis, and DNA adduct formation upon treatment with ABP in Chinese hamster ovary cells stably expressing human NAT1. Similar findings were not seen in our human fibroblast lines which led us to the investigation of total GST. We found that our human fibroblast lines express GST activity, which

may have contributed to the detoxification of the well-characterized carcinogen ABP. Due to the lack of ABP-induced toxicological outcomes in the human cells used in the present study, we have concluded that epidemiology studies may benefit from studying the effects of genetic differences in multiple XMEs that contribute to carcinogen metabolism and cancer susceptibly. These combinatory functional genomic studies may provide insight to the effects of complex phenotypes, a trait caused by two or more genes and environmental factors, on individual risk to environmental carcinogen-induced cancer.

Small molecule inhibition of NAT1

Computational modeling studies were used to identify effective small molecule inhibitors of human NAT1. Upon confirming effective small molecules of NAT, we evaluated the effects of therapeutic inhibition of NAT1 on carcinogen metabolism and cancer progression. The data in this dissertation show that NAT1 inhibition decreases ABP O-acetylation and ABP-induced DNA adducts in CHO cells stably transfected with human NAT1. Our studies also support previous findings that suggest that NAT1 plays an important role in cell proliferation and cell invasion. The most effective inhibitor, Compound 10, in this study decreased cell proliferation and cell invasion in human breast cancer cell lines. These findings suggest that pharmacological inhibitors of NAT1 could lay the foundation for cancer therapeutic applications that use NAT1 as a molecular target. Future protein-ligand binding studies are required to confirm NAT1 protein binding. In addition to confirming NAT1 binding, it is important to determine off-target effects caused by NAT1 inhibition using our lead compound.

We could utilize computational systems that explore structural and metabolomic data to identify and to compare ligand binding sites on protein structures. This future study will allow the prediction of off-target binding sites across the human proteome. This type of computational study, as described by Chang et. al. (2010) uses a novel integration of structural and systems biology to screen the human proteome to identify off-target drug-binding sites. We can utilize this list of potential off target binding sites to focus on putative metabolic off-targets. Our laboratory could then consider the off-targets that impact cancer progression to confirm that the inhibition of cancer progression is a NAT1 inhibition response.

NAT1 inhibition and cell cycle regulation

We utilized Compound 10 to investigate the mechanistic role that NAT1 plays in cancer progression. We performed pathway –focused RT^2 Profiler PCR arrays to evaluate the gene expression of 84 genes that regulate signal transduction and other biological processes during human breast cancer progression. In this study, inhibition of NAT1 in human breast cancer cells (MCF-7) was associated with differential expression of genes that play a role in human breast cancer including genes that are important in cell cycle, adhesion, apoptosis, and angiogenesis. Because our data also showed an increase in mitotic index after treating human breast cancer cells with our NAT1 inhibitor, we were especially interested in the differential expression of the profiled cyclins. Although cyclin B, a M phase cyclin, was not included in the PCR array, we confirmed by Western Blotting that after Compound 10 treatment there was a significant increase in cyclin B expression. These findings suggest that

independent of carcinogen metabolism, NAT1 plays an important role in carcinogenesis through cell cycle regulation, moreover mitotic progression.

Folate is a water-soluble B vitamin that is essential for DNA synthesis, DNA methylation, and cell division. Folate is especially important during periods of rapid cell division making rapidly dividing cells more susceptible to folate metabolism disruption (Minchin et al., 2012). P-aminobenzyolglutamate (PABG), a folate catabolite, is the only known endogenous NAT1 substrate (Minchin et al., 2012). PABG is acetylated by NAT1 and the acetylated product is excreted from the cell. This process influences the regulation of folate metabolism. PABG can compete with folic acid for folate-binding protein causing it to act as an antagonist to some folate dependent enzymes (Minchin et al., 1995). Studies have shown that in transgenic mice, high NAT1 activity is associated with low folate levels. Therefore, NAT1 is suspected to be a modulator of folate catabolism (Cao et al., 2010).

We postulate that inhibiting NAT1 decreases the *N*-acetylation of PABG, which increases PABG cellular levels resulting in feedback inhibition of the folate catabolism pathway. As reported in the literature, a disruption in folate metabolism results in impaired cell division, reduced cell growth, decreased DNA repair, and changes in epigenetic modifications (Krupenko et. al., 2002). Although our hypothesis needs to be further investigated, our results suggest that NAT1 inhibition plays an important role in cell proliferation and mitosis by indirectly modulating cellular folate levels.

REFERENCES

Adam, P. J., Berry, J., Loader, J. A., Tyson, K. L., Craggs, G., Smith, P.,Terrett, J. A. (2003). Arylamine N-acetyltransferase-1 is highly expressed in breast cancers and conveys enhanced growth and resistance to etoposide in vitro. *Molecular cancer research, 1*(11), 826-835.

Bell, D. A., Badawi, A. F., Lang, N. P., Ilett, K. F., Kadlubar, F. F., & Hirvonen, A. (1995). Polymorphism in the N-acetyltransferase 1 (NAT1) polyadenylation signal: association of NAT1*10 allele with higher N-acetylation activity in bladder and colon tissue. *Cancer research, 55*(22), 5226-5229.

Beland F. A., Beranek D.T., Dooley K.L., Heflich R.H., Kadlubar F.F. (1983) Arylamine-DNA adducts in vitro and in vivo: their role in bacterial mutagenesis and urinary bladder carcinogenesis. *Environmental health perspectives*, 49(62),125-34

Bendaly, J., Doll, M. A., Millner, L. M., Metry, K. J., Smith, N. B., Pierce, W. M., Jr., & Hein, D. W. (2009). Differences between human slow N-acetyltransferase 2 alleles in levels of 4-aminobiphenyl-induced DNA adducts and mutations. *Mutation research, 671*(1-2), 13-19.

Bendaly, J., Zhao, S., Neale, J. R., Metry, K. J., Doll, M. A., States, J. C.,Hein, D. W. (2007). 2-Amino-3,8-dimethylimidazo-[4,5-f]quinoxaline-induced DNA adduct formation and mutagenesis in DNA repair-deficient Chinese hamster ovary cells expressing human cytochrome P4501A1 and rapid or slow acetylator N-acetyltransferase 2. *Cancer epidemiology, biomarkers & prevention 16*(7), 1503-1509.

Bradford, M.(1976). A Rapid and Sensitive Method for the Quantitation of Microgram Quantities of Protein Utilizing the Principle of Protein-Dye Binding. *Analytical Biochemistry.* 72,248-254.

Cascorbi, I., Drakoulis, N., Brockmoller, J., Maurer, A., Sperling, K., & Roots, I. (1995). Arylamine N-acetyltransferase (NAT2) mutations and their allelic linkage in unrelated Caucasian individuals: correlation with phenotypic activity. *American journal of human genetics, 57*(3), 581-592.

Cao, W. Strnatka D., McQueen C.A., Hunter R.J., Erickson R.P. (2010) N-acetyltransferase 2 activity and folate levels. *Life Sciences*, 86(3)103-106.

Chang R.L., Xie L., Xie L., Bourne P.E., Palsson B.Ø. (2010) Drug Off-Target Effects Predicted Using Structural Analysis in the Context of a Metabolic Network Model. *PLoS Computational Biology* 6(9):1-18.

Dairou, J., Petit, E., Ragunathan, N., Baeza-Squiban, A., Marano, F., Dupret, J. M., & Rodrigues-Lima, F. (2009). Arylamine N-acetyltransferase activity in bronchial epithelial cells and its inhibition by cellular oxidants. *Toxicology and applied pharmacology, 236*(3), 366-371.

de Azevedo, W.F., Jr, Caceres R.A., Pauli I., Timmers L.F., Barcellos G.B., Rocha K.B., Soares M.B.(2008) Protein-drug interaction studies for development of drugs against Plasmodium falciparum. *Current Drug Targets*, 11(3), 271-278.

Doll, M.A., & Hein, D.W. (2002) Rapid genotype method to distinguish frequent and/or functional polymorphisms in human N-acetyltransferase-1. *Analytical biochemistry,* 301(2):328-32.

Fretland, A. J., Doll, M. A., Leff, M. A., & Hein, D. W. (2001). Functional characterization of nucleotide polymorphisms in the coding region of N-acetyltransferase 1. *Pharmacogenetics, 11*(6), 511-520.

Gal, E.M., Fung F.H., Greenburg D.M. (1952) Studies on the biological action of malononitriles. II. Distribution of rhodanese (transulfurase) in the tissues of normal and tumor-bearing animals and the effect of malononitriles thereon. *Cancer research*, 12(8), 574-579.

Grant, D. M., Morike, K., Eichelbaum, M., & Meyer, U. A. (1990). Acetylation pharmacogenetics. The slow acetylator phenotype is caused by decreased or absent arylamine N-acetyltransferase in human liver. *The Journal of clinical investigation, 85*(3), 968-972.

Hein, D.W., Ferguson, R.J., Doll, M.A., Rustan, T.D., and Gray, K. (1994). Molecular genetics of human polymorphic N-acetyltransferase: enzymatic analysis of 15 recombinant human wild-type, mutant, and chimeric NAT2 allozymes. *Human Molecular Genetics* 3:729-734.

Hein, D. W. (2000). N-Acetyltransferase genetics and their role in predisposition to aromatic and heterocyclic amine-induced carcinogenesis. *Toxicology letters, 112-113*, 349-356.

Hein, D. W. (2002). Molecular genetics and function of NAT1 and NAT2: role in aromatic amine metabolism and carcinogenesis. *Mutation research, 506-507,* 65-77.

Hein, D. W. (2006). N-acetyltransferase 2 genetic polymorphism: effects of carcinogen and haplotype on urinary bladder cancer risk. *Oncogene, 25*(11), 1649-1658.

Hein, D. W. (2009). N-acetyltransferase SNPs: emerging concepts serve as a paradigm for understanding complexities of personalized medicine. *Expert opinion on drug metabolism & toxicology, 5*(4), 353-366.

Hein, D.W., Doll, M.A., Fretland, A.J., Leff, M.A., Webb, S.J., Xiao, G.H., Feng,Y. (2000). Molecular genetics and epidemiology of the NAT1 and NAT2 acetylation polymorphisms. *Cancer epidemiology, biomarkers & prevention, 9*(1), 29-42.

Hein, D. W., Doll, M. A., Gray, K., Rustan, T. D., & Ferguson, R. J. (1993). Metabolic activation of N-hydroxy-2-aminofluorene and N-hydroxy-2-acetylaminofluorene by monomorphic N-acetyltransferase (NAT1) and polymorphic N-acetyltransferase (NAT2) in colon cytosols of Syrian hamsters congenic at the NAT2 locus. *Cancer research, 53*(3), 509-514.

Hein, D. W., Doll, M. A., Rustan, T. D., Gray, K., Ferguson, R. J., & Feng, Y. (1994). Construction of Syrian hamster lines congenic at the polymorphic acetyltransferase locus (NAT2): acetylator genotype-dependent N- and O-acetylation of arylamine carcinogens. *Toxicology and applied pharmacology, 124*(1),16-24.

Husain, A., Zhang, X., Doll, M. A., States, J. C., Barker, D. F., & Hein, D. W. (2007a). Functional analysis of the human N-acetyltransferase 1 major promoter: quantitation of tissue expression and identification of critical sequence elements. *Drug metabolism and disposition, 35*(9), 1649-1656.

Husain, A., Zhang, X., Doll, M.A., States, J.C., Barker, D.F. and Hein, D.W. (2007b) Identification of N-acetyltransferase 2 (NAT2) transcription start sites and quantitation of NAT2-specific mRNA in human tissues. *Drug Metabolism and Disposition* 35(10): 721-727.

Kawamura T., Mutoh H., Tomita Y., Kato R., Honda,H. (2008) Cancer DNA microarray analysis considering multi-subclass with graph-based clustering method. *Journal of bioscience and bioengineering,* 106(5):442-8.

Krupenko S.A., Oleinik N.V. (2002) 10-formyltetrahydrofolate dehydrogenase, one of the major folate enzymes, is down-regulated in tumor tissues and possesses suppressor effects on cancer cells. *Cell growth and differentiation,* 13(5), 227-236.

Lipinski, C.A. (2000) Drug-like properties and the causes of poor solubility and poor permeability. *Journal of pharmacological and toxicological methods,* 44(1):235-49.

Liu, L., Von Vett, A., Zhang, N., Walters, K. J., Wagner, C. R., & Hanna, P. E. (2007). Arylamine N-acetyltransferases: characterization of the substrate specificities and molecular interactions of environmental arylamines with human NAT1 and NAT2. *Chemical research in toxicology, 20*(9), 1300-1308.

Liu, L., Wagner, C. R., & Hanna, P. E. (2008). Human arylamine N-acetyltransferase 1: in vitro and intracellular inactivation by nitrosoarene metabolites of toxic and carcinogenic arylamines. *Chemical research in toxicology, 21*(10), 2005-2016.

Noguti J., Barbisan L.F., Cesar A., Seabra C.D., Choueri, R.B., Ribeiro, D.A. (2012). In Vivo Models for Measuring Placental Glutatione-S-transferase (GST-P 7-7) Levels: A Suitable Biomarker for Understanding Cancer Pathogenesis. *In Vivo*. 26(4):647-50.

Martin, R. J., & Downer, R. G. (1989). Microassay for N-acetyltransferase activity using high-performance liquid chromatography with electrochemical detection. *Journal of chromatography, 487*(2), 287-293.

Metry, K. J., Zhao, S., Neale, J. R., Doll, M. A., States, J. C., McGregor, W. G., . . . Hein, D. W. (2007). 2-amino-1-methyl-6-phenylimidazo [4,5-b] pyridine-induced DNA adducts and genotoxicity in chinese hamster ovary (CHO) cells expressing human CYP1A2 and rapid or slow acetylator N-acetyltransferase 2. *Molecular carcinogenesis, 46*(7), 553-563.

Millner, L.M., Doll, M.A., Cai, J., States, J.C. and Hein, D.W. (2012). NATb/*NAT1*4* promotes greater N-acetyltransferase 1 mediated DNA adducts and mutations than NATa/*NAT1*4* following exposure to 4-aminobiphenyl. *Molecular Carcinogenesis,* 51,636-646.

Minchin, R. F. (1995). Acetylation of p-aminobenzoylglutamate, a folic acid catabolite, by recombinant human arylamine N-acetyltransferase and U937 cells. *The Biochemical journal,* 307(1), 1-3.

Minchin, R. F., Hanna, P. E., Dupret, J. M., Wagner, C. R., Rodrigues-Lima, F., & Butcher, N. J. (2007). Arylamine N-acetyltransferase I. *The international journal of biochemistry and cell biology, 39*(11), 1999-2005.

Russell, A. J., Westwood, I. M., Crawford, M. H., Robinson, J., Kawamura, A., Redfield, C., Sim, E. (2009). Selective small molecule inhibitors of the potential breast cancer marker, human arylamine N-acetyltransferase 1, and its murine homologue, mouse arylamine N-acetyltransferase 2. *Bioorganic & medicinal chemistry, 17*(2), 905-918.

Sanderson, S., Salanti, G., & Higgins, J. (2007). Joint effects of the N-acetyltransferase 1 and 2 (NAT1 and NAT2) genes and smoking on bladder carcinogenesis: a literature-based systematic HuGE review and evidence synthesis. *American journal of epidemiology, 166*(7), 741-751.

Skipper P.L., Kim M.Y., Sun H.L., Wogan G.N., & Tannenbaum S.R. (2010) Monocyclic aromatic amines as potential human carcinogens : old is new again. *Carcinogenesis,* 31(1):50-8.

States, J. C., & Myrand, S. P. (1996). Splice site mutations in a xeroderma pigmentosum group A patient with delayed onset of neurological disease. *Mutation research, 363*(3), 171-177.

States, J. C., Reiners, J. J., Jr., Pounds, J. G., Kaplan, D. J., Beauerle, B. D., McNeely, S. C., McCabe, M. J., Jr. (2002). Arsenite disrupts mitosis and induces apoptosis in SV40-transformed human skin fibroblasts. *Toxicology and applied pharmacology, 180*(2), 83-91.

Sugamori, K. S., Brenneman, D., Wong, S., Gaedigk, A., Yu, V., Abramovici, H., . . . Grant, D. M. (2007). Effect of arylamine acetyltransferase Nat3 gene knockout on N-acetylation in the mouse. *Drug metabolism and disposition: the biological fate of chemicals, 35*(7), 1064-1070.

Sugamori, K. S., Wong, S., Gaedigk, A., Yu, V., Abramovici, H., Rozmahel, R., & Grant, D. M. (2003). Generation and functional characterization of arylamine N-acetyltransferase Nat1/Nat2 double-knockout mice. *Molecular pharmacology, 64*(1), 170-179.

Tiang, J. M., Butcher, N. J., Cullinane, C., Humbert, P. O., & Minchin, R. F. (2011). RNAi-Mediated Knock-Down of Arylamine N-acetyltransferase-1 Expression Induces E-cadherin Up-Regulation and Cell-Cell Contact Growth Inhibition. *PloS one, 6*(2), e17367.

Tiang, J. M., Butcher, N. J., & Minchin, R. F. (2010). Small molecule inhibition of arylamine N-acetyltransferase Type I inhibits proliferation and invasiveness of MDA-MB-231 breast cancer cells. *Biochemical and biophysical research communications, 393*(1), 95-100.

Walker, K., Ginsberg, G., Hattis, D., Johns, D. O., Guyton, K. Z., & Sonawane, B. (2009). Genetic polymorphism in N-Acetyltransferase (NAT): Population distribution of NAT1 and NAT2 activity. *Journal of toxicology and environmental health, 12*(5-6), 440-472.

Walraven, J. M., Trent, J. O., & Hein, D. W. (2008). Structure-function analyses of single nucleotide polymorphisms in human N-acetyltransferase 1. *Drug metabolism reviews, 40*(1), 169-184.

Westwood I.M., Bhakta S., Russell A.J., Fullam E., Anderton M.C., Kawamura A., Mulvaney A.W., Vickers R.J., Bhowruth V., Besra G.S., Lalvani A., Davies S.G., Sim E. (2010). Identification of arylamine N-acetyltransferase inhibitors as an approach towards novel anti-tuberculars. *Protein and cell,* 1(1):82-95.

Wu, H., Dombrovsky, L., Tempel, W., Martin, F., Loppnau, P., Goodfellow, G., Grant, D., Plotnikov, A. (2007). Structural Basis of Substrate-binding Specificity of Human Arylamine *N*-Acetyltransferases. *The journal of biological chemistry.* 282(41)30189–30197.

Zang,Y., Doll, M.A., Zhao,S., States,J.C., & Hein, D.W. (2007). Functional characterization of single-nucleotide polymorphisms and haplotypes of human N-acetyltransferase 2. *Carcinogenesis, 28*(8), 1665-1671.

Zheng, W., Deitz, A. C., Campbell, D. R., Wen, W. Q., Cerhan, J. R., Sellers, T. A., Hein, D. W. (1999). N-acetyltransferase 1 genetic polymorphism, cigarette smoking, well-done meat intake, and breast cancer risk. *Cancer epidemiology, biomarkers & prevention, 8*(3), 233-239.

CURRICULUM VITAE

NAME: Carmine S. Leggett

ADDRESS: Department of Pharmacology and Toxicology
Clinical and Translational Research Building – Room 352A
University of Louisville School of Medicine
505 S. Hancock St
Louisville, KY 40202-1617

EDUCATION

Institution/Location	Degree	Year	Field of Study
Spelman College; Atlanta, GA	B.S.	2006	Chemistry
Delaware State University; Dover, DE	M.S.	2008	Chemistry
University of Louisville School of Medicine Louisville, KY	M.S.	2010	Pharmacology/ Toxicology
University of Louisville School of Medicine Louisville, KY	Ph.D.	2012	Pharmacology/ Toxicology

RESEARCH AND TRAINING EXPERIENCE

2008 – Present   Doctoral Candidate, NIH/NIEHS Fellow

Department of Pharmacology/Toxicology,
University of Louisville School of Medicine, Louisville, KY

M.S. Thesis Topic: Functional effects of *CYP1A2*, *NAT1*,
and *NAT2* genetic variants in nucleotide excision repair-deficient
human fibroblasts: Implications for toxicological risk
from environmental arylamines

Dissertation Topic: Role of human arylamine *N*-acetyltransferase
in carcinogen metabolism and human breast cancer progression

Dissertation Director: David W. Hein, Ph.D.

111

2007 - 2008	Graduate Student Research Assistant
	Brookhaven National Laboratory; Upton NY
	Thesis Topic: Development and validation of [^{11}C]SSR149415 and indole derivatives as Positron Emission Tomography agents for imaging of cannabinoid(CB$_1$) and vasopressin (V$_{1B}$) receptors
	Thesis Director: Joanna Fowler, Ph.D.
2004 - 2006	NSF Model Institute for Excellence Research Fellow
	Spelman College; Atlanta, GA
	Research Topic: Synthesis of aniline and benzimidazole derivatives for anti-proliferative agents; Utilizing Simulation Software ADMET Predictor® to measure QSAR Descriptors of heterocyclic molecules
	Research Mentor: Leyte Winfield, Ph.D.
Summer 2005	NSF Alliance for Graduate Education and the Professoriate Research Assistant
	University of Iowa; Iowa City, IA
	Research Topic: Biotransformation of Indene by *Candida* Strains to produce indandiol and indanoxide using strain UI-9773 analyzed by NMR and TLC
Summer 2004	Multicultural Academic Opportunity Program (MAOP) Research Assistant
	Virginia Polytechnic Institute and State University Virginia Bioinformatics Institute (VBI); Blacksburg, VA
	Research Topic: Sequence Data Annotation of Expressed Sequence Tags of *Phytophthora*
Summer 2002	Health Careers Opportunity Program (HCOP) Research Assistant
	Albany State University; Albany, GA
	Research Topic: Utilizing susceptibility test to optimize antibiotic therapy

RESEARCH AND PROFESSIONAL SOCIETIES
- American Society for Pharmacology and Experimental Therapeutics; Member

- Black Biomedical Graduate Student Organization; President (2011-2012), Vice-President (2010-2011), Secretary (2009-2010)

- American Chemical Society; Member

- National Organization for the Professional Advancement of Black Chemist and Chemical Engineers (NOBCChe); Member

HONORS AND FELLOWSHIP AWARDS

2012   American Society for Pharmacology and Experimental Therapeutics Minority Graduate Student Travel Award, Experimental Biology Annual Meeting

2011   First Place Doctoral Basic-Science Graduate Student Award, University of Louisville Research!Louisville

2010   NIH/NIEHS Environmental Health Sciences Training Program Fellowship, University of Louisville School of Medicine (T32-ES011564)

2010   Center for Genetics and Molecular Medicine Graduate Student Travel Award, 5th International Workshop on Arylamine N-Acetyltransferase, Paris, France

2008   Integrated Programs in Biomedical Sciences Fellowship, University of Louisville School of Medicine

2006   National Science Foundation Greater Philadelphia Alliance for Minority Participation Bridge to the Doctorate Fellowship, Delaware State University

2006   Graduate Research Internship Program Fellowship, Brookhaven National Laboratory

2004   National Science Foundation Model Institute for Excellence Fellowship, Spelman College

2004   Organic Chemistry Laboratory Teaching Assistantship, Chemistry Department, Spelman College

2002   The State of Georgia Helping Outstanding Pupils Educationally (HOPE) Scholarship, Spelman College

Leggett, C.S., Doll, M.A, States, J.C., Trent, J.O., and Hein, D.W.: Identification and characterization of novel arylamine *N*-acetyltransferase small molecule inhibitors. *Proceedings of 2012 Experimental Biology*, San Diego, CA. April 2012.

Leggett, C.S., Doll, M.A, States, J.C., Trent, J.O., and Hein, D.W.: Identification and characterization of novel arylamine *N*-acetyltransferase small molecule inhibitors. *Proceedings of the Sixth Annual NIH National Graduate Student Research Conference*, Bethesda, Maryland, October 2011.

Leggett, C.S., Doll, M.A, States, J.C., Trent, J.O., and Hein, D.W.: Small molecule inhibition of arylamine *N*-acetyltransferase 1: A novel molecular target for cancer prevention. *Proceedings of the 10th Annual James Graham Brown Cancer Center Retreat*, Louisville, Kentucky, October 2011.

Leggett, C.S., Doll, M.A, States, J.C., Trent, J.O., and Hein, D.W.: Small molecule inhibition of arylamine *N*-acetyltransferase 1: A novel molecular target for cancer prevention. *Proceedings of Research!Louisville, Louisville*, Kentucky, October 2011.

Leggett, C.S., Doll, M.A, States, J.C., Trent, J.O., and Hein, D.W.: Identification and characterization of novel arylamine *N*-acetyltransferase small molecule inhibitors. *Ohio Valley Society of Toxicology summer student meeting*, Louisville, Kentucky, August 2011.

Leggett, C.S., Barker, D.F., Doll, M.A, Millner, L.M., States, J.C., and Hein, D.W.: Functional effects of CYP1A2, NAT1, and NAT2 genetic variants in nucleotide excision repair-deficient human fibroblasts: Implications for toxicological risk from environmental arylamines. *Proceedings of the 9th Annual James Graham Brown Cancer Center Retreat*, Louisville, Kentucky, November 2010.

Leggett, C.S., Barker, D.F., Doll, M.A, Millner, L.M., States, J.C., and Hein, D.W.: Functional effects of CYP1A2, NAT1, and NAT2 genetic variants in nucleotide excision repair-deficient human fibroblasts: Implications for toxicological risk from environmental arylamines. Proceedings of Research!Louisville, GRM-12, Louisville, Kentucky, October 2010.

Leggett, C.S., Barker, D.F., Doll, M.A., Millner, L.M., States, J.C., and Hein, D.W.: Construction and functional characterization of nucleotide excision repair-deficient SV40-transformed human fibroblasts expressing human CYP1A2 and NAT2 genetic variants. *Proceedings of the Fifth International Workshop on the Arylamine N-acetyltransferases*, Paris, France, September 2010.

Leggett, C.S., Doll, M.A., Trent, J.O., Walraven, J.M., Millner, L.M., and Hein, D.W.: Identification and characterization of novel arylamine *N*-acetyltransferase small molecule

inhibitors. *Proceedings of the 8th Annual James Graham Brown Cancer Center Retreat*, Louisville, Kentucky, November 2009.

Leggett, C.S., Doll, M.A., Trent, J.O., Walraven, J.M., Millner, L.M., and Hein, D.W.: Identification and characterization of novel arylamine *N*-acetyltransferase small molecule inhibitors. *Proceedings of Research!Louisville*, Louisville, Kentucky, October 2009.

Leggett, C.S., Fowler, J., Hooker, J., Makryannis, A., Reid, A., and Zvonok, A.: Development and Validation of [^{11}C]SSR149415 and Indole Derivatives as PET agents for Imaging of Cannabinoid(CB$_1$) and Vasopressin(V$_{1b}$) Receptors. *Proceedings of Brookhaven National Laboratory Research Symposium*. Upton, NY, August 2007.

Leggett, C.S. and Winfield, L.: Using ADMET Predictor to Measure Parameters of Heterocyclic Molecules. *Proceedings of Spelman College Annual Research Day*. Atlanta, GA, 2006.

Leggett,C.S., Ankudey,E., and Peeples,T.: Biotransformation of Indene by Candida strains. *Proceedings of the AGEP Summer Research Symposium*. Iowa City, IA, 2005.

Leggett, C.S., Thomas, E., and Winfield, L.: Synthesis of Benzimidazole Derivatives. *Proceedings of the Model Institute of Excellence Annual Research Day*. Spelman College. Atlanta, GA, 2005.

Leggett, C.S., Waller, L., and Tyler, B.: Sequence Data Annotation of Expressed Sequence Tags of *Phytophthora*. *Proceedings of the Virginia Tech Summer Research Symposium*. Blacksburg, VA, 2004.

PUBLICATIONS

Schönberger, M., **Leggett,C.S.**, Kim, S.W., and Hooker, J.M.: Synthesis of [^{11}C]SSR149415 and preliminary imaging studies using positron emission tomography. *Bioorganic and Medical Chemistry Letters* 15: 3103- 3106, 2010. [PMID: 20400305]

Hein, D.W., Millner, L.M., **Leggett, C.S.** and Doll, M.A.: Relationship between *N*-acetyltransferase 2 single nucleotide polymorphisms and phenotype. *Carcinogenesis* 31: 326-327, 2010. [PMCID: 2812573]

Winfield, L., Smith, D.M., Halemano, K., and **Leggett, C.S.**: A Preliminary Assessment of Structure- Activity Relationship of Benzimidazole-Based Anti-Proliferative Agents. *Letters in Drug Design and Discovery* 5: 369-376, 2008. [ISSN:1570-1808]

SCIENTIFIC TRAINING, WORKSHOPS, AND SEMINARS

March 30, 2012   Pfizer Investigator Training Program:
                 The workshop is based on principles of ICH-GCP and includes the

following topics: planning and preparation, recruitment and enrollment, in-trial procedures, safety in clinical trials, monitoring, audits, inspections, and publications, the drug development process, and additional regulations governing clinical trials.

October 2009	Grant Writing Workshop: NIH Training and Career Development Programs, Research!Louisville, University of Louisville School of Medicine
2008 -	Department of Pharmacology and Toxicology, University of Louisville School of Medicine Seminar Series
2008 -	James Graham Brown Cancer Center Memorial Lecture Series, James Graham Brown Cancer Center, University of Louisville Louisville, KY
2008 -	Center for Genetics and Molecular Medicine Seminar Series, University of Louisville

PROFESSIONAL SERVICE AND COMMITTEE ASSIGNMENTS

2011 -	University of Louisville School of Medicine Diversity Committee
2010 -	Department of Pharmacology and Toxicology liaison for prospective/visiting graduate students, University of Louisville School of Medicine